Emergent collective decision-making: control, model and behavior

Tian Shen

A Dissertation
Presented to the Faculty
of Princeton University
in Candidacy for the Degree
of Doctor of Philosophy

Recommended for Acceptance
by the Department of
Mechanical and Aerospace Engineering
Adviser: Naomi E. Leonard

January 2015

Abstract

In this dissertation we study dynamics of collective decision-making in social groups with time-varying interactions and heterogeneously informed individuals. First we analyze a continuous-time dynamical systems model motivated by animal collective motion with heterogeneously informed subpopulations, to examine the role of informed and uninformed individuals in collective decision-making with dynamic social interactions. We find through formal analysis that adding uninformed individuals increases the likelihood of a collective decision. In particular, increasing the population of uninformed individuals decreases the critical preference direction difference for stable decision and increases the parameter space for which the region of attraction for a stable decision is large.

Secondly, we propose a mathematical model for human shared decision-making with continuous-time feedback and where individuals have little information about the true preferences and incentives of other group members. We study the equilibria of the model through bifurcation analysis to understand how the model would predict decisions based on the critical threshold parameters that represent an individual's tradeoff between social and environmental influence.

Thirdly, we analyze data of pairs of human subjects performing an experimental shared tracking task using our second proposed model in order to understand behavior and the decision-making process. In this tracking experiment, a pair of players share the control over a virtual object and perform a tracking task while they are given possibly differing stimulus, represented by differing reference paths. Differing reference paths induce possibly conflicting preferences of the players. A player is said to have a "hard" preference when *only one* reference path is given. A player is said to have a "soft" preference when two reference paths on opposite sides are given to the player and one is wider and easier to track inducing a preference for the player for that track. We focus on the case in which one player has a hard preference which is

in conflict with the soft preference of the other player. Statistical analysis of the start and end status of the decision behaviors alone is not sufficient to explain why the players reach certain shared decisions. With this as motivation, we investigate the evolution of the decision-making with our model to find explanations for the decision-making process. We fit the model to data and show that it reproduces a wide range of human behaviors surprisingly well. This suggests that the model may have captured the mechanisms behind some of the behaviors observed in the experiment.

Finally, we take a different perspective and study game-theoretic behavior in the above-mentioned shared tracking task as a repeated coordination game with incomplete information. We show that for our game formulation the majority of the players are able to converge to playing Nash equilibrium strategies in the final rounds of the repeated game. Lastly we show through simulations that the mean field evolution of strategies resemble characteristics of replicator dynamics, suggesting that the underlying individual based strategic responses may be myopic. Even though individuals may not know what game is being played, the population as a whole could learn to play the Nash equilibrium strategies in time.

Decisions form the basis of control and problems involving deciding collectively between alternatives appear in many engineering applications as well. Understanding how multi-agent groups make decisions provides insight for designing robust decentralized control laws for many engineering applications, from mobile sensor networks for environmental monitoring to collective construction robots. With this dissertation we hope to provide additional methodology and mathematical models for understanding the behavior and control of collective decision-making in multi-agent systems.

Acknowledgements

First and foremost I wish to thank my advisor and mentor, Professor Naomi E. Leonard. Naomi has supported me not only by providing a research assistantship for over six years, but also academically and emotionally through the road to finish this dissertation. Thanks to her amazing intelligence and creativity, boundless patience and passion, I have had the opportunity to study this exciting subject of dynamics and control of collective decision-making. Naomi helped me come up with the initial research topic and guided me over six years of development, passing the General Exam, making the first progress in research and preparing manuscripts for publication. During the difficult times when research was at a stall, she gave me moral support and the freedom I needed to move on.

My PhD committee guided me through all these years as well. Thank you to Professor Holmes and Professor Levin for serving on my PhD committee. Professor Holmes gave me the opportunity to present at a PACM Dynamical Systems and Nonlinear Science seminar in 2011, which was my first experience speaking about my work in front of an audience from different fields. Professor Levin helped me with my General Exam preparation and introduced me to the mathematical modeling of biological systems. I am thankful for your motivating comments and discussions. I also thank Professor Holmes for being my examiner and I thank Professor Levin for being my reader.

I am grateful to Professor Kasdin for taking time to be my dissertation reader and being willing to offer me advice especially in my first year here. I thank Professor Stengel, Professor Rowley, Professor Ju and Professor Pacala for taking their time to help me prepare and review for the General Exam. I also thank Professor Rowley for being my dissertation examiner. I thank Professor Couzin for introducing me to the exciting field of animal collective behaviors. I am very honored to have been taught and helped by all of you.

During my graduate studies I was also supported by a first-year fellowship from the Princeton University Graduate School, a prize from the Department of Mechanical and Aerospace Engineering and the Larisse Rosentweig Klein Award established by the Bellan family. My research was also supported in part by the Office of Naval Research Grant N00014-09-1-1074. I am grateful for the support that I have received.

Dozens of friends have helped me and shared life experiences with me at Princeton. I would like to thank fellow and former graduates students in the Dynamical Control Systems Laboratory. Andy Steward and Ming Cao introduced me to the Lab and the Department when I visited Naomi in 2007. Dan Swain and Kendra Cofield welcomed me to the office as soon as I arrived here in 2008, and we had many interesting conversations on research. Darren Pais and Stephanie Goldfarb helped me prepare the General Exam and we exchanged many ideas. Thank you to my peers Anand Ashok, Fadi Abdeljawad, Brandt Belson, Paul Reverdy, Dan Sirbu, Yucheng Tsai, Fujia Wu, Elizabeth and George Young for studying and working together.

A special acknowledgement goes to my research collaborators of many years, Michael Schwemmer and Elliot Ludvig. Mike has helped me and taught me numerical simulations in his spare time and introduced me to model fitting. Elliot has inspired me to read and think about research in psychology and neuroscience. I also thank Raphaela Groten who generously shared her experimental data with us so that I could build my project. I am also grateful for the help and advice from Benjamin Nabet and Luca Scardovi, who were among my first collaborators in research at Princeton. I thank Katie Fitch, Will Scott, Vaibhav Srivastava and Carlos Caicedo for conversations and brainstorming. I thank Ioannis Poulakakis, Alex Olshevsky and Brendan Andrade for listening to my presentations and sharing their feedback.

I took part in other activities outside the Lab, with countless people teaching and helping me every step. Thank you to Jill Ray and Jessica O'Leary for helping me with academic affairs within the Department. A special thank you goes to the

Program in Applied and Computational Mathematics, for allowing me to use the computational resources there, without which some results of this dissertation would not exist. Thank you to GWISE mentoring advisor Professor Gmachl for encouraging conversations. Thank you to the Writing Center for giving me advice in academic writing.

I met many amazing people outside my academic circle who have befriended and encouraged me over the years since I came to the U.S. In particular, I thank Amy Glennon, Tomoko Shibata, Aiching He, Feifei Chu, Lei Fan, Zi Chen, Josh Rivas, Andy Akiho, Jaspreet Dhupia, Andy Madden, Joosup Lim, Akira Saito, Cindy Lau and Jonathan Luk for sharing good times with me.

I finish with briefly thanking the people I owe the deepest debt of gratitude, simply because it is hard to put into words how much I am grateful for them. The love I have received from my parents have been unconditional all these years, and I thank them for cheering me up and always cherishing me in their hearts no matter what.

This dissertation carries the number T-3294 in the records of the Department of Mechanical and Aerospace Engineering.

To my parents.

Contents

List of Tables

List of Figures

Chapter 1

Introduction

Social organisms such as fish schools, bird flocks, and honeybees have amazing capabilities for rapidly deciding collectively among many alternatives and yet still maintaining group cohesion. For example, ants make collective decisions through "stigmergy" about where to go for foraging [68], homing pigeons decide collectively about which route to take [6], honeybees decide collectively about where to build a new home [56, 67], and migratory birds decide collectively for actual departure in the wild [16]. Animals move collectively in groups in their daily activities for benefits such as increased survival probability and enhanced foraging efficiency among other benefits[55, 11, 42]. Often such social activities include groups of huge sizes such that collective motion is largely an emergent and self-organized phenomenon due to the limited sensing capabilities of individuals within such huge groups. Self-organization refers to the fact that emergent collective behaviors arise from local interactions of individuals with their nearby neighbors and local environmental information, without the influence of a known leader, or centralized external signals [11]. Animal groups that make decisions together can be huge but they react to their ecological environment very quickly. Many efforts have been carried out to understand the mechanisms that lead to such high capabilities at the group level despite that individually they may be relatively simple organisms [55, 63].

Mathematical modeling has proven to be helpful in revealing the underlying principles of collective behaviors (for a review, see [20]). In fact, early insights on principles of collective motion came from analysis and simulation of a mathematical model from particle physics [2]. By studying the model it was revealed that collective level phenomenon can arise from individual interactions. Another principle, later discovered also through computational modeling, is that for the same individual interaction rules, the group level behavior can have multiple stable modes. Such multi-stability allows collective behaviors to serve different functions while individuals interact according to the same general rules. It is now well known that social animals are capable of switching between different behavior patterns quickly and efficiently [20]. These transitions are often understood as being due to changing behavioral parameters and environmental factors.

It can prove useful to understand how and why animals can change collective states or make collective decisions quickly and efficiently in a self-organized way without the danger of a major group fragmentation. Answering such questions not only helps in understanding the nature of collective behaviors and complex biological phenomena that arise out of simple interactions, it also helps in addressing many problems in engineering fields, such as designing collective control laws for mobile sensor networks for environmental monitoring, as well as problems in wildlife habitat management [54, 28].

Following [58], we define "collective decision-making" as a process by which a group of individuals use social and environmental information to achieve group level coordination without explicit signaling and prescribed leadership. In this dissertation, decision-making involves choosing between two alternatives in a relatively short amount of time, although in the broader context, it can mean choosing between many different alternatives over longer temporal and spatial scales. The way we define what a "decision" is differs from chapter to chapter. In Chapter 3, a "collective decision" means that the majority of the group will move in a direction that favors an informed opinion. In Chapters 3 and 4, where the main focus is on a two-person shared decision-making problem, a "collective decision" is equivalent to the mean of the two individual decisions.

By social interaction, we mean that individuals can sense the state of the others. We will assume that such interaction is undirected, meaning that all pairwise sensing is bi-directional and symmetric. Complex signaling is certainly a form of social interaction in the fields of animal behavior; it is excluded from the scope of this dissertation where the focus is generally on mathematical models for decision-making based on sensing interactions. Social interactions play a crucial role in collective deicision making across different scales from bacteria [58] to humans [22]. Social interaction is a key principle underlying a diverse range of collective behaviors providing a mechanism for information transfer through the group [16]. But not all collective decisions arise out of social interaction. Some striking collective patterns and highly polarized motions can arise when non-social agents respond in a seemingly coordinated fashion to some environmental influence or stimulus such as phototrophic bacteria swimming in light gradients [64]. In such processes, social interaction plays no role [58] suggesting the importance of environmental influence.

It is generally believed that social organisms with high collective decision-making capability trade off dynamically between environmental influence and social information [58, 19]. An individual can trade off between responding to environmental versus social influences by increasing or decreasing its sensing range with which it accepts or declines more social information. Or it can also choose to forget about its environmental information in order to adapt to social interactions. Mathematically, such a tradeoff can be modeled with agent-based particle dynamics and can be studied using methods that range from numerical simulation models that incorporate many realistic but "hard" to analyze factors [21, 19] to continuous-time models that are reduced to include the key mechanisms making the problem analytically tractable [51, 41].

The balance that individuals make between environmental versus social information is often heterogenous across the group. To quantitatively understand how an individual's balance between social and environmental influences affects the group level behavior is one of the recurring themes of this dissertation, from models on animal motion to human behaviors.

For groups that consists of uninformed individuals who have no direct access to the environmental information, but only contribute to the collective coordination by social interactions, what roles do the uninformed individuals play? This is the first question that we address in this dissertation. In Chapter 2 we analyze a continuous-time model for collective social decision-making dynamics of a group traveling in the plane, consisting of two informed subgroups with different directional preferences, and one uninformed subgroup with no preference [41]. We show the parameter conditions for stability of collective decision-making, and derive the critical value of the magnitude of conflict that serves as a threshold for a collective decision as opposed to a compromise. The results agree qualitatively with the results of the numerical study based on the more complex discrete-time model of [19]. We demonstrate that we can use the continuous-time model to explore the subtle but important role of the uninformed individuals in collective decision-making. In particular, we quantify the sensitivity of the collective decision-making to the population size of the uninformed individuals, showing that increasing numbers of uninformed individuals increases the likelihood that the group will make a collective decision. This work builds on the dissertation of Benjamin Nabet [50].

Mathematical modeling of human decision-making has gained increasing interest as more evidence emerges showing that collective behavior among human crowds tends to display similar principles and tendencies as seen in animal groups [40, 36]. Traditionally human behaviors are generally observed in experimental settings and analyzed using sophisticated statistical methods. Single person decision-making dynamics has been successfully studied using drift-diffusion models [7]. Interactive human decision-making where there are two or more alternatives have started to gain interest from modelers only relatively recently [52, 5, 40].

In this dissertation we develop a mathematical model for human shared decision-making as a step toward understanding human behavior in collective decision-making in groups. In particular, in Chapter 3 we propose an agent-based dynamical systems model of human behavior in a situation where individuals in a group have to coordinate their decisions only with the feedback of their combined actions and in the presence of conflicting individual preferences. Our model can produce a rich variety of trajectories, which can be interpreted as human behaviors given different balances on social versus environmental influence. In particular, in the two-agent case, we show that the bifurcation of decision parameters can be used as a way to predict and explain decision outcomes. We find that the model can display bistability of decision outcomes (i.e., two stable decision outcomes for the same parameter values) for certain decision parameter ranges, but only displays a single stable solution for other parameter ranges. When the system has two stable equilibria, it is sensitive to initial conditions and noise and we will show that in this case the initial condition can play an important role in deciding the decision outcome. In regions of the parameter space where there is only one stable equilibrium, the decision outcome is always the same regardless of the initial conditions suggesting a robustness of decision outcome for certain parameter values. Bistability is ubiquitous in biological systems, and has been shown to be a key phenomenon in decision-making processes at the cellular level [1].

We consider our model parameters as having two aspects. One is the computational aspect, which means that we can produce a variety of trajectories by altering the parameters. The other is the psychological aspect, meaning that the parameters can be interpreted in terms of explanations of behaviors. We can fit the model parameters to the data and use this to make an interpretation of the psychology of the interactions and behaviors of the individuals.

In Chapter 4, we perform a model validation on the data of pairs of human subjects performing a shared tracking experiment by Groten and Feth et.al. [26]. In this tracking experiment, a pair of players share the control over a virtual object which moves according to the mean of the players inputs, and perform a tracking task while they are given possibly differing stimulus, represented by differing reference paths.

Differing reference paths induce possibly conflicting preferences of the players. A player is said to have a "hard" preference when *only one* reference path is given. A player is said to have a "soft" preference when two reference paths on opposite sides are given to the player and one is wider and easier to track, inducing a player preference for that track. In Chapter 4, we focus on the case in which one player has a hard preference which is in conflict with the soft preference of the other player, a type of decision scenario which we refer to as "Hard-Soft Conflict". We study this decision scenario because the greatest variety of decision behaviors are seen in this conflict case in the data.

The model is fitted to all data sets available for the Hard-Soft Conflict decision scenario type, which corresponds to all cases when one of the players has a hard preference and the other has a conflicting soft preference. There are a total of 244 sets of data and each data set consists of 5000 ms of trajectories for both players. We show that our proposed model from Chapter 3 can reproduce a wide range of human behaviors surprisingly well, suggesting that the model may have captured the mechanisms behind some of the behaviors observed in the experiment. Statistical analysis suggest that the player with a soft preference starts out more often than the player with a hard preference, but does not win the decision more often. We explain in terms of model parameters the transient processes of decision-making between the two human subjects performing the tracking task.

An advantage of our model is that it can describe in relatively simple form the decision-making behaviors in a large group of individuals, where no one can guess the intention of the rest of the group. While our analysis focuses on two-person interactions, the model can be extrapolated to larger dimensional systems with many more participating decision makers.

In Chapter 5 we take a different approach to studying decision-making from a game-theoretic perspective. First we formulate the shared tracking problem of Chapter 4 as a normal form repeated game. We show that the majority of equilibrium strategies of the two players in the experimental data correspond to Nash equilibrium strategies. This indicates that in the given experiment players are able to eventually converge onto the Nash equilibrium strategies despite the fact that they do not know the reward structures of their opponent. We then show that the mean field (i.e., population level) evolution of strategies of the two players in the data resembles that of a two-population three-strategy replicator dynamics. Such dynamics is typical of interactions between biological populations where players play their myopic strategies, which means that players only consider their current individual reward and not the future rewards.

In Chapter 6 we summarize our contributions and state future work.

Decisions form the basis of control and problems involving deciding collectively between alternatives appear in many engineering applications as well. Understanding how multi-agent groups make decisions provides insight for designing robust decentralized control laws for many engineering applications, from mobile sensor networks for environmental monitoring to collective construction robots. For example, when a group of autonomous vehicles is searching for a target together they must decide which alternative is true, or they must decide which direction to follow when they confront an obstacle. Our investigation on human behaviors provides incentives for collaboration and compromise when it can be most helpful. This approach also suggests that we can back out certain human behavioral characteristics from interactive tasks and holds promise for using what we learn towards human-robot interaction system designs.

Chapter 2

Role of uninformed individuals in animal collective planar motion [1]

2.1 Background

In this chapter we investigate the role of the number of uninformed individuals and the individual sensing ranges on collective directional decision-making of a heterogeneously informed population of agents in motion together.

The analysis presented here was part of a bigger research project on modeling and understanding of mechanisms of decision-making in a population of self-steered individuals consisting of two informed sub-populations with conflicting preferences and a remaining uninformed sub-population with no preference [41]. The bigger research project, for which Leonard, Nabet, Couzin, Levin and Scardovi laid the foundations and did previous work [51, 41, 50], aimed to develop and rigorously analyze a biologically plausible yet analytically tractable model of animal group motion and collective decision-making with dynamically changing interaction topology. The overall goal

[1] This chapter is essentially the paper [41] verbatim except for Section 2.1.1. I am not the lead author of the paper but I did make important contributions to the analysis. So I include the paper as it appeared.

was to provide mechanisms that explain global behavior of animal groups as a function of individual level responses to the environment and local social interactions. My contribution was to formally investigate the role of key parameters in affecting the collective decision outcome. The results of the research project give new insights for collective decision-making and information transfer mechanisms and provide inspiration for developing future experiments, more refined modeling work, as well as engineering design for real world applications. The model used in this work also has informed the modeling work for the shared decision-making dynamics investigated in Chapters 3 and 4 of this dissertation.

The text and figures in this chapter (except for this and the preceding paragraphs) are for the most part taken verbatim from [41] (for which I am second author), and in some cases re-stated and complemented with additional proofs. In particular, my three proofs on conditions for stability that do not appear in [41] are presented in this dissertation chapter as appendix information. The foundation of my analysis and other results reported in this chapter (and also seen in [41]) derives from the previous work of Nabet, Leonard, Couzin and Levin [51] and Nabet's PhD dissertation [50]. In particular, the model in this chapter was defined by Leonard, Nabet and Scardovi in consultation with Couzin and Levin. Leonard and Nabet also formulated the fast and slow dynamics for this model and formally proved the time-scale separation and parametric conditions for stability of the majority of manifolds and equilibria of interest. Leonard and Scardovi proposed the qualitative critical condition for collective decision versus compromise. I contributed to the remaining proofs for parametric conditions for stability of manifolds and/or equilibria, as well as analysis of algebraic conditions that determine the role of uninformed individuals in terms of the region of parameter space where the collective group decision is uniquely stable. I also contributed to the interpretations, which were developed in collaboration with

Leonard, Nabet, Scardovi, Couzin and Levin. For completeness, all results from [41] are presented in this chapter.

The research has been motivated by the discrete-time model of [19], which investigated, through computation, mechanisms of information transfer, decision-making and emergent leadership in animal groups moving in the plane. In [19], it is shown that even without signaling or identification of the informed individuals, a group can make a collective decision with two informed subgroups of equal population (one subgroup per preference alternative) and a larger subgroup of uninformed individuals. A collective decision to move in one of the two preferred directions is made with high probability as long as the magnitude of the preference conflict, i.e., the difference in preferred directions, is sufficiently large. For small conflict, the group follows the mean of the two preferred directions. When there is only one subgroup of informed individuals, as the total group size increases, the proportion of the informed individuals needed to successfully lead the group to a collective decision decreases, suggesting that increasing the number of uninformed individuals does not hinder the emergence of leadership in the group, but instead enhances the efficiency of information transfer. It is not tested in [19] whether or not the size of the uninformed subgroup plays a similar role in the case of two informed subgroups with conflicting preferences. However simulations in [50] indicate that increasing the population size of uninformed individuals (i.e. decreasing the proportion of informed individuals in the population) lowers the threshold on magnitude of conflict for group decision to emerge, making it “easier” for a collective decision to be made.

Results on collective motion in groups of interacting individuals have been studied predominantly with numerical methods [19, 21, 27, 40, 39, 18]. Parameterized computational studies such as in [19] are highly suggestive, but because their discrete-time models contain many degrees of freedom, it is difficult to identify the influences of particular mechanisms.

Motivated by the simulations of [19], Nabet, Leonard, Couzin, and Levin developed a continuous-time model in [51] of animal groups in planar motion, with simplifying assumptions of two informed sub-populations and no uninformed individuals. In [51] it is further assumed that the social interactions between the group members is all-to-all interaction for all times. Each agent is modeled as a particle moving in the plane at constant speed with steering rate dependent on inter-particle measurements and deviation from a preferred direction. They showed that the model exhibits fast and slow time scales, as observed in the simulations of [19], and therefore, from a large-scale particle model, the model in [51] can be formally reduced to a planar model using time-scale separation from nonlinear systems theory. The time scale separation is proven and the slow dynamics analyzed. In particular, in the fast dynamics, individuals within the same subgroups (i.e. with the same directional preference) reach consensus, and in the slow dynamics, the two different subgroups' mean direction (now synchronized across the subgroups) evolves. The stable solutions for the slow dynamics correspond to compromise by the two subgroups of conflicting preferences. While the model of [51] is analytically tractable and exhibits time-scale characteristics of the discrete-time model by [19], the results of only being able to make a compromise but not a group decision for one of the two preferences suggest that the model of [51] has not fully captured the outcomes as predicted in [19].

Motivated by the discrepancies between the predictions of the continuous-time model of two informed sub-populations with all-to-all interaction in [51], and the discrete time model of dynamic interactions and three sub-populations (one uninformed subgroup) of [19], Leonard, Nabet and Scardovi [50] further proposed a refinement by relaxing two simplifying assumptions. First, they allowed the model to have a third subpopulation of uninformed individuals without directional preferences. Second, they restricted inter-agent interaction to be based on how close two agents are in terms of travel direction. By doing so, they could define an interaction topology that is dynamically changing and state-dependent. Following the same procedure of time scale separation, Leonard and Nabet identified eight important manifolds of the slow dynamics that correspond to interesting group level behavior, and proved conditions on stability for the majority of those manifolds (see [50, 41] for details). Similar to the previous model [51], in the fast time-scale, alignment is established within each subgroup of agents with the same preference (or lack of preference), while in the slow time-scale, the reduced-order model describes the mean motion of each of the two informed subgroups and the uninformed subgroup.

The refined model as well as the derived conditions for stability of slow manifolds by Leonard and Nabet are the foundation of my analysis [50]. The model equations are reviewed below (taken from [41] verbatim with minor adjustments) and all results involving my contribution in [41] are presented in this chapter (taken verbatim from [41] with minor adjustments).

2.1.1 Dynamics of animal collective motion in the plane [2]

Let N be the total number of individuals in a population; each individual is modelled as a particle moving in the plane at constant speed v_c. The direction of motion of individual j at time t is denoted by the angle $\theta_j(t)$. Then, the planar velocity of j at time t is the vector $\mathbf{v}_j = (v_c \cos\theta_j(t), v_c \sin\theta_j(t))$. (Throughout this thesis, we will be denoting vectors and matrices using bold math symbols.)

Every individual is associated with one of three subgroups: the N_1 individuals in subgroup 1 have a preference to move in the direction defined by the angle $\bar{\theta}_1$, the N_2 individuals in subgroup 2 have a preference to move in the direction defined by the angle $\bar{\theta}_2$ and the N_3 individuals in subgroup 3 have no preference. The total population is N, with $N = N_1 + N_2 + N_3$.

[2]This section is from [41] verbatim.

Then, the rate-of-change of direction of motion is defined for each individual in subgroup 1 as

$$\frac{d\theta_j}{dt} = \sin(\bar{\theta}_1 - \theta_j(t)) + \frac{K_1}{N}\sum_{l=1}^{N} a_{jl}(t)\sin(\theta_l(t) - \theta_j(t)), \tag{2.1}$$

in subgroup 2 as

$$\frac{d\theta_j}{dt} = \sin(\bar{\theta}_2 - \theta_j(t)) + \frac{K_1}{N}\sum_{l=1}^{N} a_{jl}(t)\sin(\theta_l(t) - \theta_j(t)), \tag{2.2}$$

and in subgroup 3 as

$$\frac{d\theta_j}{dt} = \frac{K_1}{N}\sum_{l=1}^{N} a_{jl}(t)\sin(\theta_l(t) - \theta_j(t))\,. \tag{2.3}$$

The constant parameter $K_1 > 0$ weights the attention paid to other individuals versus the attention paid to the preferred direction. The dynamic variable $0 \leq a_{jl}(t) \leq 1$ defines the weight individual j puts on the information it gets from individual l at time t. A value $a_{jl} = 0$ implies that j cannot sense l. Social interaction (coupling) weights $a_{jl}(t)$ are modeled as evolving in time according to saturated integrator dynamics that depend on how "close" individuals are from one another, where closeness is defined in terms of relative heading:

$$\begin{aligned} \frac{d\eta_{jl}}{dt} &= K_2(\rho_{jl}(t) - r), \\ a_{jl}(t) &= \frac{1}{1 + e^{-\eta_{jl}(t)}}. \end{aligned} \tag{2.4}$$

In the model of Eq. 2.4, $\eta_{jl} = \eta_{lj}$ is an integrated variable, the constant parameter $K_2 > 0$ quantifies the speed at which the interaction gains evolve, $\rho_{jl} = |\cos(\frac{1}{2}(\theta_j - \theta_l))|$ gives a measure of synchrony of direction of motion of l and j, and $0 \leq r \leq 1$ is a chosen fixed threshold representing an individual's sensing range. It holds that $\rho_{jl} = 1$ if l and j move in the same direction and $\rho_{jl} = 0$ if they move in opposite directions.

If $\rho_{jl} > r$, then j and l are close enough to sense each other so η_{jl} increases and a_{jl} eventually converges to the maximum interaction strength of 1. If $\rho_{jl} < r$, then j and l are not close enough to sense each other so η_{jl} decreases and a_{jl} eventually converges to 0. Eq. 2.4 is equivalent to

$$\frac{da_{jl}}{dt} = K_2(1 - a_{jl}(t))a_{jl}(t)(\rho_{jl}(t) - r). \tag{2.5}$$

As it can be seen from the equation, equilibrium solutions correspond to $a_{jl}(t) = 0$ and $a_{jl}(t) = 1$. The state space for the model of Eqs. 2.1 - 2.3 and 2.5 is compact since each θ_j is an angle and each a_{jl} is a real number in the interval $[0, 1]$.

2.1.2 Reduced model and invariant manifolds [3]

Leonard and Nabet have shown in [50] that the above model exhibits fast and slow time-scale behavior even for moderate values of gains K_1 and K_2. In particular, they have shown that for an initially aggregated group, the fast dynamics correspond to the individuals in each subgroup quickly becoming tightly coupled with one another (corresponding coupling weights $a_{jl}(t) = 1$ for j and l in subgroup k (for each $k = 1, 2, 3$)), and the direction of motion $\theta_j(t)$ for j in subgroup k converges to a common angle, which is the subgroup mean direction of motion. As we will use the subgroup mean direction of motion in the following analysis, we denote it by $\Psi_k(t)$ for each subgroup k. In addition, for each pair of subgroups, the coupling weights between the subgroup members quickly approach a common value 0 or 1. Thus, after the fast transient, individuals in each subgroup move together in the same direction and the coupling between subgroups becomes constant; the slow dynamics describe the evolution of the mean direction of each of the three possibly interacting subgroups. Leonard and Nabet have shown in [50] and [41] that the time-scale separation and

[3] This section is also from [41] verbatim.

the fast and slow time-scale dynamics in the case that $\epsilon = \max\left(\frac{1}{K_1}, \frac{1}{K_2}\right) << 1$ can be derived using singular perturbation theory [37].

Consequently, they have shown through the formal reduction that the fast dynamics have a number of isolated solutions [50]. For the analysis in this chapter, only isolated solutions that correspond to synchronized speeds within the subgroups and all-to-all interactions within the subgroups (i.e. $a_{jl} = 1$, for both j and l in subgroup k for $k = 1, 2, 3$) are considered. These solutions correspond to those that emerge from groups that are initially aggregated and correspond to every individual j in subgroup k heading in the same direction Ψ_k. It follows that for these solutions, every coupling weight a_{jl} between an individual j in subgroup 1 and an individual l in subgroup 2 takes the same value A_{12}. Likewise, $a_{jl} = A_{13}$ for j in subgroup 1 and l in subgroup 3 and $a_{jl} = A_{23}$ for j in subgroup 2 and l in subgroup 3. Each of A_{12}, A_{13} and A_{23} can take the value 0 or 1; so there are a total of eight such solutions.

Each of these eight solutions defines an invariant manifold: each invariant manifold is defined such that if the dynamics start with synchronized subgroups and interconnections between subgroups defined by constants A_{12}, A_{13}, A_{23} each having value of 0 or 1, then they remain so for all time.

The eight manifolds can be defined as follows. Manifold $\mathcal{M}_{101}$ is defined by $(A_{12}, A_{13}, A_{23}) = (1, 0, 1)$ and manifold $\mathcal{M}_{110}$ by $(A_{12}, A_{13}, A_{23}) = (1, 1, 0)$. $\mathcal{M}_{101}$ describes the case in which the two informed subgroups 1 and 2 are coupled but the uninformed subgroup 3 is coupled only with informed subgroup 2; $\mathcal{M}_{110}$ describes the symmetric case in which subgroups 1 and 2 are coupled and subgroup 3 is coupled only with subgroup 1. Manifold $\mathcal{M}_{000}$, defined by $(A_{12}, A_{13}, A_{23}) = (0, 0, 0)$, corresponds to decoupled subgroups. Manifold $\mathcal{M}_{010}$ is defined by $(A_{12}, A_{13}, A_{23}) = (0, 1, 0)$ where the coupling is between informed subgroup 1 and the uninformed subgroup 3 as shown on the left in Fig. 2.1. Manifold $\mathcal{M}_{001}$, defined by $(A_{12}, A_{13}, A_{23}) = (0, 0, 1)$, describes the case symmetric to $\mathcal{M}_{010}$, where the coupling is between informed subgroup 2 and the uninformed subgroup 3 as shown on the right in Fig. 2.1. Manifold $\mathcal{M}_{100}$, defined by $(A_{12}, A_{13}, A_{23}) = (1, 0, 0)$, corresponds to coupling only between the two informed subgroups 1 and 2. Manifold $\mathcal{M}_{011}$, defined by $(A_{12}, A_{13}, A_{23}) = (0, 1, 1)$, describes the case in which the uninformed subgroup 3 is coupled with each informed subgroup 1 and 2, but the two informed subgroups are not coupled with each other. Manifold $\mathcal{M}_{111}$, defined by $(A_{12}, A_{13}, A_{23}) = (1, 1, 1)$, corresponds to coupling among all three subgroups.

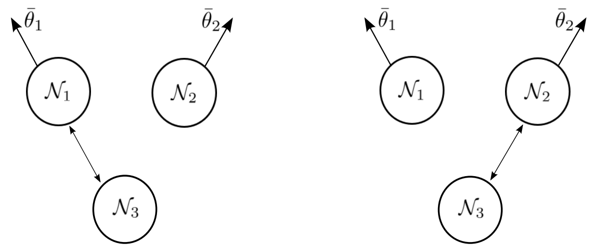

Figure 2.1: Coupling in manifolds $\mathcal{M}_{010}$ (left) and $\mathcal{M}_{001}$ (right) among subgroups 1, 2 and 3 as indicated by arrows.

The slow dynamics on each of the eight manifolds are defined by the rate-of-change of the mean direction of motion for each of the three subgroups:

$$
\begin{aligned}
\frac{d\Psi_1}{dt} &= \sin(\bar{\theta}_1 - \Psi_1(t)) + \frac{K_1}{N}(A_{12}N_2 \sin(\Psi_2(t) - \Psi_1(t)) \\
&\quad + A_{13}N_3 \sin(\Psi_3(t) - \Psi_1(t))) \\
\frac{d\Psi_2}{dt} &= \sin(\bar{\theta}_2 - \Psi_2(t)) + \frac{K_1}{N}(A_{12}N_1 \sin(\Psi_1(t) - \Psi_2(t)) \\
&\quad + A_{23}N_3 \sin(\Psi_3(t) - \Psi_2(t))) \\
\frac{d\Psi_3}{dt} &= \frac{K_1}{N}(A_{13}N_1 \sin(\Psi_1(t) - \Psi_3(t)) \\
&\quad + A_{23}N_2 \sin(\Psi_2(t) - \Psi_3(t))).
\end{aligned}
\tag{2.6}
$$

Each of the eight invariant manifolds is defined to be stable if solutions corresponding to initial conditions near the manifold approach the manifold with time; in this case the full dynamical solution is well approximated by the stable solution of the slow dynamics of Eq. 2.6. Conditions were determined under which each of the eight manifolds is stable by computing the stability of the boundary layer dynamics (fast dynamics) evaluated at the stable solution(s) of the slow dynamics [37]. Without loss of generality, $\bar{\theta}_1 = 0$ and $0 \leq \bar{\theta}_2 \leq \pi$ was chosen; thus, the difference in preferred directions $\bar{\theta}_2 - \bar{\theta}_1$ is equal to $\bar{\theta}_2$. For the majority of the analysis, we focus on the case in which the two informed subgroups have equal population size, i.e., $N_1 = N_2$.

2.2 Role of uninformed population on stability of collective decision [4]

Formal analysis in [50] shows that manifolds $\mathcal{M}_{101}$ and $\mathcal{M}_{110}$ (where the uninformed subgroup couples with only one of the coupled informed subgroups) are always unstable, but there are conditions such that the remaining six manifolds are stable. The manifolds $\mathcal{M}_{010}$ and $\mathcal{M}_{001}$ (where the uninformed subgroup couples with only one of the *uncoupled* informed subgroups) are both stable if and only if

$$\left|\cos\left(\frac{\bar{\theta}_2}{2}\right)\right| - r < 0,$$

i.e., if and only if the difference in preferred direction $\bar{\theta}_2 > \bar{\theta}_\mathrm{c}$, where the critical difference in preference direction $\bar{\theta}_\mathrm{c}$ is given by

$$\bar{\theta}_\mathrm{c} = \cos^{-1}(2r^2 - 1). \tag{2.7}$$

On the other hand, manifold $\mathcal{M}_{111}$ (where all subgroups are coupled) is stable if $\bar{\theta}_2 < \bar{\theta}_\mathrm{c}$, i.e., if

$$\left|\cos\left(\frac{\bar{\theta}_2}{2}\right)\right| - r > 0.$$

[4] This section is from [41] verbatim. I contributed to proving, analyzing, and interpreting the remaining stability conditions.

The dependency of the stability of the manifolds on the critical angle $\bar{\theta}_c$ can be interpreted as follows. Given a value of sensing range parameter r, for sufficiently large difference $\bar{\theta}_2$ between the two preferred directions, the two informed subgroups will be pulled enough in their preferred directions such that they will lose direct connection with each other. Depending on initial conditions the uninformed subgroup may become connected with one or the other of the two informed subgroups corresponding to the interconnections on $\mathcal{M}_{010}$ or $\mathcal{M}_{001}$ of Fig. 2.1. On the other hand, for sufficiently small difference $\bar{\theta}_2$ between the two preferred directions, the two informed subgroups can stay connected with each other and with the uninformed subgroup corresponding to the fully connected case of $\mathcal{M}_{111}$.

The stable solution of the slow dynamics Eq. 2.6 on the manifold $\mathcal{M}_{010}$ corresponds to all of the informed individuals in subgroup 1 and all of the uninformed individuals (subgroup 3) moving steadily in the preferred direction $\bar{\theta}_1$; the informed individuals in subgroup 2 are disconnected from the greater aggregation and move off by themselves in their preferred direction $\bar{\theta}_2$. This solution is classified as (most of) the group making a decision for preference 1. Likewise, the stable solution on the manifold $\mathcal{M}_{001}$ corresponds to all of the informed individuals in subgroup 2 and all of the uninformed individuals (subgroup 3) moving steadily in the preferred direction $\bar{\theta}_2$; the informed individuals in subgroup 1 are disconnected from the greater aggregation and move off by themselves in their preferred direction $\bar{\theta}_1$. This solution is classified as (most of) the group making a decision for preference 2.

Fig. 2.3 shows a simulation of $N = 30$ individuals obeying the dynamics of Eqs. 2.1-2.4 with $N_1 = N_2 = 5$ and $N_3 = 20$. Here $r = 0.9$, which corresponds to $\bar{\theta}_c = 52°$. Further, $\bar{\theta}_2 = 90°$ which is greater than $\bar{\theta}_c$ so that $\mathcal{M}_{010}$ and $\mathcal{M}_{001}$ are both stable. Indeed, for the initial conditions illustrated on the plot of Fig. 2.2, the solution converges to a group decision for preference 1 as in the slow dynamics on $\mathcal{M}_{010}$.

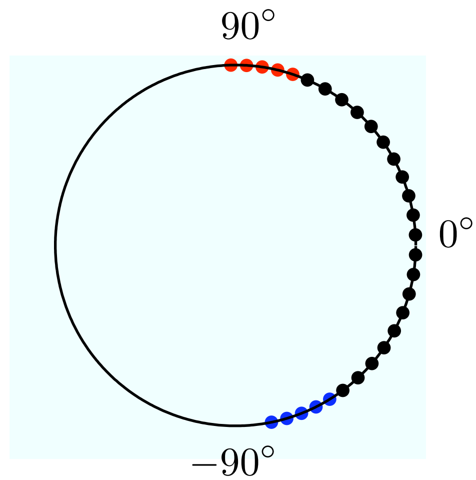

Figure 2.2: The initial direction of motion $\theta_j(0)$ for each $j = 1, \ldots, N$ is displayed on the unit circle. The $\theta_j(0)$ are evenly collective between $-78.5°$ and $-58.5°$ for the $N_1 = 5$ individuals in subgroup 1 (blue dots), between $71.5°$ and $91.5°$ for the $N_2 = 5$ individuals in subgroup 2 (red dots), and between $-53.5°$ and $66.5°$ for the $N_3 = 20$ individuals in subgroup 3 (black dots). All initial values of interaction gains $a_{lj}(0)$ are taken from a uniform distribution with mean 0.2 and standard deviation 0.1.

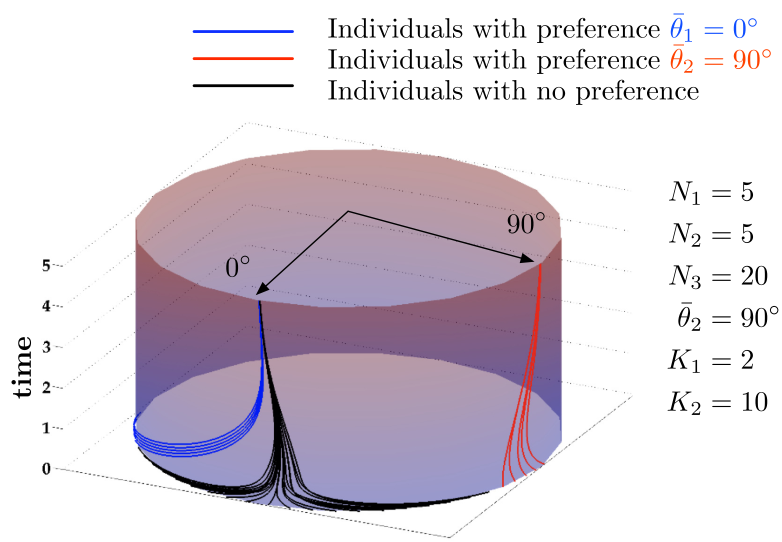

Figure 2.3: Simulation of dynamics of Eqs. 2.1-2.4 with $N = 30$ individuals, $r = 0.9$, and $\bar{\theta}_1 = 0°$ and $\bar{\theta}_2 = 90°$ as shown with black arrows on the top of the cylinder. The solution for each individual is shown evolving on the surface of the cylinder; the azimuth describes the angle θ_j and the vertical axis describes time t. For this example, $\bar{\theta}_2 > \bar{\theta}_c = 52°$ and it can be observed that a decision is made for preference 1.

Depending on parameters, the slow dynamics Eq. 2.6 on the manifold $\mathcal{M}_{111}$, corresponding to the fully connected case, can have up to two stable solutions. In the first stable solution each of the two informed subgroups compromises between its preferred directions and the mean of the two preferred directions, while the uninformed subgroup travels in the mean of the two preferred directions. Fig. 2.4 shows a simulation of $N = 30$ individuals obeying the dynamics of Eqs. 2.1-2.4 with $N_1 = N_2 = 5$ and $N_3 = 20$. Here $r = 0.6$, which corresponds to $\bar{\theta}_c = 106°$. As in the previous example, $\bar{\theta}_2 = 90°$, but now this is less than $\bar{\theta}_c$ so that $\mathcal{M}_{010}$ and $\mathcal{M}_{001}$ are unstable and $\mathcal{M}_{111}$ is stable. Indeed, for the initial conditions of Fig. 2.4 (the same as in Fig. 2.3), the solution converges to the compromise as in the first stable solution of the slow dynamics on $\mathcal{M}_{111}$. If $N_3 > 2N_1$, i.e., for a sufficiently large population of uninformed individuals, $\mathcal{M}_{111}$ is *only* attractive near the first stable solution if $\bar{\theta}_2 < \bar{\theta}_c$. The proof for the sufficient condition for $\mathcal{M}_{111}$ to be unstable is shown in Appendix A as Lemma A.1.1.

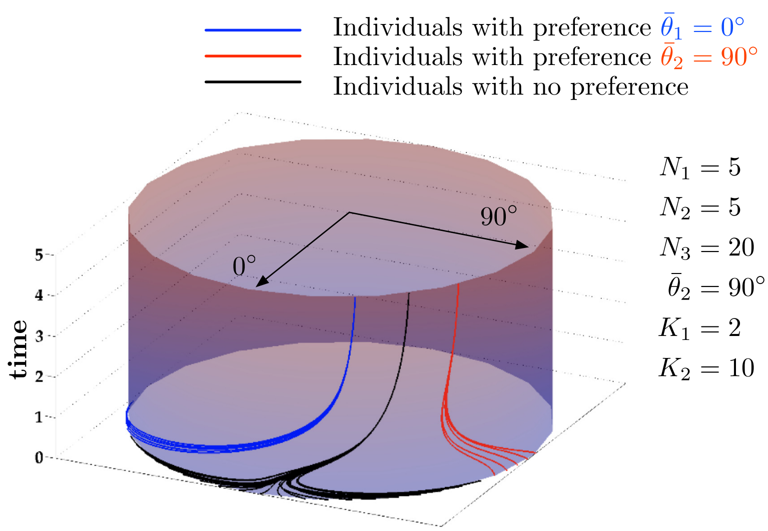

Figure 2.4: Simulation of dynamics of Eqs. 2.1-2.4 with $N = 30$ individuals, $r = 0.6$, and $\bar{\theta}_1 = 0°$ and $\bar{\theta}_2 = 90°$. For this example, $\bar{\theta}_2 < \bar{\theta}_c = 106°$ and it can be observed that no decision is made. Instead, the agents collect in subgroups that compromise.

The second stable solution of Eq. 2.6 on the manifold $\mathcal{M}_{111}$ is symmetric to the first stable solution: the uninformed subgroup moves in the direction 180° from the mean of the two preferred directions and each informed subgroup compromises between this direction and its preferred direction. This is a somewhat pathological solution that is very far from a group decision. However, this second solution does not exist in the presence of a sufficiently large population of uninformed individuals, notably in the case that

$$\left(\frac{N_3}{2N_1}\right)^{2/3} > 1 - \left(\frac{2N_1K_1}{N\sin(\bar{\theta}_2/2)}\right)^{2/3}. \tag{2.8}$$

Inequality Eq. 2.8, which derives from the stability analysis (see [50], Chapter 6 page 143), is always satisfied for $N_3 > 2N_1$ or for sufficiently large strength of social interactions given by $K_1 \geq 2$. Thus, under the condition $N_3 > 2N_1$, $\mathcal{M}_{111}$ is unstable precisely when $\mathcal{M}_{010}$ and $\mathcal{M}_{001}$ are stable. Fig. 2.5 illustrates stability of decisions (on M_{010} and M_{001}) versus compromise (on M_{111}) as a function of preference difference $\bar{\theta}_2$.

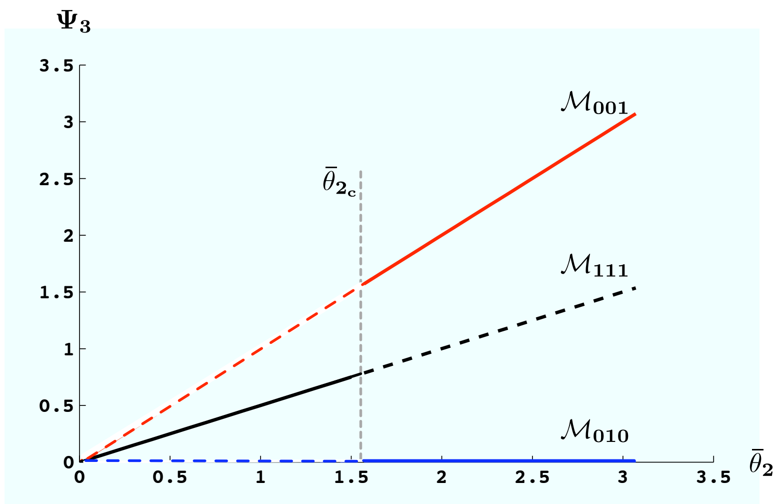

Figure 2.5: Stability of decisions (on M_{010} and M_{001}) versus compromise (on M_{111}) illustrated on plot of direction of uninformed subgroup Ψ_3 as a function of preference difference $\bar{\theta}_2$. Here $r = .707$ and so $\bar{\theta}_{2_c} = \pi/2$. A solid line denotes a stable solution and a dashed line denotes an unstable solution.

Fig. 2.6 (top left) plots r as a function of $\bar{\theta}_2$ given by Eq. 2.7; this defines the critical condition for stability of a collective decision for preference 1 as defined by the solution on $\mathcal{M}_{010}$ and for preference 2 as defined by the solution on $\mathcal{M}_{001}$. The shaded region illustrates the parameter space corresponding to stability of a collective decision. The decision is unstable in the parameter space defined by the white region, which corresponds to the stability of a compromise. Given a fixed value of r, the curve provides a lower bound $\bar{\theta}_c$ on the preference difference $\bar{\theta}_2$ for which a decision is stable.

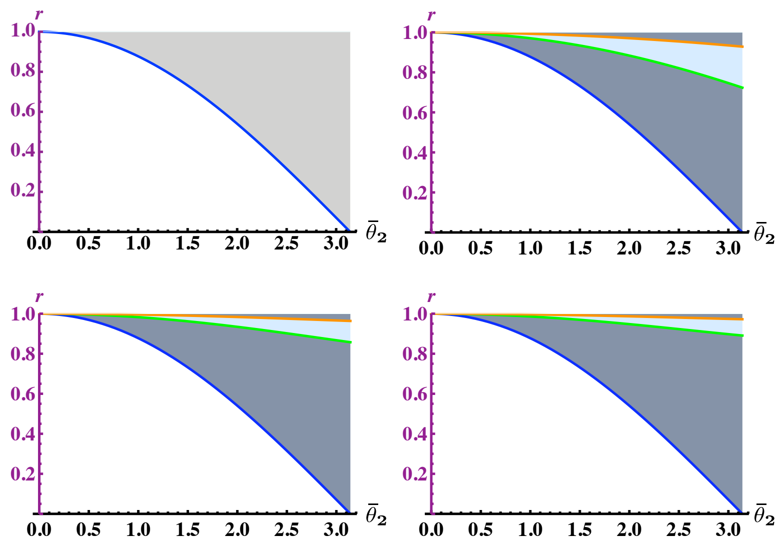

Figure 2.6: Curves in the space of parameters $\bar{\theta}_2$ and r that determine the stability of manifolds $\mathcal{M}_{010}$ and $\mathcal{M}_{001}$, and, thus, the stability of a collective decision. In all plots, $K_1 = 2$ and $N_1 = N_2 = 5$. Top left: Light grey parameter space corresponds to stability of $\mathcal{M}_{010}$ and $\mathcal{M}_{001}$, independent of N_3. Top right: $N_3 = 11$. Bottom left: $N_3 = 50$. Bottom right: $N_3 = 500$. Dark grey parameter space corresponds to $\mathcal{M}_{010}$ and $\mathcal{M}_{001}$ being the only stable manifolds among the eight invariant manifolds studied. The dark grey parameter space increases with increasing number of uninformed individuals N_3.

Now suppose that a number of uninformed individuals are added to the aggregation, i.e., the density is increased. For any individual to retain roughly the same number of neighbors after the addition of individuals as before, it can decrease its sensing range. A decrease in sensing range corresponds to an increase in r. As seen in Fig. 2.6, an increase in r corresponds to a decrease in the lower bound $\bar{\theta}_c$, i.e., with increased numbers of uninformed individuals, a collective decision is stable for lower values of preference difference $\bar{\theta}_2$.

For some range of parameter values for which $\mathcal{M}_{010}$ (i.e. collective decision for $\bar{\theta}_1$) and $\mathcal{M}_{001}$ (i.e. collective decision for $\bar{\theta}_2$) are stable, it is possible that $\mathcal{M}_{000}$, $\mathcal{M}_{100}$ and/or $\mathcal{M}_{011}$ are also stable. This means that even if $\mathcal{M}_{010}$ and $\mathcal{M}_{001}$ are stable, for some initial conditions the solution may converge to the stable solutions of $\mathcal{M}_{000}$, $\mathcal{M}_{100}$ and/or $\mathcal{M}_{011}$, none of which correspond to a collective decision for preference 1 or 2. In fact, the only stable solution on $\mathcal{M}_{000}$ corresponds to the three subgroups moving apart (i.e. the group splits). $\mathcal{M}_{100}$ can have up to two stable solutions and $\mathcal{M}_{011}$ can have one stable solution; all of these correspond to compromise solutions. Therefore, we examine the conditions for stability of $\mathcal{M}_{000}$, $\mathcal{M}_{100}$ and $\mathcal{M}_{011}$ in order to isolate the parameter space in which $\mathcal{M}_{010}$ and $\mathcal{M}_{001}$ are the *only* stable manifolds among the eight under investigation.

The condition $\bar{\theta}_2 > \bar{\theta}_c$ is necessary for stability of $\mathcal{M}_{000}$. However, $\mathcal{M}_{000}$ is unstable as long as the initial mean heading of the uninformed individuals is greater than $-\bar{\theta}_2$ and less than $2\bar{\theta}_2$, i.e., as long as the uninformed individuals are not headed in a direction that is dramatically different from the mean of the two preferred directions. The latter is not so likely for initially aggregated individuals. Further, the likelihood of $\mathcal{M}_{000}$ being stable shrinks as $\bar{\theta}_2$ grows (see [50] Chapter 6 page 140 for proof).

$\mathcal{M}_{100}$ (coupled informed subgroups) is also unstable if the initial mean heading of the uninformed is not dramatically different from the mean of the two preferred directions [50]. Otherwise, if $\bar{\theta}_2 < \bar{\theta}_c$, $\mathcal{M}_{100}$ is stable about its first stable solution. The second stable solution of $\mathcal{M}_{100}$ does not exist if $K_1 < 2N/N_1$ and is not attracting if

$$r > \sqrt{1-d^2}, \quad d = \frac{N\sin(\bar{\theta}_2/2)}{2N_1K_1}. \tag{2.9}$$

For the proof of the condition for non-existence and the condition for instability of the second solution of $\mathcal{M}_{100}$, refer to Lemma A.2.1 in Appendix A.

The condition $\bar{\theta}_2 > \bar{\theta}_c$ is a necessary condition for stability of $\mathcal{M}_{011}$ (uninformed coupled to uncoupled informed subgroups). However, $\mathcal{M}_{011}$ is unstable if either of the following is satisfied ([50] Chapter 6 page 142):

$$r < \frac{1}{\sqrt{1+\nu^2}} \quad \text{or} \quad r > \sqrt{\frac{1}{2} + \frac{1}{2\sqrt{1+\nu^2}}} \tag{2.10}$$

where

$$\nu = \frac{N \sin(\bar{\theta}_2/2)}{N_3 K_1 + N \cos(\bar{\theta}_2/2)}.$$

We show in Appendix A (Lemma A.3.1) that $\mathcal{M}_{011}$ can be stable in the range of parameters for which $\mathcal{M}_{010}$ and $\mathcal{M}_{001}$ are also stable.

Table 2.1 summarizes the possible coexistence of stable manifolds for different parameter ranges, assuming $N_3 > 2N_1$. For the initial conditions we consider, $\mathcal{M}_{000}$ and $\mathcal{M}_{100}$ will be unstable, in which case, when $\mathcal{M}_{111}$ is stable, it is exclusively stable among the eight manifolds. Further, the parameter values that yield the exclusive stability of $\mathcal{M}_{010}$ and $\mathcal{M}_{001}$ among the eight invariant manifolds are those that satisfy Eq. 2.10; these are shown as dark grey regions in the parameter space plots of Fig. 2.6.

Table 2.1: Possible combinations of stable (S) and unstable (U) manifolds given $N_3 > 2N_1$

$\mathcal{M}_{101}$	$\mathcal{M}_{110}$	$\mathcal{M}_{000}$	$\mathcal{M}_{010}$	$\mathcal{M}_{001}$	$\mathcal{M}_{100}$	$\mathcal{M}_{011}$	$\mathcal{M}_{111}$
U	U	S	S	S	U	U	U
U	U	S	S	S	U	S	U
U	U	S	S	S	S	U	U
U	U	S	S	S	S	S	U
U	U	U	U	U	S	U	S

In the remaining three plots in Fig. 2.6, the green curve plots r as a function of $\bar{\theta}_2$ in case of equality in the first condition of Eq. 2.10, and the orange curve plots r as a function of $\bar{\theta}_2$ in case of equality in the second condition of Eq. 2.10. In each of the plots, $N_1 = N_2 = 5$ and $K_1 = 2$. The number of uninformed individuals N_3 ranges from $N_3 = 11$ (top right) to $N_3 = 50$ (bottom left) to $N_3 = 500$ (bottom right). The plots show the dark grey region expanding with increasing N_3, i.e., the region of parameter space that ensures unique stability of the collective decision for one or the other preference expands with increasing number of uninformed individuals. An increase in strength of social interaction K_1 also increases this parameter space, since K_1 is multiplied to N_3 in the condition.

2.3 Randomness and asymmetric informed populations

The model studied above is defined as having deterministic dynamics and retains dynamically changing, local social interactions. However, it neglects some of the details of the zonal-based interaction rules of [19]. Nonetheless, it provides the same fundamental result in the case $N_1 = N_2$ without requiring any additional modeling terms such as a forgetting factor on information that is not reinforced [51]. Here we show with simulations of the model with uniform noise that the model produces similar results, suggesting that the analytical results are robust.

Fig. 2.7 shows two simulations of the dynamics of Eqs. 2.1-2.4 with the same initial conditions and parameter values as for the simulations shown in Figs. 2.3 and 2.4, but with randomness added. For each j, we let w_j be an independent random variable drawn from a uniform distribution with mean 0 and standard deviation 0.5. Eqs. 2.1- 2.3 are modified to include a random term as follows:

$$
\begin{aligned}
\frac{d\theta_j}{dt} &= \sin\left(\bar{\theta}_1 - \theta_j\right) + \frac{K_1}{N}\sum_{l=1}^{N} a_{jl}\sin\left(\theta_l - \theta_j\right) + w_j, \quad && j \text{ in subgroup 1} \\
\frac{d\theta_j}{dt} &= \sin\left(\bar{\theta}_2 - \theta_j\right) + \frac{K_1}{N}\sum_{l=1}^{N} a_{jl}\sin\left(\theta_l - \theta_j\right) + w_j, \quad && j \text{ in subgroup 2} \\
\frac{d\theta_j}{dt} &= \frac{K_1}{N}\sum_{l=1}^{N} a_{jl}\sin\left(\theta_l - \theta_j\right) + w_j, && j \text{ in subgroup 3.}
\end{aligned}
\tag{2.11}
$$

Fig. 2.7 exhibits the same net behavior as in the case with no randomness, i.e., for $r = 0.9$ a decision is made for preference 1 and for $r = 0.6$ there is a compromise solution. The use of uniform noise is a conservative choice for examining robustness since as compared to Gaussian noise it gives a higher probability of large random deviations. The noise corrupted model Eq. 2.11 is integrated in MATLAB by first partitioning the time interval into time steps of 0.01 and then use ode113 in the time duration of 0.01 to integrate the system recursively. This method is consistent with the Euler-Maruyama method for integrating stochastic differential equations.

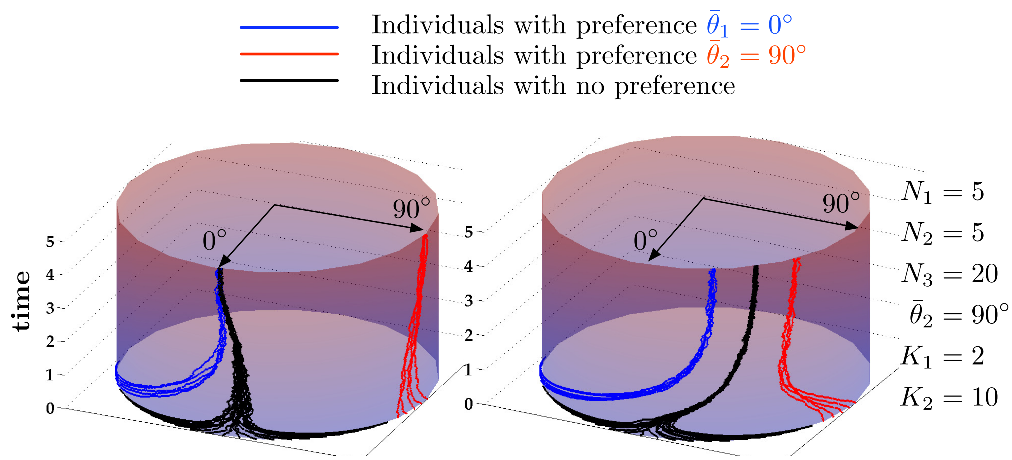

Figure 2.7: Simulation of dynamics of Eqs. 2.1-2.4 modified by additive randomness as given by Eq. 2.11. The left plot corresponds to $r = 0.9$ and the right plot to $r = 0.6$. The solution for each individual is shown evolving on the surface of the cylinder; the azimuth describes the angle θ_j and the vertical axis describes time t. Blue corresponds to subgroup 1, red to subgroup 2 and black to subgroup 3. Initial conditions and parameter values are the same as in Figs. 2.2 and 2.3.

Furthermore, in the case of asymmetric uninformed individuals $N_1 \neq N_2$, the model yields the same necessary and sufficient conditions for stability of a decision. In the case of a decision, simulations show a dominating region of attraction for the decision to move in the preferred direction of the majority informed subgroup, consistent with [19].

Fig. 2.8 shows simulations of the dynamics of Eqs. 2.1-2.4 with the same initial conditions and parameter values as for the simulations shown in Figs. 2.3 and 2.4, but for an asymmetry in the sizes of the informed subgroups. Here we let $N_1 = 4$ and $N_2 = 6$. In the left plot of Fig. 2.8, as in Fig. 2.3, $r = 0.9$ and a decision is made. In the right plot of Fig. 2.8, as in Fig. 2.4, $r = 0.6$ and a compromise is made. While in the simulation of Fig. 2.3, the solution is attracted to the manifold $\mathcal{M}_{010}$ where a decision for preference 1 is made, in the left simulation of Fig. 2.8 with $N_2 > N_1$, the solution is attracted to the manifold $\mathcal{M}_{001}$ where a decision for preference 2 is made.

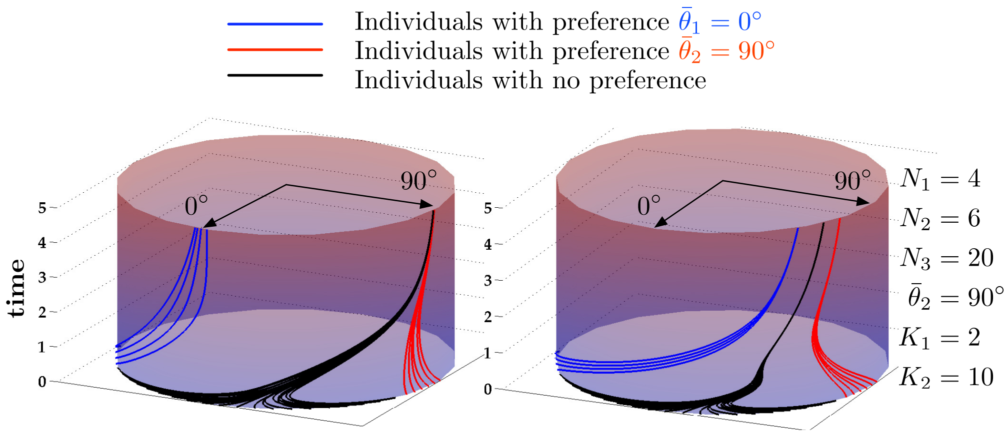

Figure 2.8: Simulation of dynamics of Eqs. 2.1-2.4 with informed subgroup sizes $N_1 = 4$ and $N_2 = 6$. Initial conditions and all other parameters are the same as in Figs. 2.3 and 2.4. The left plot corresponds to $r = 0.9$ and the decision is made for preference 2. The left plot corresponds to $r = 0.6$ and a compromise is made between the two preferred directions and slightly closer to preference 2.

In the following chapters, we will use the insights we gained from analyzing the model for animal decision-making in group motion and propose a model for human social decision-making in collective settings where individuals hold possibly conflicting preferences. The mechanisms of balancing between social and environmental influence will prove to be essential for the human social decision model as well. However, a difference in social interaction will be assumed when applying the mechanism to human behavior. In this chapter we have shown formal evidence on the role of the uninformed population in improving collective decision making, and in the following chapter, we will examine more closely, with our new model, how parameters that reflect individual decision thresholds affect the collective decision outcome.

Chapter 3

Dynamics of collective decision-making between two alternatives

3.1 Background

Consider a real life social coordination situation in which people interact in order to reach a certain private or group goal that is important for each of the individuals. For example, commuters in a traffic network choose routes to take to work. Each commuter's choice affects congestion on the roads in the network and ultimately affects the choices of other commuters. Every commuter wants to save time and/or travel the shortest distance possible. Single commuters probably don't know the goals of other commuters or have little control over the overall traffic. From experience, we know that collective decision trends in these kinds of situations emerge through decisions by individuals at the local level without a central control telling each single commuter what to do. It is not clear, though, what kind of individual decision rules give rise to the group level coordination and if there are better ways than what happens "naturally". In order to answer questions like this, one would like to have a quantitative procedure that can describe and maybe even predict how coordination emerges out of individual decisions. While mechanisms of animal group decision-making have been proposed and validated for various decision-making scenarios, mathematical models and experimental validation for human continuous-time decision-making in multi-alternative choice situations have only started to gain attention recently.

In this dissertation we make contributions towards understanding social coordination of humans in complex decision situations with a focus on choosing among multiple possibilities. Over the next two chapters we develop a model for human social decision-making and shared control in the case when agents with different preferences for goals have to reach a group level decision in continuous-time with feedback of only their mean action. Our objective is to propose an effective model for human social decision-making that can converge to a collective decision even in situations where individuals have little information about the true preferences and incentives of other group members. This is much in the spirit of, and indeed motivated by, the collective animal behavior and model studied in Chapter 2.

As in the model of Chapter 2, we incorporate both social influences and self-interested goals in the model. We show how the model can help us gain insights into the mechanisms and psychology of behaviors. Using the model we show that different collective behaviors corresponding to the decisions favoring different preferences in the group can arise out of different ranges of parameters that represent human individual tendencies, notably the resistance or willingness to forgo a preference in order to coordinate. The fact that we can link parameters to decision outcomes at the collective level allows us to predict what outcome would arise given an interaction between individuals with different tendencies as defined by the parameters. Then in Chapter 4 we use the model to explain real human data in controlled experimental settings suggesting possible behavioral mechanisms. The results in these two chapters also appear in [59].

Before we describe the model, we start with a broader motivation than the aforementioned traffic control example. Consider a group of decision-making agents (humans, or humans and computers) simultaneously deciding the motion of an object in order to perform a coordination task within a given time limit. The object to be controlled can be a single vehicle moving in some terrain, or a representation of the moving center of mass of a group of vehicles, each controlled by a different decision maker. For example, suppose in the latter case that each vehicle is a mobile sensor platform moving in the ocean and the vehicles are to move together as a sensor array for environmental monitoring. Suppose also that each decision maker may hold different information about the environment that cannot be communicated to others during the task. The differences in information may induce conflicting directional preferences for the controlled object's motion. Possible reasons for the restriction of information exchange could be that communication channels between decision makers are not available, have temporarily experienced some system failure, or simply are too costly to be used. To reach an overall desirable group-level decision in the presence of conflicting individual directional preferences requires a dynamic process of coordination among the individuals in the group. Fig. 3.1 illustrates an example of shared decision-making in the application of vehicle teleoperation. Fig. 3.2 illustrates an example where the two operators' judgements about the environment are different, and therefore conflicting individual decisions are made that may cause their combined decision to reach a deadlock.

Deciding collectively among alternatives is also ubiquitous in nature and in human daily life. For example, migratory flocks must decide when to take off, and humans must decide which route to take to work. The decision variable can be a timing, or a route choice, or an opinion. For tasks like these, individuals are affected by other

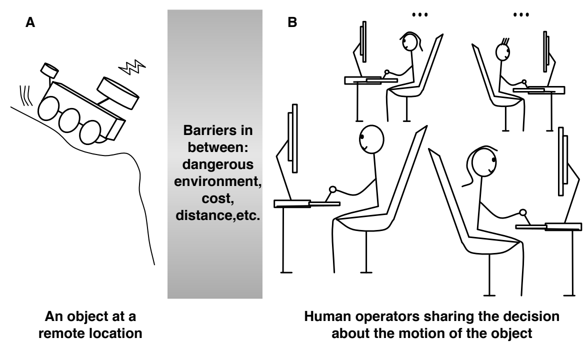

Figure 3.1: Coordinated shared decision-making in vehicle teleoperation. Two or more human and/or computer programs work at non-collocated control stations generating commands via input devices and receiving feedback from displays (see panel B). The remote vehicle, which executes the combination of all input commands is equipped with sensors but has limited autonomy (see panel A). The operators and the vehicle are separated by some barrier (environment, distance, etc.), and information between them is exchanged via some communication channel. The operators at the control station share the decisions over the vehicle motion but cannot communicate with one another i.e., they cannot exchange what they know about the environment or what feedback they get from the vehicle. Operators are only linked through their combined decisions as can be seen from the vehicle's motion.

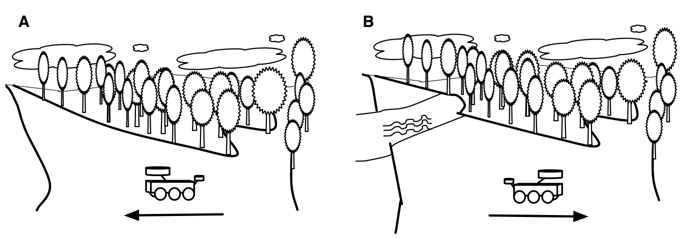

Figure 3.2: Conflict of interest due to different views about the environment. Two operators (a human-human or human-computer dyad) are coordinating and sharing a decision about which route the vehicle should take to avoid running into the forest and possibly colliding with trees. Different information about the environment observed by the operators, combined with good judgement result in the illustrated two conflicting views of the environment and directional preference. A) Both routes are accessible, but the left one is straight and wider. B) The left route is dangerous. Only the right one is accessible.

decision makers, and not just by the external environment. In order to predict and facilitate collective decisions in such social situations, we seek to quantify underlying mechanisms that help explain the coordination process. In particular, when humans interact with robots in human-robot applications, the quantified mechanisms could be used to enable the robots to better anticipate human actions and coordination efficiency between human and robotic systems might improve. On the other hand, quantifying human behaviors can help us further design experiments for investigating more complex behaviors in human interactions. If we can identify different human tendencies as personalities through parameterized modeling, we can then simulate a certain personality with robots and observe and study how human subjects respond.

With understanding human social behavior in complex scenarios such as cooperation and problem solving as a future goal, we focus here on quantifying human decision-making behaviors and hypothesizing testable decision rules for simple alternative choice tasks in social interactive settings where no complex communication is allowed. In particular, we look at situations where a group of individuals have to choose collectively (i.e. through shared control) between two alternatives and do so in fixed time. Each individual has a scalar, real-valued decision state that evolves continuously in time. The decisions that we consider are equilibrium states of a dynamic process that requires the coordination through continuous-time feedback of the joint (mean) decision state.

We adopt a unified approach combining both agent-based modeling and experimental validation to understand collective decision-making behaviors in humans with different preferences. First, we propose an ordinary differential equation model that effectively captures the decision-making processes for each of the individuals in a shared decision-making task. The formalism of nonlinear deterministic coupled ordinary differential equations is simple enough to allow us to clearly distinguish different factors that influence the decisions, yet it can incorporate key features that lead to complex behaviors, such as conflicting individual preferences and dynamic social interactions. Second, the model is suitable for being fitted to experimental data of human behaviors. By interpreting the parameter values of human data fitted to our mathematical model, we develop an understanding of the processes of decision-making from a psychological perspective. This perspective is one that we are unable to derive based on data analysis alone. That is, the model serves a critical purpose.

Decision-making among alternatives by a single person without interactions with others has been extensively studied in various fields, from neuroscience [25, 7], to psychology [32, 17], to engineering [57]. Human decision-making in an interactive setting where the decision outcome is not influenced by just one individual but by the interactions and inputs of many decision makers has garnered more attention of late. Modeling and especially model validation work on human collective decision-making are even more recent, while most previous works have a single focus on experiments or modeling.

From the cognitive sciences, computational models confirmed by empirical observations have been proposed on human perception and action control in individual decision-making [45, 29, 57, 62, 12].

In [57], Reverdy, Srivastava and Leonard presented a formal algorithmic model of single human decision-making behavior when choosing among multiple options with uncertain rewards. They examined heuristics that humans use in exploit-explore tasks (formally as multi-armed bandit problem) from a Bayesian perspective and used it to analyze and interpret empirical data from human decision-making experiment where the goal of the participants was to collect the maximum number of total points when making decisions about navigating a cursor in a 10x10 virtual spatial grid. The reward points associated with the location for which the participants had decided to move the cursor to was defined by a reward landscape embedded in the grid but unknown to the participants. Reverdy, Srivastava and Leonard demonstrated that the observed performance in terms of regret in rewards were captured by their proposed algorithm with model parameters representing prior quality, belief about the reward and decision noise [57]. The findings of [57] provide a formal method for assessing human performances in explore-exploit tasks of single human decision maker in real time.

In an earlier work by Stewart, Cao, Nedic, Tomlin and Leonard [62], a stochastic decision-making model has been studied and fit to human behavioral data from groups of humans performing a two-alternative forced choice task while receiving feedback on the choices of others in the group. They derived analytically the steady-state probability distributions for decision and performance of decision makers as a function of parameters such as the strength and path of social feedback [62]. Their analytical prediction produced the same trends as with empirically validated model of earlier work of Nedic et al. [52] and also from their experimental data. Preceding the work of combining modeling and data fitting of [62], Cao, Stewart and Leonard presented two models on human decision-making in two-alternative forced-choice tasks in [12], and proved convergence to behavior that was strongly supported by psychology experiments (for reference see [12]). The model of [12] provided further simulation study on an application problem but was not fit to real human data.

In a recent study, Bassett et al. [5] built a discrete-time model of decision-making for agents making binary decisions when given information from multiple sources. The goal was to study information transmission and decision dynamics for a group of socially connected individuals. Given external information and social connections, the decision state of an agent in the group was modeled to evolve according to a deterministic averaging rule, consistent with models of opinion formation [33]. When the decision state reached a certain individual-dependend decision threshold, the agent was assumed to make a certain action out of a binary set of available actions. The simulations of [5] highlighted the importance of local interactions among agents in predicting collective decision-making behavior of the group as a whole. The model was not validated on experimental data, but Carlson et al. [15] reported an experiment based on the aforementioned work to identify the factors that influence the decisions about whether or not to evacuate in case of a natural disaster. Consistent with Bassett et al. [5], Carlson et al. [15] assumed that individuals were given many kinds of different external information.

The studies above show how unifying modeling with experimental data can be more helpful than traditional methods of analyzing experimental data only. In the studies of [62] and [12] specifically, the model helps to prove analytical results and make testable predictions.

From a social neuroscience perspective, Bosse et al. [8] have studied collective decision-making that involves adaptation of one's mental state, such as belief, emotions and intentions, in social interactions with others. In particular, the authors presented an agent-based computational model based on neural mechanisms revealed by recent developments in social neuroscience to explain the process that enables individual intentions to converge to an emerging consensus and simultaneously to achieve shared individual beliefs and emotions. They then applied their agent-based computational model to a case study of a real-life panic-driven evacuation incident during a public gathering. They showed that by including the contagion of mental states of the agents, the model resulted in better reproduction of the reported observations of people's evacuation trajectories than without including the mental states. As with [5], the model in [8] assumed that the key mechanisms of updating of decision states involved threshold dynamics, and that the thresholds represent individual tendencies. However, the model proposed contained too many sub-processes and parameters to be analytically tractable.

3.2 Collective decision-making with continuous-time feedback

While experimental work is crucial in observing and understanding human behaviors, there are many unique advantages to studying human behaviors using mathematical models and validation of such models by fitting the model to empirical data. The primary reason is that behavioral data can be hard to understand. For human actions that change in time, it can be difficult to back out the features of such dynamic processes using statistical measures alone. Formulating and fitting dynamical models can help us identify important parameters and mechanisms that are otherwise not possible to single out. If the model can accurately reflect some behavior of the real-world problem of interest, then one can gain an improved understanding of the problem by analyzing the mathematical model. Additionally, one can use the model to predict behavior and to derive testable hypotheses. Further experiments can be used to refine the model.

We propose an agent-based dynamical system model to understand human behaviors in the above-mentioned situation where individuals in a group have to coordinate their decisions only with the feedback of their combined actions and in the presence of conflicting individual preferences. The proposed model is inspired by mechanisms proposed in various prevous studies on single- and multi-agent decision-making of humans and animal groups. In particular, our modeling approach is influenced by empirical observations and computational and analytical models on animal collective motion and multi-agent self-organization [41, 19]. It is related to previous modeling and/or model validation work in the general framework of agent-based collective decision dynamics in the presence of external influences that are potentially conflicting. Several modeling studies have proposed mechanisms that typically comprise the balancing between social interactions and external influences [41, 19, 46, 24, 23, 18, 5, 15].

However our model has two features not present in the current animal motion or human coordination literature. First, we allow the individuals to make a conditional tradeoff between two possibly different preferences. Consider again the vehicle teleoperation example in Fig. 3.2. While the individual has an induced preference (for example, a road that is preferred over the other), when facing two available options, she may ignore her induced preference gradually if the vehicle is already closer to an alternative option.

Second, traditional flocking and opinion formation models have assumed that the interaction dynamics between agents are of homophilious nature, meaning that the closer two agents get, the stronger their influence on each other [44, 33]. We use the contrary assumption on social interaction, namely heterophilious interactions [49]. Heterophilious interactions imply that individuals in a social network experience weaker influence by those who are nearby spatially or holding a similar decision variable (e.g. opinion), and experience stronger influence by those who are far away or holding a different decision variable. Motsch and Tadmor [49] showed through analysis that heterophilious interactions better enhance group cohesion as compared to the traditionally assumed homophilious interactions. We adopt heterophilious interaction dynamics in our model because it is consistent with empirical evidence showing that in a social setting, people tend to copy others' behaviors when there is a larger individual difference, and tend to differ in behavior when there is a smaller individual difference [48].

We consider our model parameters as having two key aspects. One is the computational aspect, which means that we can produce a variety of trajectories by altering the parameters. The other is the psychological aspect, meaning that the parameters can be interpreted as suggestions for explanations of behaviors such as quantifying mood or personality traits. Therefore we can fit the model parameters to the data and gain some insights into the psychology associated with the interactions and behaviors of the individuals.

Throughout the dissertation, we say that a decision has reached *deadlock* for the group if the decision has converged to a state in which every individual in the group insists on a different opinion or two or more intransigent opposing parties have formed. In our setting, deadlock is the worst case since the decision then will not favor anyone's preference and will result in lost time at the very least. If the decision to be made is about which route to take to avoid collision with an obstacle, then deadlock can lead to a real problem such as illustrated in Fig. 3.2.

Now we formally introduce the model. Let N be the size of a group of decision-making individuals interacting socially as they share control over the group mean state. The state of each individual is its real-valued decision variable. Although the state can represent an abstract opinion, we will refer to it as a scalar position in keeping with our concrete example of shared control over the motion of a vehicle or vehicles. The position of individual i, for $i = 1, ..., N$, at time t is denoted by $x_i(t) \in \mathbb{R}$. We define the mean position of all individuals at time t as $\bar{x}(t)$:

$$\bar{x}(t) = \frac{1}{N} \sum_{i=1}^{N} x_i(t). \tag{3.1}$$

In general, $x_i(t)$ is a decision variable of the player i that can represent anything to be decided on. For this reason, we consider the decision to be evolving in one dimension, even though in real application problem a decision can evolve in higher dimension (such as in our example of motion control, where motion is in the plane). When the decision is about motion in higher dimensions, we assume that the decision of motion in all but one dimension stay in consensus across all individuals and therefore are not part of the decision process. In the motion control example, the decision is in the horizontal direction.

We consider the case in which there are two alternative options at -1 and 1, such that if $\bar{x}$ converges in time to -1 then the group has decided for one option and if it converges to 1 then it has decided for the other alternative. If $\bar{x}$ converges to 0, then it is in deadlock. We initialize all agents at $x_i(0) = 0$ so that the mean is not biased towards either alternative from the beginning.

When a decision maker i is the only decision maker in the group, two possible environmental factors that can contribute to the decision-making process include the decision maker i's preference, denoted by $p_i \in \{-1, 1\}$, and the proximity of the closer option, denoted by $c_i \in \{-1, 1\}$. For example, for the decision maker in panel A of Fig. 3.2, p_i is the reference path that is straight and wider, while c_i is the reference path that is closer.

We quantify the relative weighting of the two options p_i and c_i by a sigmoidal preference weight function, denoted by $\alpha_i \in [0, 1]$. If $\bar{x}$ is far from p_i, where distance is determined by a preference threshold parameter $\delta_i \in \mathbb{R}_+$, namely, if $|p_i - \bar{x}| > \delta_i$, then $\alpha_i > 0.5$, and c_i is the dominating stimulus. By stimulus, we mean that it affects the player as a self-interested goal. If however, $\bar{x}$ is close to p_i, namely, if $|p_i - \bar{x}| < \delta_i$, $\alpha_i < 0.5$ and the preference p_i is the dominating stimulus.

Now assume that instead of just one, there are two or more decision-making individuals, each with a continuous-time feedback measurement of $\bar{x}$. We model a second influence in decision-making based on social interaction. We assume that individuals interact in a *heterophilious* fashion, implying an individual tends to be more influenced by the mean decision variable $\bar{x}$ when it is far away from its own and less so when it is closer. The idea here is that an individual will take greatest notice of the others in a shared decision-making setting when the decision of the others diverges from her own.

For each individual i, the strength of the social interaction, relative to the strength of the stimulus, is determined by another sigmoidal weight function, $\beta_i \in [0, 1]$. The value of β_i depends on how far x_i is from $\bar{x}$, where distance is compared to a social threshold parameter $\theta_i \in \mathbb{R}_+$. The farther x_i is from $\bar{x}$, namely, if $|x_i - \bar{x}| > \theta_i$, then $\beta_i > 0.5$, resulting in a greater tendency to follow the mean.

To account for situations where the time when an individual starts her decision-making differs from others in the group, we introduce the starting time of an individual i, t_i. The value of t_i can be defined in absolute time, or it can be measured against a common time marker (defined as time at 0). A time marker, for instance, can be the time when a stimulus is a certain distance away from the group. Thus, individuals in the group may start their own decision-making at different times relative to one another. Plausible reasons for different starting times include differing reaction times, deliberation times or possible distractions during the task. There are obvious benefits to starting early, such as being able to signal a preference or to dominate the group for some time before other individuals start to respond. In general, the bigger the group gets, the smaller the influence an individual's decision can have on the group mean. We allow an extra time constant parameter τ to account for the overall speed of decision-making for a given decision. Any decision process, whether it is about deciding which side to go to when meeting in the hallway or deciding when to take off for migration, has a temporal scale and having a time constant can help normalize the remaining parameters. In our model, we consider the case when every individual in the group has the same τ.

The model is written for player i as the first order differential equation:

$$\tau \dot{x}_i = H(t, t_i)[\alpha_i(c_i - \bar{x}) + (1 - \alpha_i)(p_i - \bar{x}) + \beta_i(\bar{x} - x_i)]. \qquad (3.2)$$

$H(t, t_i)$ is a box function indicating the duration of the decision process. The value of H is 1 when $t_i \leq t \leq t_f$, and 0 elsewhere. The final time t_f is the same for all individuals. The preference weight function α_i and social interaction weight function

β_i are defined as

$$\alpha_i = \frac{1}{1 + e^{-B_i(|p_i - \bar{x}| - \delta_i)}}, \tag{3.3}$$

$$\beta_i = \frac{1}{1 + e^{-R_i(|\bar{x} - x_i| - \theta_i)}}. \tag{3.4}$$

Parameters B_i and R_i control the steepness of these sigmoidal weight functions. The greater B_i and R_i, the closer the weight functions α_i and β_i approximate step functions, resulting in a tendency to have "abrupt" changes in the weights as states $x_i(t)$ and $\bar{x}(t)$ evolve.

We study the case in which there are two decision-makers. In particular, we consider the case when the two individuals have opposite preferences. We will use the term "players" to refer to the two decision makers. The two-person case is also representative of a scenario where two parties have formed within a large group and the members of the two parties share the same key features.

In Fig. 3.3 a situation is presented of two individuals jointly controlling the horizontal position of an object represented as a solid black ball moving on a screen. The ball moves at a steady rate in the vertical direction so the vertical direction can be identified with time. The horizontal position of the ball at time t is given by $\bar{x}(t)$. The decision makers jointly control the horizontal position $\bar{x}(t)$ to track one or the other of the two vertical bars centered at -1 or 1 (shown in grey). We refer to the vertical bars as reference paths. Each player can see the same mean position $\bar{x}$ but each may see different kinds of tracks.

In Fig. 3.3 the upper plot presents the trajectory and visual feedback of player i who has *only one* reference path to track; this reference path necessarily is the preference p_i. The lower plot presents the visual feedback of player j who sees a reference path at both -1 and 1. However, one reference path (at 1) is thicker than

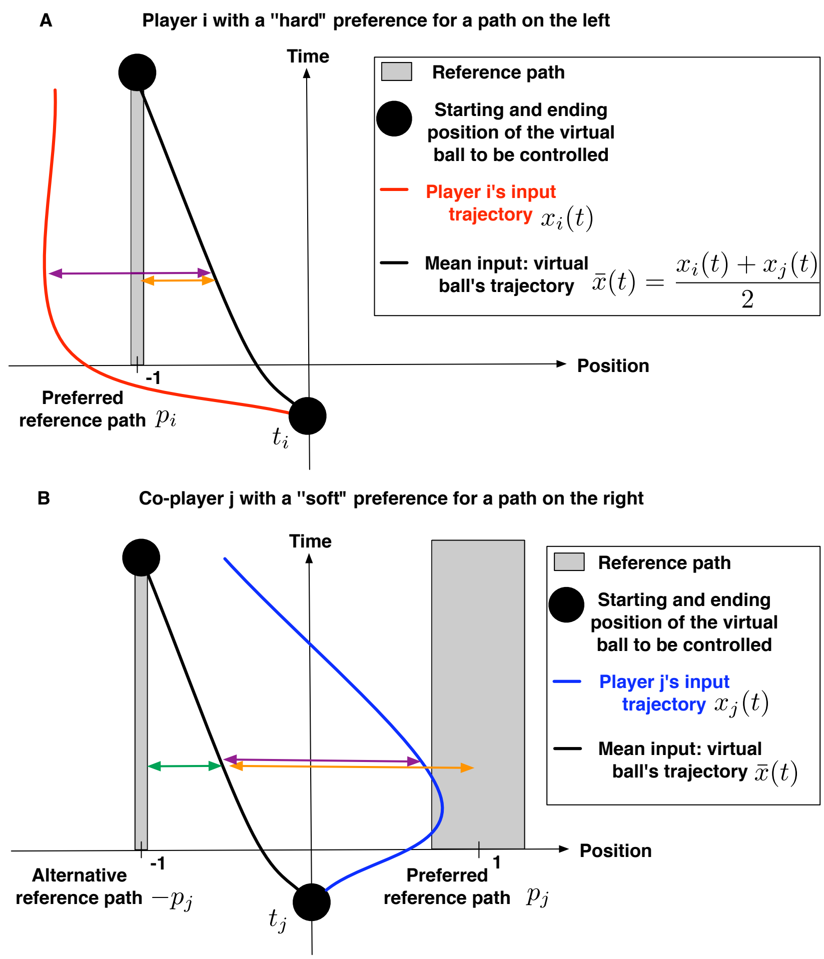

Figure 3.3: Key model components and feedback used by two players i and j. The horizontal axis is position which is the decision state. The vertical axis is time. Motion and decision dynamics start at $x_i = 0$, and $t = t_i$ for player i and $x_j = 0$ and $t = t_j$ for player j.

the other. Because the thicker path is easier to track it is representative of the preferred alternative for player j. Time is plotted on the vertical axis pointing from bottom to top, so that the vertical motion is upward. The reasons for the time axis to be plotted vertically is mainly for being consistent with the experimental set up and presentation of data for Chapter 4. We use the terms “left” and “right” to describe directionality in the decision-making dimension.

Fig. 3.3 illustrates a decision-making dynamic. The decision-making trajectory of player i, $x_i(t)$ for $t \in [t_i, t_f]$ is shown in red and of player j, $x_j(t)$ for $t \in [t_i, t_f]$ is shown in blue. The average trajectory $\bar{x}(t)$ is shown in black. Initially, each player controls the ball by moving her respective position towards her own preference as shown in the upper plot in red and in the lower plot in blue. Upon observing that the mean does not follow her intended action, player j can infer that player i may have a conflicting preference. Player j then "compromises" by giving up her preference and moving to follow the reference path that is already closer to the mean.

The feedback quantities that each player uses in her decision-making are indicated by colored arrows in Fig. 3.3. An orange arrow represents the distance between the mean $\bar{x}$ and the preference at time t. Each player compares this distance with her preference threshold δ to decide whether this preference influence is still important. When the distance exceeds the preference threshold, e.g. $|\bar{x} - p_i| > \delta_i$ for player i, the preference weight α_i will be greater than 0.5 and close to 1, depending on the steepness of the weighting function. From Eq. 3.2 we can see that when $\alpha_i > 0.5$ the influence from the preference will be less important than the influence from the option c_i. The option c_i is the reference path that is closer to $\bar{x}$ (ball). At time t, this is determined by looking at the green arrow, which is the distance between the mean and the alternative reference path. If the distance indicated by the green arrow is less than the orange arrow, the alternative reference path is the closer path.

We note that the closer reference path can be the same as the preference. Especially for player i in the upper plot who sees *only one* signal, there is no alternative reference path, which is equivalent to assuming $c_i = p_i$ for all time. The resulting dynamics for this player are equivalent to having $\alpha_i = 0$.

A purple arrow represents the distance at time t between the mean $\bar{x}$ and the individual's own position x_i. Each player compares this distance with her social threshold θ to decide whether the mean decision (i.e. the decision of the other player) is important relative to her own preference. If the distance exceeds the social threshold, e.g. $|\bar{x} - x_i| > \theta_i$ for player i, the social weight β_i will be greater than 0.5. From Eq. 3.2

we see that when $\beta_i > 0.5$ the influence from the social term, which implies reducing the difference between one's own position and that of the mean, will become comparatively important. One simplification of the model is that there is no additional gain in front of the social term, implying that given limited range of motion, the social interaction influence cannot be significantly greater than the preference influence.

3.3 Two-person shared decision-making with conflicting preferences.

We specialize the model of Eq. 3.2 to the setup illustrated in Fig. 3.3. Suppose that one of the two players has two available options but has a "soft" preference for one of those options (like player j in Fig. 3.3). We refer to this player as "Player S" or the "S Player". Suppose that the other player has *only one* option, which necessarily is preferred. We refer to this player, who has a "hard" preference, as "Player H" or the "H Player" as illustrated in Fig. 3.3.

We also assume that the soft and hard preferences are alternative options (on opposite sides of the origin) resulting in a conflict of preference between the two players. The locations of the preferences at 1 and -1 are generalizable to any locations symmetric about the origin. For convenience, the model state is called x_H for Player H, and x_S for Player S. The associated parameters for each of the players with either soft or hard preference will be labeled with the same subscripts. We will investigate closely this case and we will refer to it as the "Hard-Soft Conflict" decision scenario type. It will be seen later in Chapter 4 that human behaviors from empirical observations that the most variability in decision outcomes and unpredictable behaviors can be seen in this conflict scenario. We will also see that the "Hard-Soft Conflict" model can capture all possible decision outcomes in the experiment and the corresponding transient behaviors with fewer parameters than the full model of Eq. 3.2. We refer to the full model with opposing preferences as the "Soft-Soft Conflict" model.

In the case of Hard-Soft Conflict, because Player H has only one option, the model equations can be rewritten as

$$\begin{aligned} \tau\dot{x}_H &= H(t,t_H)[\alpha_H(c_H-\bar{x})+(1-\alpha_H)(p_H-\bar{x})+\beta_H(\bar{x}-x_H)] \\ \tau\dot{x}_S &= H(t,t_S)[\alpha_S(c_S-\bar{x})+(1-\alpha_S)(p_S-\bar{x})+\beta_S(\bar{x}-x_S)], \end{aligned} \tag{3.5}$$

where we make the following definitions:

$$\begin{aligned} \bar{x} &= \frac{x_H+x_S}{2} \\ \alpha_H &= \frac{1}{1+e^{-B_H(|p_H-\bar{x}|-\delta_H)}} \\ \alpha_S &= \frac{1}{1+e^{-B_S(|p_S-\bar{x}|-\delta_S)}} \\ \beta_H &= \frac{1}{1+e^{-R_H(|\bar{x}-x_H|-\theta_H)}} \\ \beta_S &= \frac{1}{1+e^{-R_S(|\bar{x}-x_S|-\theta_S)}}. \end{aligned} \tag{3.6}$$

For simplicity, we assume $p_H = 1$ and $p_S = -1$. Initial positions are near the origin, so that both players are initially equally far away from their preference. We also assume that for each player, regardless of the preference type, the default alternative path c_i is the instantaneous closer path, denoted by c. The instantaneous closer path c is a state-dependent function:

$$c = \begin{cases} 1 & \text{if } \bar{x} > 0 \\ 0 & \text{if } \bar{x} = 0 \\ -1 & \text{if } \bar{x} < 0 \end{cases}$$

The alternative path c_i, in general, can be any path that the player considers, including a non-existent path (possibly opposite to the preferred path) that the player cannot see but may assume it exists for the other player.

When the player has a soft preference, $c_S = c$. When the player has a hard preference, as we illustrated before, $c_H = p_H$. The resulting dynamics for her is the same as when $\alpha_H = 0$ is assumed, meaning that Player H cannot follow any alternative other than her preference.

We do, however, allow for the case when Player H does consider an alternative $c_H = -p_H$ for example. In this case the model for Player H uses $\alpha_H \neq 0$, and thus a model like Player S. Such a case is possible if Player H chooses to track a reference path that does not appear to be available for herself but which she surmises is the preference of the other player. For the remainder of the chapter we will use the assignment $\alpha_H = 0$ versus $\alpha_H \neq 0$ to distinguish the cases when Player H plays *as if* only the available reference path is considered (corresponding to $\alpha_H = 0$), versus *as if* the inferred preference of the other player is also considered (corresponding to $\alpha_H \neq 0$).

3.4 Bifurcation in parameters δ_S and θ_S

In this section we compute equilibria and bifurcations of the model of Eqs. 3.5 to investigate how the decision outcomes depend on the decision threshold parameters. In particular, we look at the decision outcomes as the steady-state solutions of the system Eqs. 3.5 under parameter variations. We let the social threshold parameters for the two players, θ_S, and θ_H, and the preference threshold parameter for Player S, δ_S, be bifurcation parameters, and we compute the bifurcation plots. For the methods for generating the bifurcation plots, see Appendix B.

In Fig. 3.4A, a two-parameter bifurcation plot is shown in the plane of θ_S and δ_S, both of which are associated with Player S. The plot shows the number of steady-state solutions of the system for different values of the parameters θ_S and δ_S in the range that is plotted. Fixed parameter values used are $p_H = 1, p_S = -1$, $R_H = 20$, $R_S = 20$, $B_S = 20$, and $\theta_H = 1.2$. We substitute the discontinuous description of c with a continuous but steep sigmoid function that saturates at -1 and 1:

$$c = \frac{2}{1 + e^{-100\bar{x}}} - 1. \tag{3.7}$$

From Fig. 3.4A, it can be seen that for high values of the preference threshold of Player S ($\delta_S > 2$), i.e., the threshold to giving up on the preference is higher, there is only one (stable) solution for all values of θ_S. For intermediate to low values, $\delta_S < 2$, depending on the values of θ_S, the system can have one (stable) or three steady-state solutions, two of which are stable, and are separated by an unstable solution. When the system exhibits two stable solution for a given set of parameters, it is called bistability. In the region of the parameter space where bistability occurs, the decision outcome can be one of the two stable solutions. When the system has two stable equilibria, it is sensitive to initial conditions and noise. We suggest that in this case the initial condition plays a deciding role in the decision outcome. In regions of the parameter space where there is only one stable equilibrium, the decision outcome is always the same regardless of the initial conditions.

Fig. 3.4B shows the one-parameter bifurcation plot with θ_S, the social threshold of Player S as the bifurcation parameter. The steady-state solutions of the mean decision variable $\bar{x}$, interpreted as the equilibrium decisions of the system, are shown as a function of the bifurcation parameter θ_S and for four different values of the preference threshold δ_S of Player S.

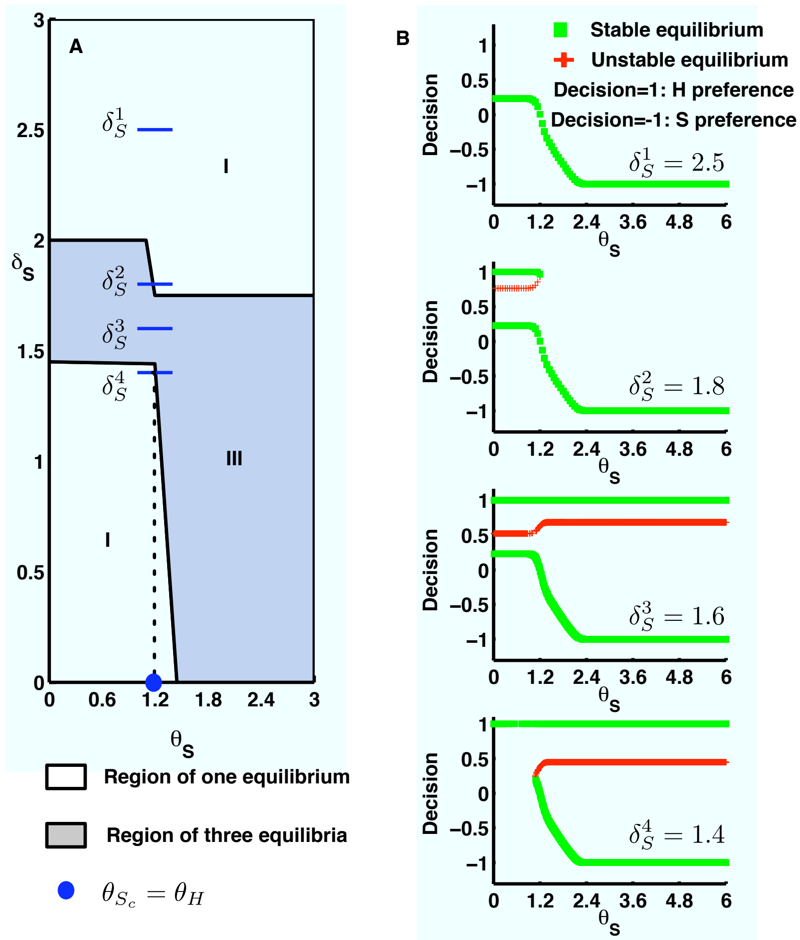

Figure 3.4: Bifurcation plots of the Hard-Soft Conflict model. The numerical computation was based on the Hard-Soft Conflict model ($\alpha_H = 0$), with parameters $R_H = 20$, $R_S = 20$, $B_S = 20$, and $\theta_H = 1.2$. The hard preference is located at 1, and the soft preference is located at -1. A). Two parameter bifurcation plot in the plane of δ_S and θ_S. There are a total of three different regions, as labeled in the figure. Two of the regions have one equilibrium, and are separated by a region with three equilibria. In the two single-equilibrium regions, the equilibrium is a nodal or spiral sink. In the three equilibria region, there are two sinks separated by a saddle point. Lines represent bifurcation points separating regions where there are different numbers of equilibria. B). The bifurcation as θ_S changes for different sections of δ_S values (labeled as δ_S^i and with a blue line segment in A indicating the regions it can cross).

For high values of δ_S ($\delta_S = 2.5$), as shown in the top plot of Fig. 3.4B, the system will stabilize at one decision for all values of θ_S. In particular, when $\theta_S < \theta_H$, the decision is around 0, which means deadlock. When $\theta_S > \theta_H$, i.e., when the threshold for dominance of the social signal is greater for Player S than for Player H, the decision gradually moves towards the soft preference as θ_S increases.

For intermediate values of δ_S, as shown in the three other plots of Fig. 3.4B, interesting bistability of decisions occur. In the second plot of Fig. 3.4B, when $\delta_S = 1.8$, for $\theta_S < \theta_H$, there are three steady-state solutions. They are the stable decision for the hard preference, the stable decision for some decision around 0 (almost deadlock), and the unstable decision for somewhere near the hard preference. As θ_S increases to $\theta_S > \theta_H$, i.e., Player S becomes less influenced by the social term, the two decisions near the H preference disappear, and just one solution remains stable which tends towards the S preference as θ_S increases.

In the third plot of Fig. 3.4B, when $\delta_S = 1.6$, for all values of θ_S, there are always three steady-state solutions. The hard preference decision is always a stable solution, and so is the other stable solution that approaches the soft preference as θ_S grows.

Finally, in the fourth plot of Fig. 3.4B, when δ_S takes a relatively low value of 1.4, for $\theta_S < \theta_H$, there is just one stable solution for the hard preference. For $\theta_S > \theta_H$, again both the hard preference decision, and the one that approaches the soft preference as θ_S grows, are stable.

As can be seen in the bifurcation plots, the critical bifurcation point for θ_S is $\theta_{S_c} = 1.2$, which is equal to the fixed value of θ_H. In general, for all values of δ_S, the soft preference decision is only stable when $\theta_S > \theta_H$. This means that regardless of how strongly Player S considers her preference (i.e. whether she gives up her preference easily or not), her preference can only be reached when she is relatively less "willing" to follow the mean (i.e., to be less "social"). On the other hand, as δ_S increases, the range of θ_S for which the hard preference decision is stable diminishes. This means that as Player S becomes more intransigent about her preference, Player H has to become relatively less social and tolerate larger differences between the mean and her own position in order to "win" the decision.

Fig. 3.5 shows the influence of θ_H on the bifurcation plots in θ_S. As θ_H increases, the range of values of θ_S for which two stable solutions occur diminish for all values of δ_S, while the range for which the hard preference decision is stable increases. This means that as Player H becomes less sensitive to the social signal, the more likely it is that her preference will be the solution. Fig. 3.6 shows the influence of the parameters R_H, R_S and B_S on the bifurcation of equilibrium. As seen, these parameters do not change the qualitative nature of the system, but they do change the sensitivity of the equilibria to the bifurcation parameter. Nullclines of the systems are plotted and compared for different values of the parameters in Fig. B.1 (see Appendix B).

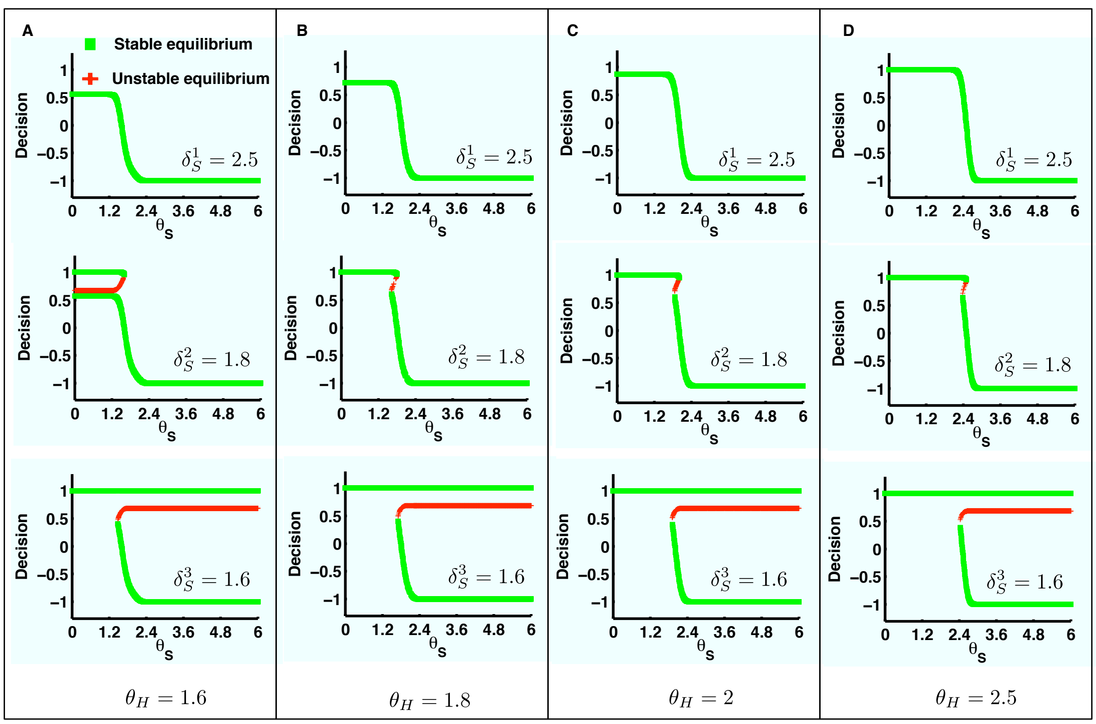

Figure 3.5: Bifurcation in parameter θ_S, for various values of θ_H and δ_S. As θ_H increases, the bifurcation point for θ_S also increases, and the ranges of values of θ_S for which bistability exists shrinks. Furthermore, for higher values of θ_H, the equilibrium values for $\theta_S < \theta_H$ tend to approach $p_H = 1$. As δ_S increases, ranges of θ_S for which bistability exists also decreases. When δ_S are θ_H are both of higher values, then there is always one equilibrium, and it is 1 for $\theta_S < \theta_H$ and -1 for $\theta_S > \theta_H$. When δ_S is of intermediate to lower value (< 1.8), for all θ_H and θ_S, the equilibrium at 1 is always stable, and the equilibrium at -1 can only be stable when $\theta_S > \theta_H$.

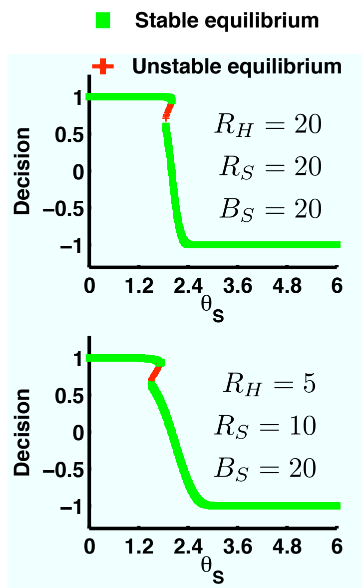

$\theta_H = 2$
$\delta_S = 1.8$

Figure 3.6: Influence of the steepness parameters R and B. Bifurcation in parameter θ_S is shown for $\theta_H = 2$ and $\delta_S = 1.8$ and for two different sets of values for the steepness parameters R_H, R_S and B_S. When the steepness parameters are greater, the bifurcation points change faster as θ_S changes, making the bifurcation curves also steeper.

Based on the bifurcations we can predict, for our model dynamics, which decision outcome is made for which values of the preference and social thresholds of the players. The interplay between the relative social thresholds and preference thresholds of the players is critical in determining the decision outcomes. For a preference to win, i.e., to become the steady state solution for the group mean decision variable, the player with that preference needs to have both a sufficiently high preference threshold δ and a sufficiently high social threshold θ relative to the other player. Having a higher threshold for just one factor does not guarantee winning a decision. In some cases, both the hard and soft preferences are stable solutions, and which preference will win depends then on the initial condition of the mean. A slight change in initial condition can result in different decision outcomes. For a decision scenario where the mean always starts around 0, this means that the starting times of the individuals will play an important role in determining the decisions to be made. The bifurcation plots also suggest that for the same initial conditions, a slight change in relative social thresholds can result in a big difference in the decision outcome.

The model analysis suggests that Player H needs to tolerate a greater deviation from the mean as compared to Player S (i.e. being less "social" than the other) in order to win a decision when Player S does not "compromise" on her preference. If, however, Player H maintains a "close" distance to the mean and is more "social" than Player S, she can win if Player S is flexible (e.g. $\delta_S < 1.4$). Otherwise when Player S is both relatively less "social" $\theta_S > \theta_H$, and relatively "intransigent" $\delta_S > 2$, then it is less likely for Player H to win the decision.

We note that the bifurcation plots imply behaviors when the dynamics have reached equilibrium. To look at the transient, we need to study the individual behaviors in time. In the next chapter, we will study how real humans play the above mentioned tracking task by examining their tracking trajectories and transient behaviors using the model and the parameters.

Chapter 4

Human behavior in experimental shared tracking task

In this chapter, we examine human behaviors from a shared tracking experiment by Groten and Feth et.al. [26] using the parameterized model developed in the previous chapter. Understanding the behavioral data using mathematical modeling is a novel approach that provides insights on transient and process characteristics, which are otherwise not possible through statistical analysis. Our goal is to show that the proposed model from Chapter 3 can reproduce a wide range of human behaviors surprisingly well, suggesting that the model may have captured the mechanisms behind some of the behaviors observed in the experiment. It also provides a predictive capability that can be used to design new experiments to test hypotheses and refine the model.

Before we begin it is important to note that Groten and Feth et.al. [26] are the original experiment designers who have run experiments and recorded the original data. We acquired the data set from one of their experiments in which participants used visual feedback. The work reported in this chapter is based on the Groten and Feth et.al. data set and is an outcome of collaboration among all authors in [59].

4.1 A two-person shared tracking experiment

In this experiment, pairs of human participants performed a tracking task that required shared decision-making and execution. Players were given limited feedback and sometimes different signals inducing conflicting individual preferences. The data set was originally recorded as part of the experiment described in [26], but the data itself was not analyzed for what is reported in the present study.

In Fig. 4.1A, the experimental setup is shown. A pair of participants sat in front of two computer screens separated by a wall, and they each used a hand knob to jointly control a cursor (displayed as a small red ball on the screen, visible to both players) to track a reference path. The position of the cursor in the vertical direction was automatically set at a constant rate. The position of the cursor in the horizontal direction was the scaled algebraic mean of each of the two player's hand knob position and was commonly visible to both players. No verbal communication was allowed between the two players, and the only feedback given to the players was the visual image of the position of the cursor and the reference path. Players could not see the position of the other. The reference path, displayed as a white line, changed in time as it moved down the screen with a constant velocity of 15mm/s. At regular time intervals the path split in a way that looked like the shape of the letter "T" into two paths that then later merged again into a single path. Each "T" meant that a shared decision for one of the two alternative paths was required for tracking. (At the instant shown in Fig. 4.1A, the red dot is at a position slightly above the split of the paths"T").

To influence the horizontal motion of the cursor, each participant had to slide a hand knob on a 1-D horizontal interface: the ball's horizontal position was rendered as the algebraic mean of the two players' hand knob positions. Both players' trajectories and the mean trajectories were recorded, and an example of the data set is shown in Fig. 4.1B.

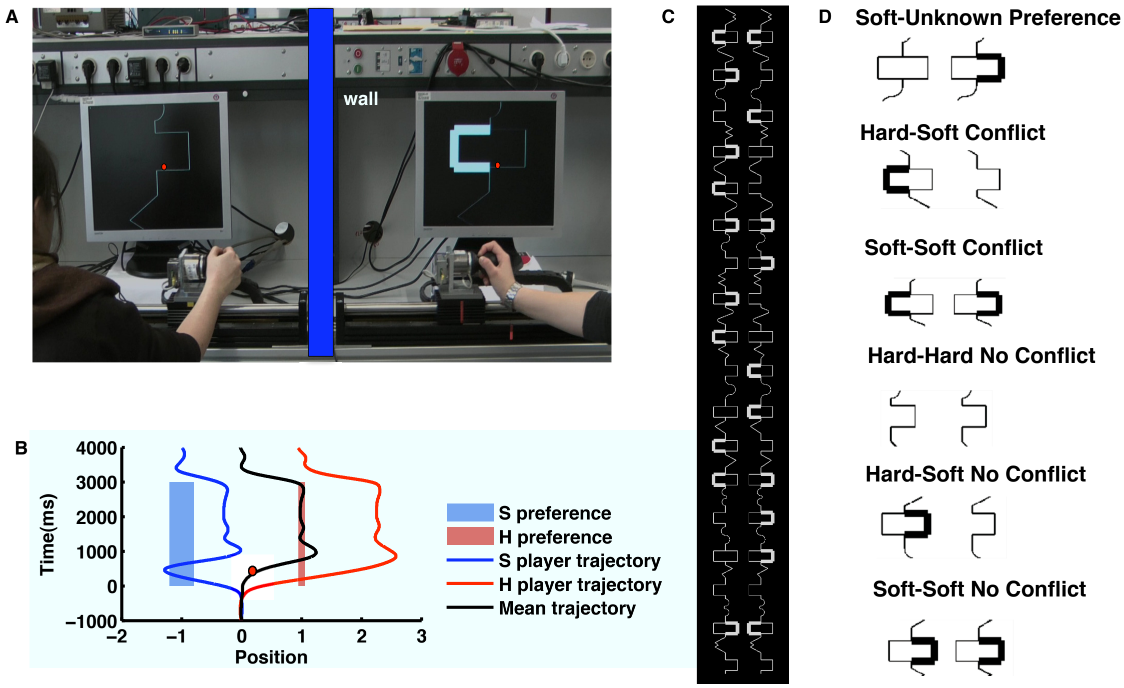

Figure 4.1: Experimental setup, data and decision scenario types. A) A video snapshot of two players performing the shared tracking task. Two players jointly control a cursor on the screen to track a given reference path. The players are separated by a wall and wear headphones with white noise playing. No direct communication is allowed. The only feedback the player receives that pertains to the other player is the continuous-time visual image of the position of the cursor. The decision scenario shown corresponds to a conflict between the players' preferred paths: one player has a "hard" preference for going right, and the other a "soft" preference for going left. B) Data collected for the case shown in A). The positions in time of the players, as well as the mean were collected. Time at 0 ms is defined as the instant when the "T" in the reference path aligns with the vertical position of the cursor (center of the screen). The duration of the decision is 3 s, i.e.; it is 3 s from the time the cursor aligns with the "T" to the time the cursor aligns with the re-joining of the reference paths. Before and after the decision, a phase for calibration occurs where both players follow the same single reference path. C) A complete trial of the experiment consists of 18 non-repeated decision scenarios occurring in random order. D) There are six types of decision scenarios. Three of them induce conflicting preference in the players. We say a player holds a "hard" preference when the player only sees one reference path (on the left or right), and holds a soft preference when there are two paths and one is thicker than the other. A player is said to hold an unknown preference, when there are two reference paths with equal width. When the two players' preferences are for opposite sides, there is a conflict.

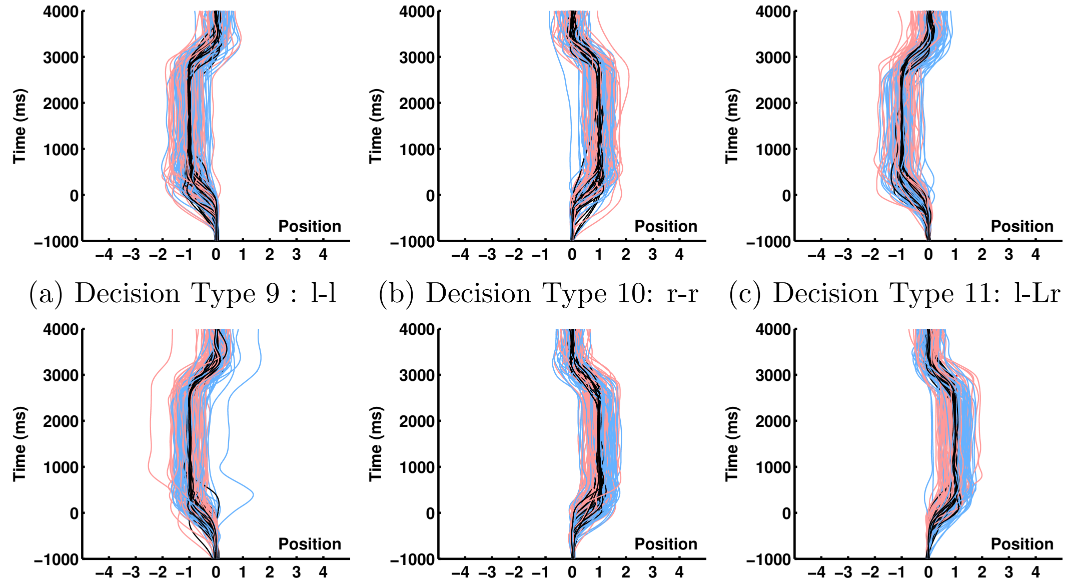

(a) Decision Type 9 : l-l (b) Decision Type 10: r-r (c) Decision Type 11: l-Lr

(d) Decision Type 12: Lr-l (e) Decision Type 13: r-lR (f) Decision Type 14: lR-r

Figure 4.2: Trajectories of players in decision scenario types Hard-Hard No Conflict and Hard-Soft No Conflict. Total number of participant pairs is 61 in each case. In the Hard-Hard No Conflict decision scenario types shown in panels (a) and (b), trajectories of the "first" Player H are in red and those of the "second" Player H are in blue. In the Hard-Soft No Conflict decision scenario types shown in panels (c) to (f), trajectories of Player H are in red and trajectories of Player S are in blue. The mean trajectories are in black.

Throughout a trial in the experiment, players saw, in random order, non-repeated decision scenarios (starting at the "T" s), such as the one shown in the snapshot of Fig. 4.1A. A complete trial consisting of 18 such decisions is shown in Fig. 4.1C. Each decision scenario was separated by a non-decision path, which was the same for both players, as a calibration procedure. In some decision scenarios, a player could only see one of the two alternative reference paths, inducing what we call a "hard" preference for that single reference path. In other decision scenarios, a player could see both alternatives, where one was a thick path and one a thin path. In this decision scenario, since it was easier to track the thicker path, the player was assumed to hold a soft preference for the thicker path. In the remaining decision scenarios, a player could see both alternative paths, which were equally thin, and is therefore said to have no induced preference, and therefore an unknown preference.

There were six general decision scenario types, as shown in Fig. 4.1D, which were pairwise combinations of hard, soft and unknown preferences for each of the two players. A conflict occurred when the preferences of the two players were for opposite sides. If the players had conflicting preferences, and both insisted on tracking their preferred directions, the decision outcome would end up in deadlock, with the ball moving along neither reference path, causing loss of time and opportunity for either player to achieve their preferred goal. Among the six decision scenario types, three were scenario types without conflict in preferences, for which the decision outcomes were straightforward, and cohered with the players' shared preferences. In those cases, the shared decision was simply to coordinate speeds. However, there were also three conflict decision scenario types, for which different decision-making behaviors and outcomes were observed, making it compelling to study those processes. In particular, the Hard-Soft Conflict decision scenario is the one that incorporates all possible human behaviors as indicated in the trajectories of this experimental data set in Figs. 4.2-4.4.

In Figs. 4.2-4.4 trajectories for all decision scenario types and each of the players are plotted by decision scenarios. The decision scenarios are called 1 to 18 and the letters l, L, r, R are used to denote the type of reference path shown to the players. l and L each denote a path shown to the left and r and R each denote a path shown to the right. A lower case letter indicates a thin path, and an upper case letter indicates a thick path. The paths are located at 1 (i.e. right) and -1 (i.e. left). If a player is shown just one reference path then just one letter will be used; otherwise two letters will be used to denote the thickness. So for example, two players that each just see a thin reference path to the left will be denoted "l-l". If "player 1" instead sees a thick path to the left and a thin path to the right, this will be denoted "Lr-l" etc. A player with one letter has a hard preference and with two letters, one upper case

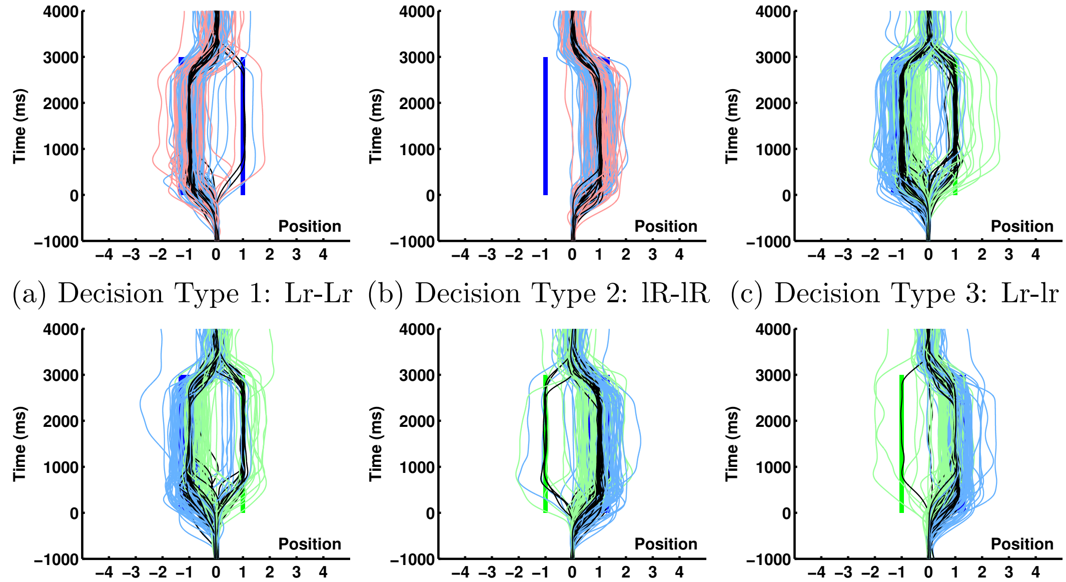

(a) Decision Type 1: Lr-Lr (b) Decision Type 2: lR-lR (c) Decision Type 3: Lr-lr

(d) Decision Type 4: lr-Lr (e) Decision Type 5: lR-lr (f) Decision Type 6: lr-lR

Figure 4.3: Trajectories of players in decision scenario types Soft-Soft No Conflict and Soft-Unknown. Total number of participant pairs is 61 in each case. In the Soft-Soft No Conflict decision scenario types, shown in panels (a) and (b), trajectories of players with the left preference are in red and trajectories of players with right preference are in blue. In the Soft-Unknown decision scenario types shown in panels (c) to (f), trajectories of players with unknown preference are in green and trajectories of players with a soft preference are in blue. The mean trajectories are in black. Location of preferences of players with soft preference in Soft-Soft No Conflict types are shown as blue panels at 1 and -1. Location of the opposite path to the preferences of Player S in the Soft-Unknown types are shown in green.

and one lower case, has a soft preference. A player with two lower case letters has an unknown preference.

It can be seen in Figs. 4.2-4.4 that the individual behaviors (as reflected in trajectories) are most unpredictable in the conflict decision scenario types. Notably, the variety of behaviors that occurred in other decision scenario types all appear in the case of the Hard-Soft Conflict decision scenario types.

In this experiment, there were a total of 58 participants. All participants were university personnels and students at the Technical University of Munich, in Munich, Germany. Out of all participants, 32 played three trials (each trial consisting of 18 decisions) with different partners each time, and 13 participants played only one

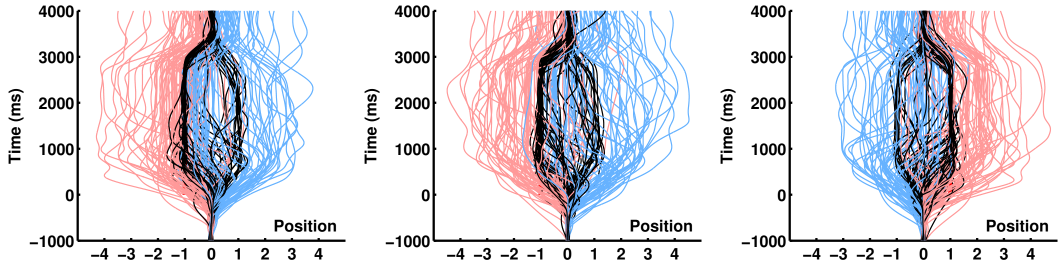

(a) Decision Type 15: l-lR (b) Decision Type 16: lR-l (c) Decision Type 17: r-Lr

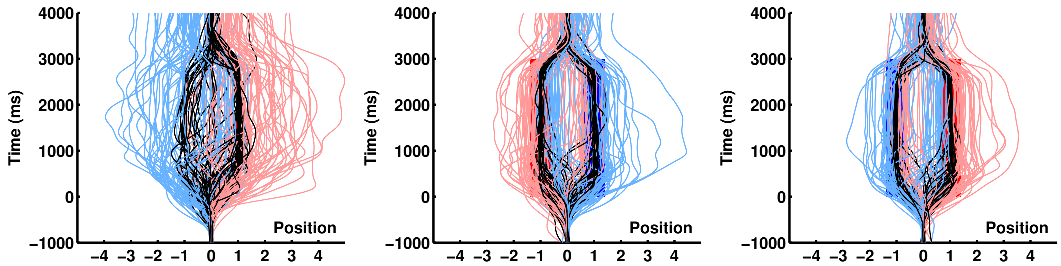

(d) Decision Type 18: Lr-r (e) Decision Type 7: Lr-lR (f) Decision Type 8: lR-Lr

Figure 4.4: Trajectories of players in decision scenario types Soft-Soft Conflict and Hard-Soft Conflict. Total number of participant pairs is 61 in each case. For Hard-Soft Conflict decision scenario types, shown in panels (a) to (d), trajectories of Player H are in red and trajectories of Player S are in blue. Location of preferences of Player S are shown as a blue stripe. Location of preferences of Player H are shown as red stripe. The mean trajectories are in black. For Soft-Soft Conflict decision scenario types, shown in panels (e) and (f), trajectories of the "first" Player S are in red and trajectories of the "second" Player S in blue. Location of preferences of the "first" Player S are shown as a red stripe and that of the "second" Player S are shown as a blue stripe. The mean trajectories are in black.

trial, with a partner who also played only one trial. The mean of the ages of all participants was 25.78, and the standard deviation was 4.87. All participants were right-handed and were incentivized to follow the track as closely as possible. Details of the reward structure and how success was measured quantitatively are presented in [26]. Participants were separated by a wall. In addition, players wore headphones in which white noise was played, so that neither direct communications, nor the noise of moving handknobs could be sensed. Players were not shown the entire track signal before the experiment. However, all participants had gone through a test run before the actual trial, where they could view both screens, and thus became aware of the different types of decision scenarios. They were also informed about the randomness of the order of decision scenarios, and that the situation combinations were not repeated. They knew that there would always be a solution, i.e., that the two players would each see at least one common path at a “T”.

The sliding motion interface was equipped with a force sensor (burster load cell 8542-E), a hand knob and a linear actuator (Thrusttube). The control of the interface modeled a virtual object with intertia only. The cursor position was defined as the mean of the two indvidual device positions. The control of the cursor motion was implemented in MATLAB/Simulink and executed on the Linux Real Time Application Interface RTAI. The graphical representation of the path was run on a separate computer and communication between the computers was realized by a UDP connection in a local area network. For further details, see Groten and Feth et.al. [26].

4.2 Model-free statistics of experimental data

As a first step to understanding the experimental observations, we collected statistics on the decision outcomes and starting order (i.e., who started first) for the three conflict cases.

For a given trial, if the mean trajectory entered a certain neighborhood of one of the two alternative reference paths and stayed there for a sufficiently long time, then the pair of players is said to have reached a decision, and we define the decision outcome to be for that particular path (for details of the methods see Appendix B). The bounds of the neighborhood for the thick path, thin path and centerline, are defined by μ_{thick}, μ_{thin}, and μ_0 respectively. Each neighborhood is defined as a box surrounding the path, with length equal to the signal duration (3000 ms) and width equal to twice the bounds centered around the path or centerline. The bounds μ_{thick}, μ_{thin}, and μ_0 are percentages of the distance between the reference paths and the centerline. Fig. 4.5A presents the decision outcomes statistics. The decisions were defined for the following criterion. The threshold on the thick path was $\mu_{thick} = 0.35$. The threshold on the thin path was $\mu_{thin} = 0.1$. The threshold for deadlock at centerline was $\mu_{zero} = 0.1$. Time required to stay within the threshold was $T_{preference} = 50$ ms for the preferences, and $T_{center} = 2000$ ms for deadlock. In the Hard-Soft Conflict decision type, the stronger preference is defined to be the hard preference. In the case of Hard-Soft Conflict, Player H was able to win the decision for 64.3% of the time. A remarkable 25.4% of the time, the decision was for the side for which Player H had no track, i.e. Player S was able to win the decision 25.4% of the time. And for the remaining 10.3% of the time, the decision outcome was other than classified above. This 10.3% consisted of deadlock, unclassified decisions and decisions that reached both hard and soft preferences in the process.

In the Soft-Soft Conflict decision type, we distinguish between left and right preferences. For 52.5% of the time, the decision outcome was for the right preference, while 47.5% of the time, it was for the left preference. In the Soft-Unknown decision type, the stronger preference was the soft preference, and 87.3% of the time, the decision outcome was for the soft preference.

In the Soft-Unknown decision type, a decision for the side opposite to the soft preference was as frequent as 11.9%. A decision for the non-preferred side may have occurred when the player with the unknown preference initiated first. For the remaining 0.8% of the time, the outcome was not accurate enough to be counted.

Fig. 4.5B presents a comparison of the starting order between the players in different conflict decision scenario types. In the Hard-Soft Conflict decision type, Player H was the initiator for 36.5% of the time. Player S was the initiator for 62.7% of the time. Only in two cases, did both players start out at the same time. In the Soft-Soft Conflict decision type, the player with the preference for the right side was the initiator for 55.7% of the time. The player with the preference for the left side was the initiator for 44.3% of the time. In the Soft-Unknown decision type, the player with the soft preference was the initiator for 82.4% of the time, and the player with an unknown preference was the initiator for 17.6% of the time.

Fig. 4.5 C-E show the decision outcomes by starting order for the three conflict decision scenario types. In the Hard-Soft Conflict decision scenario, when Player H initiated, she almost always won the decision. When Player S initiated, all decisions were possible. In the Soft-Soft Conflict decision scenario, when the left preference player initiated, the decision was most likely for the left preference, and similarly for the right preference player. In the Soft-Unknown case, when the player with a soft preference initiated, the decision was most likely for that preference, and when the player with unknown preference initiated, the decision could be both.

We performed the Chi-squared test on the Soft-Soft Conflict decision scenario, and Fisher's exact test on the Hard-Soft Conflict and Soft-Unknowns cases (see Table 4.1 below), to test the correlation between the starting order and decision outcome. The null hypothesis was that the decision outcomes were independent of the starting order of the players. For all of the cases, we computed a p-value of $p < 0.01$, indicating that the decision outcomes significantly differed by starting order of the players [13] [14]. However, statistical significance does not say exactly what role starting time plays, and how for the Hard-Soft Conflict decision type, although Player S initiated more often, she didn't win the decision more often. In the other two cases however, the player who initiated the motion was typically a proxy for the decision outcome.

One possible reason why Player S would start out more often is that the soft preference path is 40 times wider (40 pixels versus 1 pixel on the screen) than the hard preference path both vertically and horizontally, as in Fig. 4.1A. And therefore, the "T" indicating the start of the decision happens sooner for the player who sees a thick path. It is likely due to this difference that Player S started out first more often. The horizontal portion of the soft preference track would reach Player S's action level (level where the cursor moves) sooner than the hard preference does for Player H,

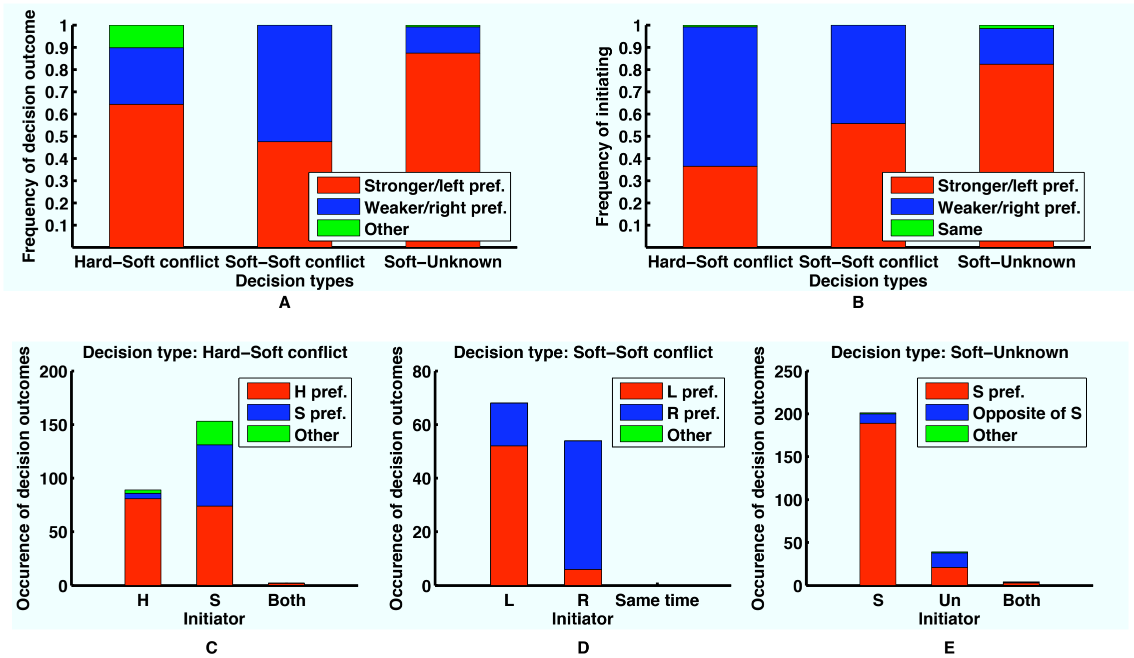

Figure 4.5: Decision outcomes and starting order. A). Frequency of decision outcomes for each of the three conflict decision scenario types. Red represents the stronger preference (i.e., the hard preference in the Hard-Soft Conflict decision scenario and the soft preference in the Soft-Unknown case). Red also represents the left preference in the Soft-Soft Conflict decision scenario. Blue represents the other preference. Green represents decisions not classified due to inaccuracy. B). Frequency of initiator for each of the three decision scenario types. Red represents the initiator being the player with the stronger preference (as defined before) and blue represents the initiator being the player with the weaker preference and green represents both players initiating at the same time. C)-E) Decision outcomes for each type of initiator for the three conflict decision scenario types. In the Hard-Soft Conflict decision scenario, when Player H initiated, she almost always won the decision. When Player S initiated, all decisions were possible. In the Soft-Soft Conflict decision scenario, when the left preference player initiated, the decision was most likely for the left preference, and similarly for the right preference player. In the Soft-Unknown decision case, when the player with a soft preference initiated, the decision was most likely for that preference, and when the player with unknown preference initiated, the decision could be both.

resulting in a noticeable time delay by design. The delay should be more obvious when the two decision scenario types are different. When both have soft preferences, there should be little influence from the delay.

Table 4.1: Cross tabulation of incidents of decision outcomes (H preference, S preference, L preference, R preference, None of the above) and incidents of initiating (Player H, Player S, Player L, Player R, Player Unknown, Both at the same time) for the three different decision scenarios

Hard-Soft Conflict	H preference	S preference	None
Player H initiates	81	5	3
Player S initiates	74	57	22
Both	2	0	0

(a) Initiator and decision outcomes for the Hard-Soft Conflict decision scenario.

Soft-Soft Conflict	L preference	R preference	None
Player L initiates	52	16	0
Player R initiates	6	48	0
Both	0	0	0

(b) Initiator and decision outcome for the Soft-Soft Conflict decision scenario.

Soft-Unknown	S preference	Opposite to S	None
Player S initiates	189	11	1
Player Unknown initiates	21	17	1
Both	3	1	0

(c) Initiator and decision outcome for the Soft-Unknown decision scenario.

These statistical findings suggest that the starting order (and therefore relative starting time) play a potentially important role. However, we also noticed that statistical analysis of the start and end status of the decision behaviors alone were not sufficient for us to understand why the players reached certain decisions. Player S started out more often than Player H, but did not win the decision more often. This motivates our investigating of the trajectories with our model to find explanations for the decision-making process.

4.3 Fitting the dynamical model to data and parameter analysis

The Hard-Soft Conflict model Eq.3.5 (including all parameters) was fitted to all data sets available for the Hard-Soft Conflict decision scenarios. There were a total of 244 sets of data, and each data set consisted of 5000 ms of trajectories for each player and for the mean. All of the parameters in the Hard-Soft Conflict model were fitted except for τ. We did not expect individuals to learn or develop a consistent personality trait in this experiment with unrepeated task trials. Therefore, we allowed the parameters to vary from trial to trial, and every trial was fit individually. We then evaluated all fits and parameter values to find a general trend on the relationship between parameters and behaviors.

We applied a time constant of $\tau = 100$ ms for all fits so that the speed of the model matches the speed for the majority of the data trajectories. The value of 100 ms for the time constant was found out based on preliminary fitting to the data by using various values of τ. The time constant affects the transient and reflects the inherent time scale of the process. We fit to the data up until $t_f = 3000$ ms and used a common Heaviside function to account for the ending of the decision phase (see methods in Appendix C).

Fig. 4.6 shows the statistics for goodness-of-fit. The mean of the root mean squared (RMS) error is 0.39 with a standard deviation of 0.18. The root mean squared error for the best fitted data is 0.08, and 0.94 for the worst fitted data. We have normalized the data such that the tracking goal is at 1 and -1. The mean of the RMS to be at 0.39 is considered good for overall fit quality, as can be seen in the trajectories fitted and discussed later on in Figs. 4.10 -4.11.

We refer to a player who changes her mind and changes course of action after some unsuccessful attempts to change the motion of the mean as someone who makes

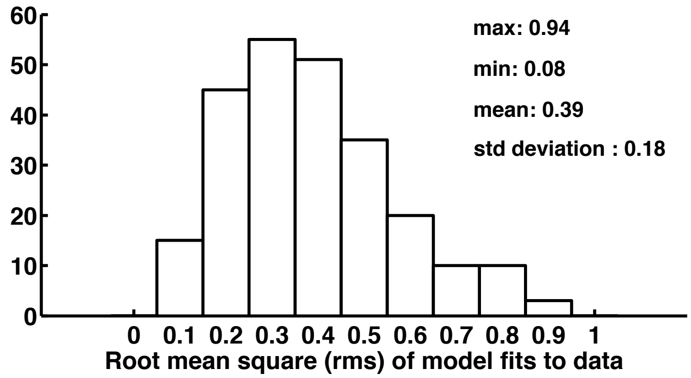

Figure 4.6: Goodness-of-fit in terms of root mean squared error. A total of 244 data sets were fitted. Each data set included three trajectories of 5000 data points (1 point per ms.)

a "compromise" in the coordination. We will use the word "compromise" in the following text to mean that the player has given up her previous intention.

There were cases in the data (less than 25 per cent of the time) when Player S and Player H behaved as if they exchanged roles. In those trials, Player S was often more forceful and did not make a "compromise" whatever the mean decision was, while Player H made a compromise soon after the task started, and even actively moved towards a side where she could see no path. We allowed for the fitting routine to select a binary parameter to decide whether $\alpha_H = 0$ or $\alpha_H \neq 0$ would better fit the case, i.e. whether Player H should be modeled as such or as Player S instead.

Fig. 4.7 shows the decision outcomes fitted with $\alpha_H = 0$, and mapped on the plane of relative social thresholds $(\theta_S - \theta_H)$ versus relative starting times $(t_H - t_S)$. It can be seen that for $t_H - t_S < 0$, i.e. Player H starting first, regardless of the values of $\theta_S - \theta_H$, the decision outcomes were exclusively for the hard preference or otherwise unclassified. For $t_H - t_S \geq 0$ all decisions were present, while for $\theta_S - \theta_H > 0$, a decision for the soft preference was more likely. It can be noticed that the starting time differences were greater for the double decisions, which were cases when the decision reached both preferences during one trial. The majority of the hard

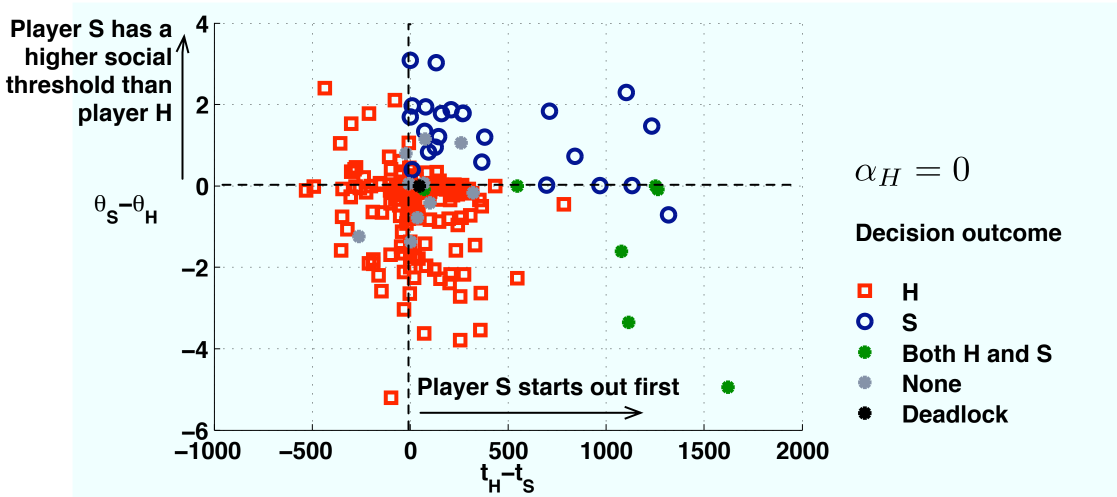

Figure 4.7: Decision outcomes mapped onto the plane of relative fitted social thresholds ($\theta_S - \theta_H$) versus relative fitted starting times ($t_H - t_S$ in milliseconds). Outcomes are identified by different markers. Red squares represent decision outcomes for the hard preference. Blue empty circles represent outcomes for the soft preference. Green filled circles represent decisions reaching both hard and soft preferences. Black filled circles represent the single occasion of deadlock (at the centerline), and gray filled circles represent outcomes which are not accurately classified as above. The definition for decision outcomes used for this case is the same as that used in Fig. 4.5. It can be seen that for the fitted data sets, a higher social threshold of Player S is a necessary condition for Player S to win when Player H plays according to the given cue ($\alpha_H = 0$), with only one exception. Player S starting first is also a necessary condition for the decision outcome to be the soft preference.

preference outcomes lie in the dense cluster in the range of $-2 < \theta_S - \theta_H < 0$ when $t_H - t_S$ was around 0, and in the range of -500 ms $< t_H - t_S < 500$ ms when $\theta_H - \theta_S$ was around 0.

Fig. 4.8 shows the decision outcomes fitted with $\alpha_H \neq 0$. For all cases fitted with Player H playing as if holding a soft preference, the decision outcome was never for the hard preference, or deadlock or double decisions, but only for the soft preference or otherwise unclassified. For all but one case, the decision outcomes for the soft preference occur when $t_H - t_S > 0$. In summary, for the decision outcome to be the soft preference where Player H played as if having a soft preference, Player S generally started earlier than Player H, with just one exception.

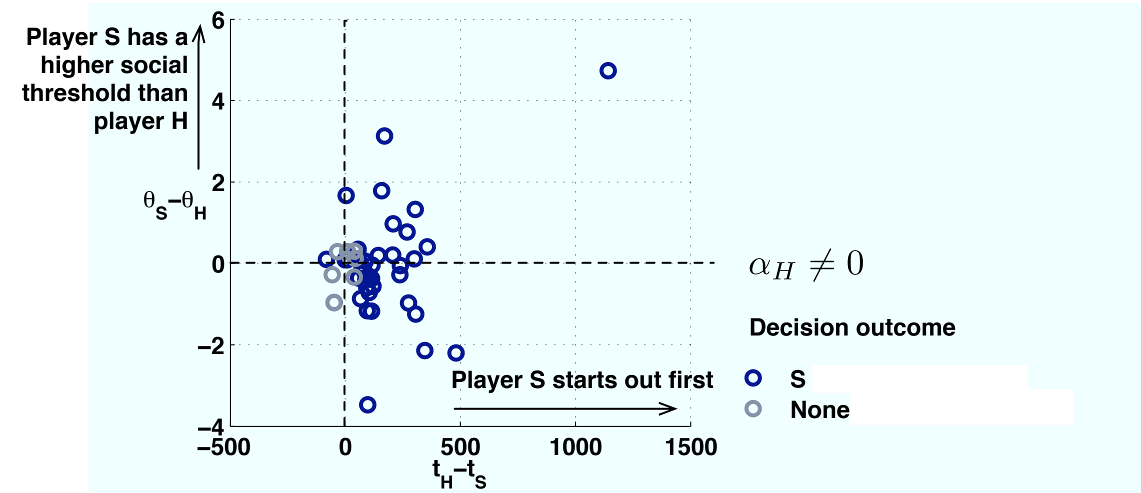

Figure 4.8: Decision outcomes mapped onto plane of relative fitted starting times ($t_H - t_S$ in milliseconds) and relative fitted social thresholds ($\theta_S - \theta_H$) when $\alpha_H \neq 0$. $\alpha_H \neq 0$ is used to fit to data sets where the player with a hard preference plays as if she had an alternative track and therefore instead of the hard preference, she had a soft preference. Outcomes are identified by different markers. Blue circles represent decision outcomes for the soft preference and gray empty circles represent decision outcomes which are not accurately classified as above. Overall, including the data sets fitted to the case when $\alpha_H = 0$, Player S starting out first is a necessary condition for the decision outcome to be the soft preference for but one exception.

Fig. 4.9 shows the decision outcomes fitted with $\alpha_H = 0$ in the plane of the fitted preference threshold δ_S for Player S versus the relative fitted social thresholds ($\theta_S - \theta_H$). When δ_S was greater than 2, the decision outcome was almost exclusively for the soft preference when $\theta_S - \theta_H > 0$. Diagonally, when δ_S was less than 2, the decision outcome was almost exclusively for the hard preference when $\theta_S - \theta_H < 0$. In general, when $\theta_S - \theta_H < 0$, that is when Player S is more "social" than Player H, the decision outcome is almost exclusively for the hard preference with only one exception. The case of deadlock had a δ_S value greater than 4, while the corresponding $\theta_S - \theta_H$ and $t_H - t_S$ were almost 0.

Mapping human behavioral parameters onto the plane of decision outcomes leads us to a closer understanding of the distribution of individual player's transient behaviors in this continuous-time social coordination task. We have seen that there is

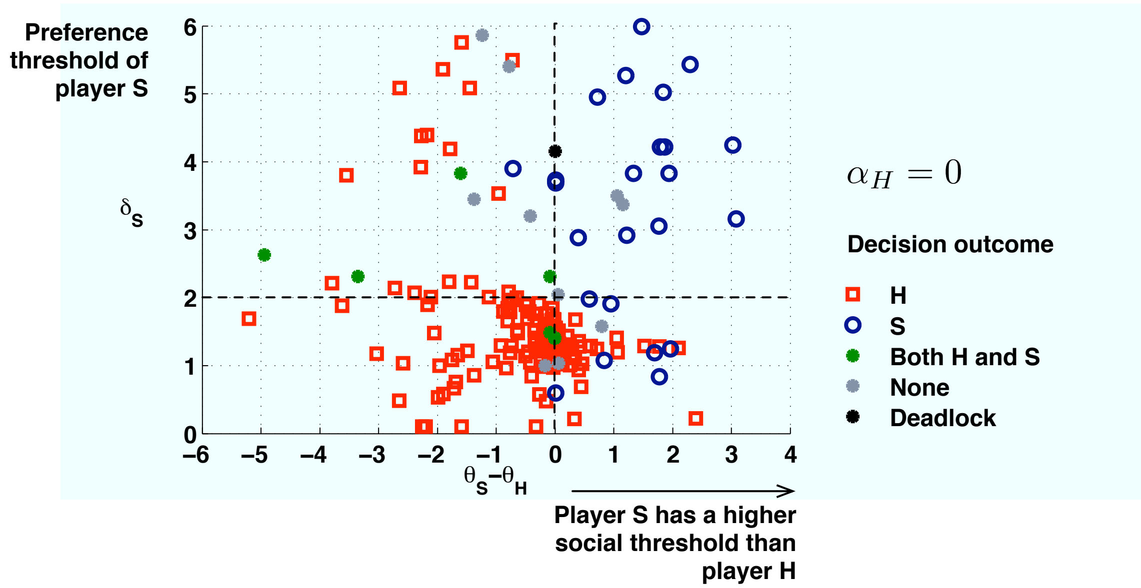

Figure 4.9: Decision outcomes mapped onto the plane of fitted preference thresholds δ_S of Player S versus relative fitted social thresholds $(\theta_S - \theta_H)$. Outcomes are identified by different markers. Red squares represent decision outcomes for the hard preference. Blue empty circles represent outcomes for the soft preference. Green filled circles represent decisions reaching both hard and soft preferences. Black filled circles represent the single occasion of deadlock (at the centerline), and gray filled circles represent outcomes which are not accurately classified as above. The definition for decision outcomes used for this case is the same as that used in Fig. 4.5. It can be seen that for a higher social threshold θ_S of Player S and a preference threshold δ_S greater than 2 the decision outcome tended to be exclusively the soft preference or on the side of the soft preference. On the other hand, when Player S had a relatively lower social threshold θ_S then for all values of δ_S the decision outcome tended to be on the side of the hard preference with one exception.

great variability in behaviors across the players from the fact that parameters are relatively broadly distributed in the parameter space. However, the parameter space is separated by stable decision outcomes and there are characteristic clusters that allow us to identify different behavior types.

4.4 Explaining behaviors in terms of dynamical processes

We compared fitted and data trajectories to show how key model parameters help explain the dynamic process behind a decision. In Fig. 4.10, five different types of decision processes are presented. The parameters for the fits are shown in Table 4.2. Fig. 4.10A presents a frequently observed decision process where the player with the hard preference (in red) started out early, and Player S (in blue) simply followed. Players adjusted their speeds and the mean reached the hard preference path accurately. It can be seen from the parameters in Table 4.2 that Player S had an intermediate value of preference threshold δ_S, which accounts for Player S ignoring the preference when the preference became too far.

Fig. 4.10B shows the case where Player S (in blue) started out first, towards the direction for which Player H had no track, and successfully pulled the mean towards the soft preference for some time. As soon as Player H started moving, Player S made a compromise and turned around. The threshold parameters revealed that it was Player S's relatively lower social threshold that led to the compromise. At the same time, Player S had a high preference threshold, implying that there was a strong determination to stick to the preference. However, the force to pursue the preference was overcome by the force of the social interaction.

Fig. 4.10C shows another frequently seen process, where the two players started out almost simultaneously and towards opposite directions. Player S reacted to the resulting deadlock quickly by turning around and making a compromise so that the hard preference was reached. Comparing the parameters for this case and that of Fig. 4.10A reveals that in this case, Player S had a slightly lower social threshold, i.e., a slighter greater willingness to compromise for coordination.

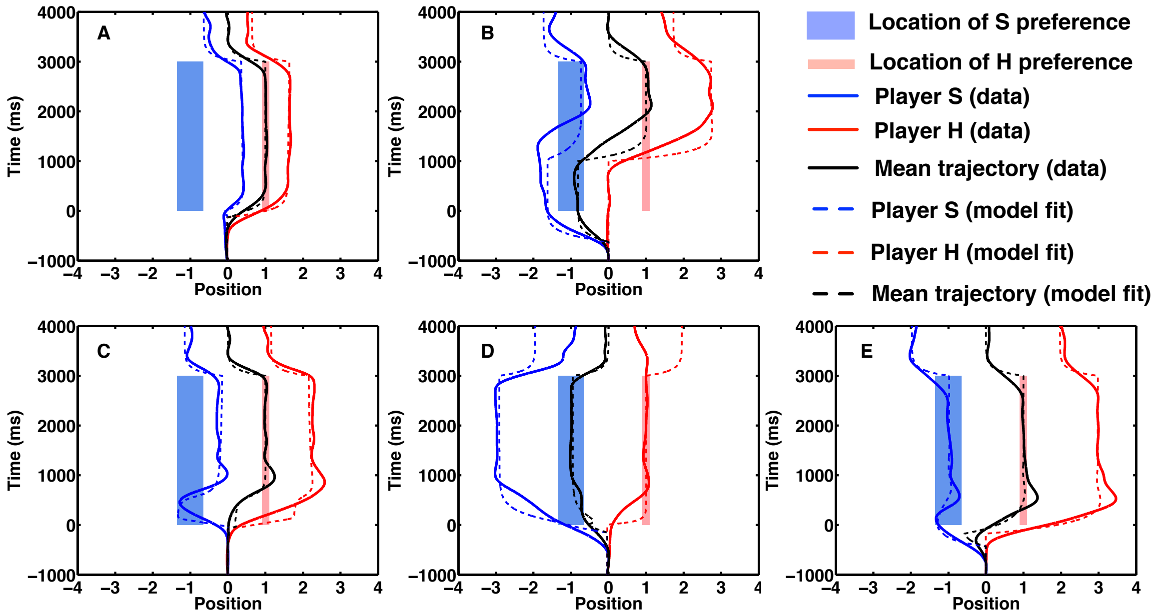

Figure 4.10: Data and model fits for representative decision processes. The parameters for the fits are shown in Table 4.2. A). Decision outcome was for the hard preference. Player H started out early, and Player S followed without pursuing her preference. B). Decision outcome was for both the hard and soft preferences. Player S started out first towards the soft preference, but as soon as Player H started moving, Player S compromised for the hard preference. C). Decision outcome was for the hard preference. The two players started out almost simultaneously and towards their respective preferences. However, Player S reacted to the resulting deadlock quickly by turning the other way and making a compromise so that the hard preference was reached. D). Decision outcome was for the soft preference. Player S started out first and insisted on the preference, while Player H gave up right around when the mean reached the soft preference. E). Decision outcome was for the hard preference. Player H acted more forceful than Player S even though Player S started out earlier.

Fig. 4.10D shows a case where the decision outcome was for the soft preference. Player S started out first and insisted on the preference, while Player H gave up after trying for a while. Parameters show that Player H had a relatively lower social threshold.

Fig. 4.10E shows a case where Player H was more forceful and Player S did not have to turn around for the mean to reach the hard preference. Parameters suggest

Figure	t_H	t_S	θ_H	θ_S	δ_S	B_S	R_H	R_S
Fig. 4.10A	-135.00	-88.48	1.51	1.80	1.24	7.90	7.20	7.08
Fig. 4.10B	999.87	-622.17	5.97	1.03	2.63	2.77	19.82	5.57
Fig. 4.10C	-80.37	-31.45	1.55	1.54	1.36	9.15	15.46	13.20
Fig. 4.10D	8.46	-150.34	0.87	2.65	0.84	6.07	6.04	5.28
Fig. 4.10E	-173.45	-429.64	4.31	0.52	2.22	8.75	16.61	1.35
Fig. 4.11A	-25.83	-73.37	0.70	0.70	4.16	11.80	3.66	3.64
Fig. 4.11C	-25.01	-161.24	1.06	1.39	1.1	14.06	1.26	4.07
Fig. 4.11D	0	-321.82	0.65	0.48	1.00	2.69	23.27	1.08

Table 4.2: Table of fitted parameters when $\alpha_H = 0$.

Figure No.	t_H	t_S	θ_H	θ_S	δ_H	δ_S	R_H	R_S	B_H	B_S
Fig. 4.11B	-18.07	-84.63	1.23	2.09	1.45	5.17	1.09	24.13	4.65	16.24
Fig. 4.11E	0.91	-299.98	1.40	1.51	1.50	1.50	3.01	5.00	14.98	5.77

Table 4.3: Table of fitted parameters when $\alpha_H \neq 0$.

that the value of the social threshold of Player H was relatively high even though the the value of the preference threshold of Player S, δ_S was also high.

Besides the above typical decision process, there are a few more worth pointing out. The one case of deadlock present in Fig. 4.5 is shown in Fig. 4.11A. In this case both players gave up trying and remained in deadlock until the end. Player S had a very high preference threshold. Fig. 4.11B shows the case where Player S played as if having a hard preference, and Player H played as if having a soft preference. As mentioned before, this case was fitted assuming $\alpha_H \neq 0$. Both Player S's preference threshold, and social threshold, were greater than those of Player H's. The parameter values for this fit are shown in Table 4.3.

Fig. 4.11C presents a case where the two players were coordinating their speeds with simultaneous overshoot and undershoot, but the mean went to the hard preference path. Here, Player S started out first, and was able to pull the mean towards her advantage, but turned around in a compromise. Both Player S's preference threshold and social thresholds were relatively low. Fig. 4.11D shows a case where the two play-

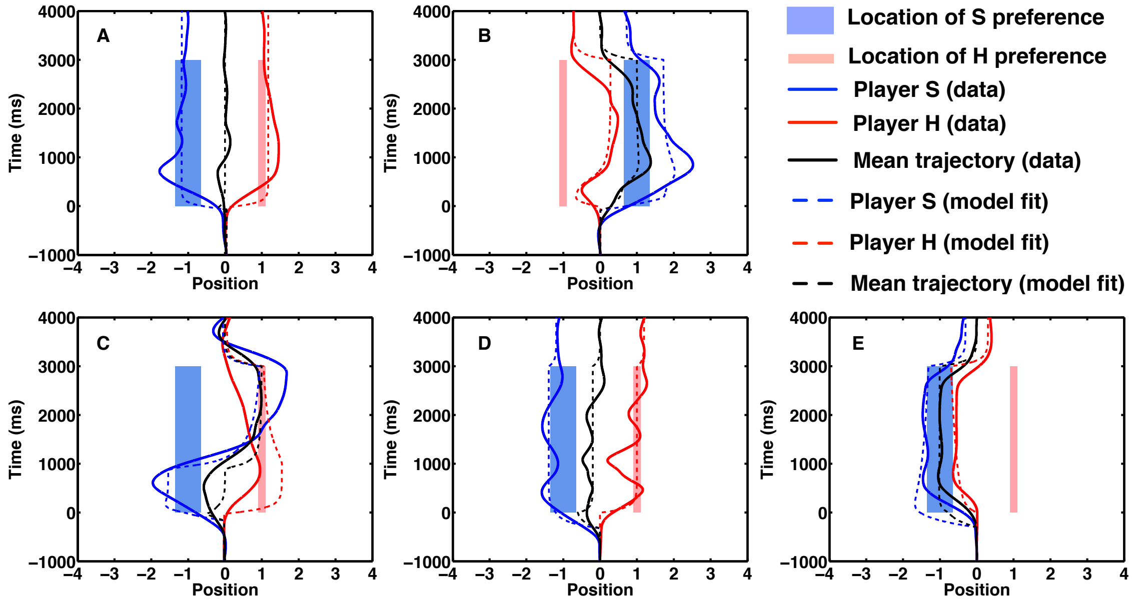

Figure 4.11: Data and model fits for less common kinds of decision processes. The parameters for the fits are shown in Table 4.2 and Table 4.3. A). Decision outcome was for deadlock. Both players gave up trying and remained in deadlock. B). Decision outcome was for soft preference. Player S played as if having a hard preference, and Player H played as if having a soft preference. C). Decision outcome was for the hard preference. Two players coordinated their speeds in the process of reaching a decision and simultaneously overshot and undershot, but the mean stayed on a path. Player S initiated the movement, but decided to turn around to compromise for Player H. D). Decision outcome not classified. Players seemed to have moved with canceling oscillations and did not try further to make the decision. E). Decision outcome was for the soft preference. Players played as if having exchanged roles. Player H followed Player S.

ers reached a decision somewhere in the middle between the soft preference and the centerline. In this case, both players seem to have moved with canceling oscillations and were not forceful enough to make the decision.

Fig. 4.11E shows a case where Player H followed Player S as if they exchanged roles and Player S was much more forceful.

In this experiment, individuals played a particular decision type once with a prescribed partner, and no learning was possible since neither the partner player, nor the decision scenario types were repeated. The parameters that we were able to extract and interpret therefore stand for the behavior for the one process that was fitted to. It remains to be tested in future experiments to see if players develop a particular social threshold or preference threshold, after repeatedly playing the game with a fixed partner player and for a fixed sequence of decision scenarios.

Our model has limitations as well, and not all decision curves of the experimental data were a good fit, as presented in Fig. 4.12. Fig. 4.12A is an example of deadlock by compromise, where both players moved opposite each other in a gesture of compromise. While the resulting decision looks like a deadlock, it was not counted as a deadlock decision since it is not in the close-enough vicinity of the centerline. We were able to reproduce this decision outcome, but could not capture the transient behavior. If we introduce one more parameter as a gain in front of the social interaction term, we should be able to capture such deadlock cases, since it is possible that in this case, the social interaction is a stronger term than we have assumed.

Fig. 4.12B shows a case where Player H suddenly increased speed after the decision had reached the soft preference side (which Player H could not see). We have used a constant time constant for all trials, and could not produce sudden changes in the speed in one direction that required a higher time constant. If we introduced one more gain into the model, or allowed the time constant to change for each data set, we should be able to capture such processes.

From a cognitive science perspective, these results could also be due to the fact that players did not always act consciously in this task [35, 43]. Interactive tasks where players cannot see each other can be very complex. In cases where players seem to be not taking action or being consistently stubborn and "single-minded", it may be because these trials happened when players were not consciously performing an interactive task (i.e. not being "social" or "deciding" at all). We therefore suggest that social interaction is a conscious act that may require some form of cueing, and simply displaying the mean trajectory may not be enough to motivate players to consciously interact with the "invisible" other player. Nevertheless, our model has shown potential usefulness in explaining human behaviors in decision-making processes that are otherwise not able to be described with data analysis alone.

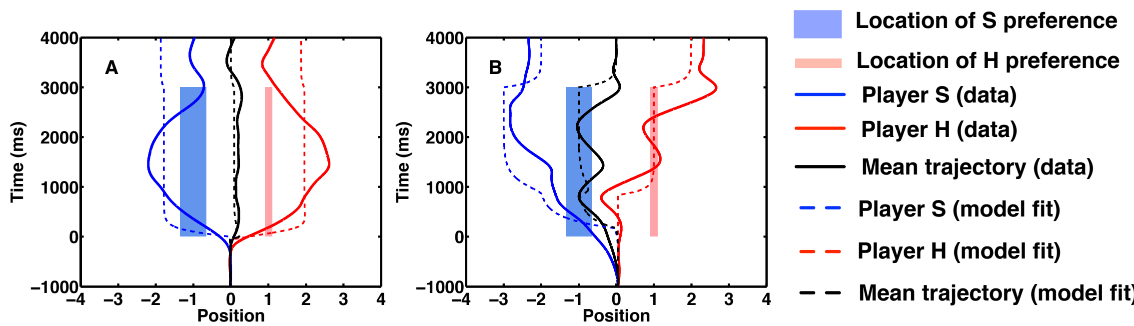

Figure 4.12: Trajectories that were not well fitted with the model. A. Deadlock by compromise. B. Change in time constant is present. It is of future work to investigate how to capture these transient processes, while our current model can only capture the outcomes for these cases.

Chapter 5

Game-theoretic analysis of behavior in the shared control task

5.1 Background

In this chapter we study human behaviors in Chapter 4 from a game-theoretic perspective, and examine evolution of strategies at the population level. A game is an interactive decision-making setting where two or more players make independent decisions (without communication or prior agreement) in a strategic situation where their individual reward is influenced by the joint decision of all players in the game [53]. Game theory examines how incentives affect individual decisions in a strategic setting. To use game theoretic tools, we assume that players make rational decisions. By rational, we mean that they will always prefer a strategy that will help them achieve the best rewards for themselves given the responses of others.

A normal form game is defined by the rewards given to the players and carries the form of a reward matrix, which we will introduce in detail later. In this chapter, we analyze the shared control task from Chapter 4 using the formulation of a repeated normal form game formulation, and investigate if players make decisions that achieve joint strategies corresponding to game-theoretic equilibria, even though players cannot compute such equilibria (due to incomplete information). Nash equilibrium is an important concept in game theory. A Nash equilibrium, named after the mathematician John Nash, is a set of strategies, one for each of the players in a game, that has a special property that each player's choice is his best response to the choices of all other players. A Nash equilibrium corresponds to the players playing the strategies in which no one can be better off by unilaterally deviating. In other words, at a Nash equilibrium, nobody has the incentive to deviate from the equilibrium unilaterally, and the strategy played is therefore a best response given the strategies of others [31, 53].

A repeated game is a type of game that maps well to continuous-time processes where the same one-shot game is repeated a number of times as the process evolves, and rewards are accumulated along the way. Repeated games allow players to adapt their strategies based on past observations and use feedback that is otherwise not possible in one-shot games [53]. Often, strategies that result in the highest individual rewards for playing a repeated game may not be the same as the strategies that result in the highest individual rewards in a one-shot game, because players can learn or adapt in a way so that they may implicitly cooperate and play a socially optimal strategy that is better than individually best response (Nash) strategies. One type of equilibrium that can be reached is called a correlated equilibrium.

First introduced by mathematician Robert Aumann in 1974 [3], a correlated equilibrium is one of the most commonly observed (in laboratory settings) and natural (by intuition) outcomes of repeatedly played coordination games that have two or more Nash equilibria. Intuitively a correlated equilibrium is best understood by considering the game to be played repeatedly, even through one-shot games can have correlated equilibrium as well. A correlated equilibrium requires the existence of at least two pure Nash equilibria. Suppose there are only two, then at the correlated equilibrium, the players reach a consensus that half of the time they will play one of the Nash equilibria and the remaining half of the time they play the other equilibrium. It is as if they were coordinated through some communication: i.e. if you switch in the next round I switch. At a correlated equilibrium, a player chooses his strategy only on the condition that the other player also chooses the correlated equilibrium strategy. The two players' strategies are correlated, hence the name. What's striking about this equilibrium concept is that correlated equilibria predict that such coordinated dividing between Nash equilibrium strategies can emerge even without communication or signaling [30, 3, 4].

In the case of a population reaching a correlated distribution of strategies over two Nash equilibria, then half of the population will play one equilibrium strategy and the other half of the population will play the other equilibrium strategy, as if someone had told them to split. The most obvious benefit of playing a correlated equilibrium is that players can avoid negative reward outcomes and play in a more "fair" way [53].

There are many notions of equilibria in game theory other than the ones we consider in this chapter [53]; however, these are not relevant to our study and hence will not be reviewed here.

Two player interactions in continuous-time coordination games have been studied by Braun et. al. in [10, 9]. Using experiments [9], Braun et. al. investigated human pairwise coordination in sensorimotor tasks that correspond to classical coordination games with multiple Nash equilibria. They found that successful coordination between two players (who were not allowed to communicate with each other) was achieved in the majority of the experimental trials and that such coordination was characterized by statistical features including increased mutual decision dependence and increased joint entropy. While they showed that players were able to converge to the Nash equilibria in the majority of the trials, how strategies evolve in time was not addressed.

The goal for this chapter is twofold. First we show that in the experiment for which we studied individual transient behaviors in Chapter 4, the majority of players are able to converge to playing the Nash equilibrium strategies as predicted by game theoretic analysis. This finding provides motivation for investigating why players are able to “learn” or converge to the Nash equilibrium strategies even though they don’t know the incentives of the other player. Second, by observing the evolution of strategies at the population level, we suggest an explanation for how convergence of Nash equilibrium strategies can take place. By analyzing the mean field strategy evolution we see that as a population, the majority of players are able to jointly converge onto the Nash equilibrium strategies in time as if they knew their co-players rewards as well. We show through simulations for two examples that the replicator dynamics can reproduce very similar strategy profiles as found in empirical observations.

5.2 A normal form coordination game with incomplete information

We first formulate the experimental task of Chapter 4 into a normal form game. At first glance the game formulation results in a reward structure that looks like an anti-coordination game instead of the classical coordination game where the highest rewards for each player are achieved when players play the same strategies. We will explain why it is appropriate to formulate the game as an anti-coordination game instead of a classical coordination game, since in this tracking experiment, it is the mean position of the two players that influences their respective rewards and not the player’s own absolute positions. There is a higher possibility of tracking the reference path more accurately if the players coordinate more freely than having to move in sync. We then show that for the different decision scenario types, the one-shot normal form game that we define can have one or more pure Nash equilibria that can be interpreted as best response individual strategies for the players. In the scope of this chapter, we are only interested in pure Nash equilibria in the games we are going to describe.

The game formulation of the experiment as summarized in Chapter 4 and conducted by Groten et. al. [26] can be formally described in terms of the language of game theory as follows. Two players, who we refer to as Player 1 and Player 2 for now, repeatedly interact in a game setting where the game outcome depends on the joint strategies of the players, which also decides their respective rewards. For each player $i = 1, 2$, the set of strategies are called left (L), right (R) and center (C). A strategy of L corresponds to a model decision variable z_i with a value $z_i \leq -1$. A strategy of R corresponds $z_i \geq 1$. The strategy of C corresponds to the value $z_i \in (-1, 1)$. This provides a map from continuous values on the real line onto the three distinct sets identified with the three distinct strategies L, R and C.

We define each trial of the task of Chapter 4 that lasts from -1000 ms (1000 ms before the reference path splits at a "T") to 3000 ms when the reference paths merge as a repeated game of the one-shot game with the three strategies L, R and C. The number of repeated rounds of the one-shot game depends upon the resolution we use to discretize the 4000 ms time period. We use the resolution of one round per millisecond so that the total number of rounds is 4000. The goal of the game (as in the experiment) is for the two players to coordinate their decisions so that the mean $\frac{1}{2}(z_1 + z_2)$ reaches 1 or -1. In our game theoretic formulation, we assume that a reward is accumulated in each round by each player throughout the repeated play. Each individual therefore try to maximize her average reward in each repeated play.

Reward to the players is modeled as reflecting the probability of achieving higher accuracy in tracking the preferred reference path. Intuitively, in order to achieve coordination and therefore to get a nonzero reward, the players should not choose the same strategies (as this may result in overshoot), and should not choose joint strategies that are opposite to each other (as this may result in deadlock), and furthermore, should not choose joint strategies that are both at the center (as this may result in no action similar to deadlock). The only joint strategies that will earn at least one of the players a nonzero reward is the joint strategy that consists of one player playing center, and the other player playing left or right depending on the game's reward structure. Even though this is a coordination game, the way we discretize the strategy space makes the game similar to an anti-coordination game as opposed to the classical coordination game in the literature.

The strategies, besides being called left, right and center, may also be called "preference (P)", which means that it corresponds to a side for which the player will gain higher reward, "opposite of the preference (O)", indicating a side for which the player may not have any reward or lower reward, and " no preference(C)", meaning that the player chooses to not make a strong move and not indicating obvious preference. For clarity, we will stick with the definitions of the strategies as left (L), right (R) and center (C) until later when we introduce the replicator dynamics in the next section, where we will use the P, C and O notation if necessary.

Given two players and three strategies, the reward for each player is contained in a three-by-three reward matrix in which the rows are the strategies for the player who has been assigned the reward, and the columns are the strategies of the co-player. For instance, consider a "Hard-Soft Conflict game", corresponding to the Hard-Soft Conflict decision scenario type as described in Chapter 4, where the first player has a hard preference for left (for instance), and the second player has a soft preference for right. We denote such a game as l-lR, following the notation of Chapter 4 in Section 4.1. We define the reward matrix $\mathbf{A_l}$ for Player 1 (with a hard preference for Left) as

$$\mathbf{A_l} = \begin{array}{c|ccc} & L & R & C \\ \hline L & 0 & 0 & \alpha \\ R & 0 & 0 & 0 \\ C & \alpha & 0 & 0 \end{array}$$

Player 1 can only receive a non-zero reward α, which we explain later, if the joint strategy is Player 1 playing C and the other player playing L (denoted by (C,L)) or Player 1 playing L and the other player playing C (denoted by (L,C)). Depending on the other player's incentives, Player 1 needs to adjust the strategy accordingly. At these two strategies (given that the other player plays accordingly) the mean has a higher probability of reaching -1 (L), which is Player 1's preference. Similarly, we define the reward matrix $\mathbf{B_{lR}}$ for Player 2 (with a soft preference for Right) as

$$\mathbf{B_{lR}} = \begin{array}{c|ccc} & L & R & C \\ \hline L & 0 & 0 & \gamma \\ R & 0 & 0 & \beta \\ C & \gamma & \beta & 0 \end{array}$$

We define the reward matrix for a player with unknown preference, denoted by $\mathbf{A_{lr}}$ as

$$\mathbf{A_{lr}} = \begin{array}{c|ccc} & L & R & C \\ \hline L & 0 & 0 & \gamma \\ R & 0 & 0 & \gamma \\ C & \gamma & \gamma & 0 \end{array}$$

The values α, β, γ in the reward matrices are chosen to indicate the relative measure of rewards for different joint strategies. We assume that $\alpha, \beta, \gamma \geq 1$ and that $\alpha > \beta > \gamma$. The player who has a hard preference for Left, will always have the reward matrix $\mathbf{A_l}$ regardless of the co-player's rewards. By combining and permutating the above three reward matrices we can reproduce joint strategy reward structures (tables) that define the two-player three-strategy games for the experiment corresponding to the 18 decision scenario types as in Chapter 4. Example reward tables for the six qualitatively different game types, namely the Hard-Hard No Conflict game, Hard-Soft No Conflict game, Soft-Soft No Conflict game, Soft-Soft Conflict game, Soft-Unknown game and Hard-Soft Conflict game, are shown in Tables 5.1-5.6. In the reward tables, the pure Nash equilibrium or equilibria are colored whereas other joint strategies are not. Different colors are used for the two players' payoffs and the player's position (Player 1 or Player 2) are colored accordingly. Player 1 is always the row player meaning that she selects the row strategies and Player 2 is always the column player selecting the column strategies.

		Player 2		
		L	R	C
	L	(0,0)	(0,0)	(α,α)
Player 1	R	(0,0)	(0,0)	(0,0)
	C	(α,α)	(0,0)	(0,0)

Table 5.1: Reward table for the Hard-Hard No Conflict game. Both players have a hard preference for left (L).

		Player 2		
		L	R	C
	L	(0,0)	(0,0)	(α,β)
Player 1	R	(0,0)	(0,0)	(0,γ)
	C	(α,β)	(0,γ)	(0,0)

Table 5.2: Reward table for the Hard-Soft No Conflict game. Player 1 has a hard preference for left (L) and Player 2 has a soft preference for left (L).

Classical game theory predicts outcomes of game play in terms of equilibrium strategies by computing the equilibria of the normal form game. All normal form games have at least one Nash equilibrium, which may not be a pure Nash equilibrium. But in our case, all games (corresponding to the decision scenario types in Chapter 4) have pure Nash equilibria. A pure Nash equilibrium (of a one-shot game) is a set of

		Player 2		
		L	R	C
Player 1	L	(0,0)	(0,0)	(β,β)
	R	(0,0)	(0,0)	(γ,γ)
	C	(β,β)	(γ,γ)	(0,0)

Table 5.3: Reward table for the Soft-Soft No Conflict game. Both players have a soft preference for left (L).

		Player 2		
		L	R	C
Player 1	L	(0,0)	(0,0)	(γ,β)
	R	(0,0)	(0,0)	(γ,γ)
	C	(γ,β)	(γ,γ)	(0,0)

Table 5.4: Reward table for the Soft-Unknown game. Player 1 has no preference and Player 2 has a soft preference for left (L).

strategies that yield the best rewards for both players so that no one has an incentive to deviate from the equilibrium strategy if the other player does not choose to play otherwise as well. As the game is repeated, always playing the Nash equilibrium may not result in the best average reward because once the co-player's strategies become predictable, it is possible to achieve higher reward by "cheating" for example. In the experiment of Chapter 4, players do not know the reward matrices of the other player and as will be seen in the data analysis later, players do not switch between Nash equilibria within a trial of 4000 rounds. However, across trials, and therefore as a population, if there is more than one Nash equilibrium, the population can be seen to divide and distribute over the Nash equilibria solutions. Specifically, players who played a certain Nash equilibrium strategy in one trial (of 4000 rounds) switched to a another Nash equilibrium strategy in another trial. At the population level, this corresponds to a correlated equilibrium distribution over strategies. But within trial (within the 4000 rounds), players when converged onto a joint strategy do not switch between Nash equilibrium strategies.

		Player 2		
		L	R	C
Player 1	L	(0,0)	(0,0)	(γ,β)
	R	(0,0)	(0,0)	(β,γ)
	C	(γ,β)	(β,γ)	(0,0)

Table 5.5: Reward table for the Soft-Soft Conflict game. Player 1 has a soft preference for right (R) and Player 2 has a soft preference for left (L).

		Player 2		
		L	R	C
Player 1	L	(0,0)	(0,0)	(α,γ)
	R	(0,0)	(0,0)	(0,β)
	C	(α,γ)	(0,β)	(0,0)

Table 5.6: Reward table for the Hard-Soft Conflict game. Player 1 has a hard preference for left (L) and Player 2 has a soft preference for right (R).

5.3 Equilibrium strategies in experimental data

We discretize the strategy space in the experimental data according to the aforementioned game formulation such that the player strategies (even though evolving in continuous space) can be mapped onto the three discrete strategies corresponding to the game formulation above. By doing so we can show our first result that the majority of equilibrium strategies of the two players in the experimental data correspond to the Nash equilibria.

We computed the mean individual position during the time frame from 1500 ms to 2500 ms and recorded the frequency in the population of each joint strategy. We used this to determine which joint strategy was reached at the end of the game. We will refer to this joint strategy as the "endpoint" strategy or as "equilibrium strategy" since in the majority of cases, the strategies have converged. The equilibrium strategies for Hard-Soft Conflict games and Soft-Soft Conflict games are shown in Fig. 5.1 where the color scale represents the frequency of a certain joint strategy of Players 1 and 2. The total number of trials is 61. According to our game-theoretic formulating of the experiment, the type of game changed every 4000 rounds and each game scenario is only played for one trial. Players did not know the joint reward table but only their own rewards and therefore were unable to recognize which game they were playing.

In Fig. 5.1(a), Player 1 has a hard preference for left (l) and Player 2 has a soft preference for right (lR). The game type is Hard-Soft Conflict. The Nash equilibria are Player 1 playing L and Player 2 playing C, denoted by (L,C) and Player 1 playing C and Player 2 playing L, denoted by (C,L). As can be seen, the majority of players played the joint strategy (L,C) for this game. Similarly, Fig. 5.1 (b)-(d) are all Hard-Soft Conflict game types, where the majority of players played one of the Nash equilibria. The symmetric Nash equilibrium corresponds to the same rewards, but it is not natural for players to play them and therefore not seen as frequently in the data.

Fig. 5.1(e) and (f) correspond to endpoint strategies in Soft-Soft Conflict games. In both panels (e) and (f), one of the players have a soft preference for Left and the other player has a soft preference for Right. There are four Nash equilibria in each case for the two panels, which are (L,C), (C,L), (R,C) and (C,R). The resulting endpoint strategy distribution across all trials in population shows that the number of times one player plays her preference (L) or (R) and the other player playing center (C) is almost equally distributed across the two Nash equilibria (L,C) and (C, R) in one case (panel (e)) , and (R,C) and (C,R) in the symmetric case (panel (f)).

The equilibrium strategies for Hard-Soft No Conflict games and Soft-Soft No Conflict games are shown in Fig. 5.2 where the color scale represents the frequency of a certain joint strategy of Players 1 and 2. Fig. 5.2 (a) and (b) correspond to the Hard-Hard No Conflict game where both players have the same reward matrices. The Nash equilibria for panel (a) are (L,C) and (C,L) and for panel (b) are (R,C) and (C,R).

Almost all players were able to play one of the Nash equilibria and as a population the distribution over Nash strategies corresponds to a correlated equilibria.

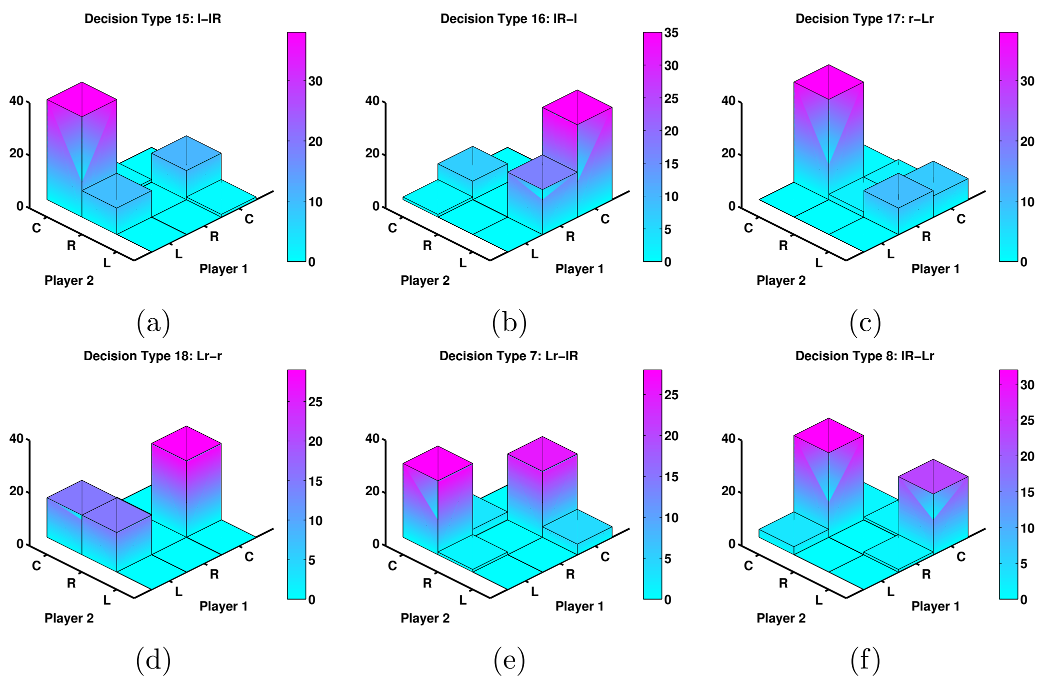

Figure 5.1: Frequency of joint strategies at equilibrium from the experimental data are binned into quadrants of the strategies of players for the Hard-Soft Conflict game (panels (a) to (d)) and the Soft-Soft Conflict game (panels (e) and (f)). Notation for the game types are defined according to the decision scenario definition in Section 4.1. The capital letters inside the figures represent strategies: L for left, R for right and C for center. As an example, the joint strategies of Player 1 playing L and Player 2 playing C produces a final position of the mean on the side of L. The Nash equilibria joint strategies for panels (a) and (b) are (L,C) and (C,L). For panels (c) and (d) are (R,C) and (C,R). And for panels (e) and (f) are (L,C), (C,L), (R,C) and (C,R).

Fig. 5.2(c) to (f) correspond to the Hard-Soft No Conflict game type where both players have the highest reward in the same joint strategy position in their respective reward matrices. In particular, the Nash equilibria for panel (c) and (d) are (L,C) and (C,L), for panel (e) and (f) they are (R,C) and (C,R). The distribution over the two Nash equilibria in each case of panels (c) to (f) differs slightly, indicating other factors possibly affecting the decision-making and not just the incentives, since the incentives are similar in these cases. One possibility is the starting times of the two players, or that there could be a bias towards the right, as can be seen in panels (e)

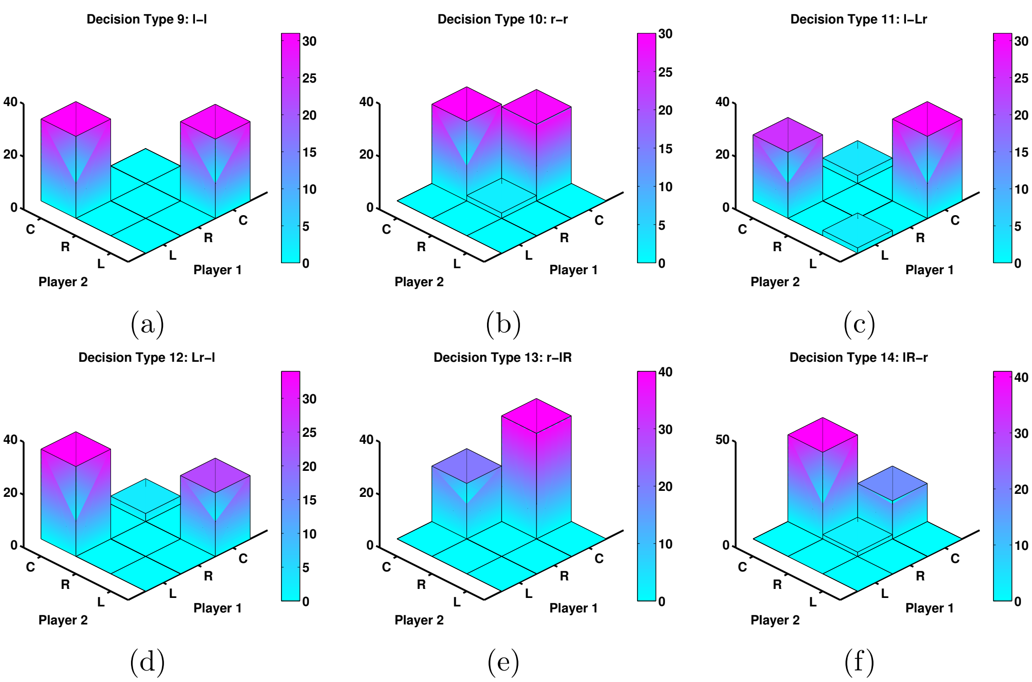

Figure 5.2: Frequency of joint strategies at equilibrium from the experimental data are binned into quadrants of the strategies of players for games types Hard-Hard No Conflict (panels (a) and (b)) and Hard-Soft No Conflict (panels (c) to (f)). The total number of participant pairs is 61 for each case. The Nash equilibria joint strategies for panels (a), (c) and (d) are (L,C) and (C,L). For panels (b), (e) and (f) are (R,C) and (C,R).

and (f) where there is a higher tendency for the player with a preference for R to play R than as seen in panels (c) and (d) where players with a preference for L play L or C almost equally frequently.

The equilibrium strategies for Soft-Soft No Conflict games and Soft-Unknown games are shown in Fig. 5.3. Fig. 5.3 (a) and (b) correspond to the Soft-Soft No Conflict game where both players have the same reward matrices. The Nash equilibria for panel (a) are (L,C) and (C,L) and for panel (b) are (R,C) and (C,R). Almost all players were able to play one of the Nash equilibria and as a population the distribution over Nash strategies is close to a correlated equilibria.

Fig. 5.2(c) to (f) correspond to the Soft-Unknown game type. In particular, the Nash equilibria for panels (c) and (d) are (L,C) and (C,L), and for panels (e) and (f) they are (R,C) and (C,R). Here in each case only one Nash equilibrium is played

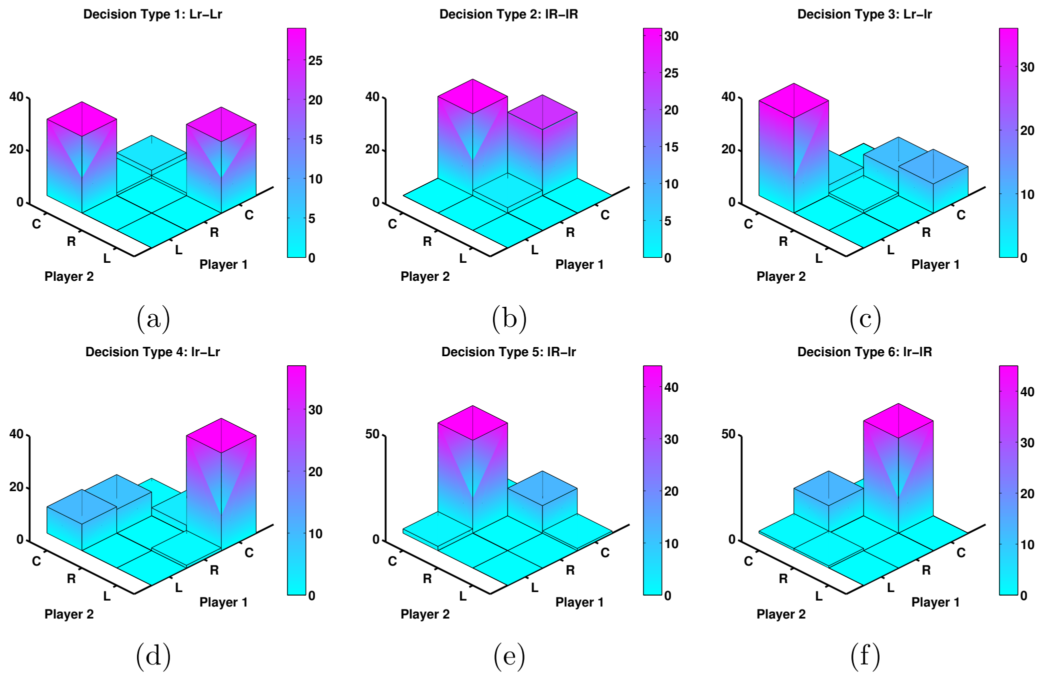

Figure 5.3: Frequency of joint strategies at equilibrium from the experimental data are binned into quadrants of the strategies of players for games types Soft-Soft No Conflict (panels (a) to (b)) and Soft-Unknown (panels (c) to (f)). The total number of trials is 61 in each case. The Nash equilibria joint strategies for panels (a), (c) and (d) are (L,C) and (C,L). For panels (b), (e) and (f) are (R,C) and (C,R).

by most players because it corresponds to the more natural way of responding to the game.

The fact that we observed the majority of the players playing the Nash equilibrium motivates us to look for a potential dynamical process that suggests how such an equilibrium converged from a given initial distribution of strategies on the population level.

5.4 Evolution of strategies in time and replicator dynamics.

To examine the dynamical process we studied how the strategies in the experiment evolved over time. First, we computed the frequency of individual strategies (rather than joint strategies) across the population of players at each millisecond throughout the 4000 ms long trial for each game of the 18 games corresponding to the 18 decision types of the experiment in Chapter 4. Then we summed up the frequency of individual strategies over the six qualitatively different game types. In the Hard-Soft Conflict game, the Soft-Unknown game and the Hard-Soft No Conflict game, the number of trials is 244. In the Soft-Soft Conflict game, the Soft-Soft No Conflict game and the Hard-Hard No Conflict game, the number of trials is 122.

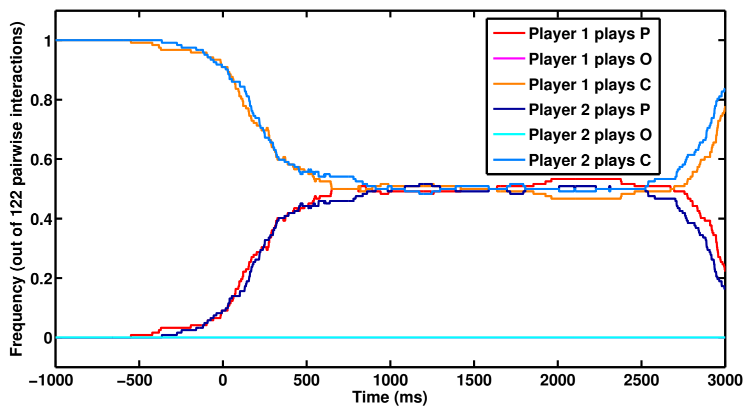

Figure 5.4: Evolution of strategies in the Hard-Hard No Conflict game. Player 1 and Player 2 have the same hard preference. Strategy P represents the common the preference of the two players. Strategy O represents the opposite of the preference and C represents center. All players start the game at strategy C.

Fig. 5.4 shows the evolution of frequency of strategies that occurred in both player populations in the Hard-Hard No Conflict game. In this game players' strategies at either position evolve from the starting condition C towards an endpoint strategy in a similar way because they have the same reward structure corresponding to the same preferences. The strategies in the population converges to a distribution similar to a correlated equilibrium where half of the population of Player 1 (red) play the strategy P, while half of the population of Player 2 (blue) play C. At the same time, the other half of the population of Player 1 play the C (orange), while the other half of the population of Player 2 play P (dark blue). A very similar process can be seen in the Soft-Soft No Conflict game as shown in Fig. 5.5. In these two games, players had identical preferences and reward matrices, therefore even though they could not see directly which game they were playing, the interactions overall between the two players in these two games are similar.

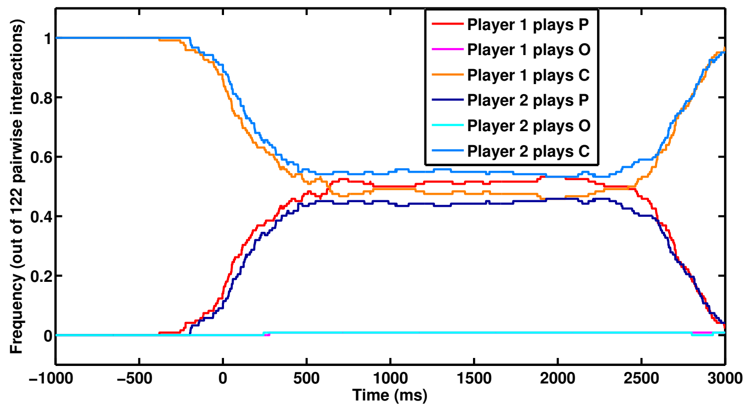

Figure 5.5: Evolution of strategies in the Soft-Soft No Conflict game. Player 1 and Player 2 have the same soft preference.

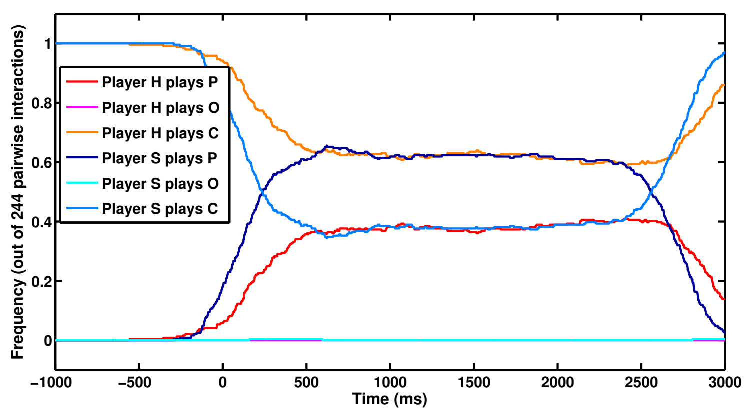

Figure 5.6: Evolution of strategies in the Hard-Soft No Conflict game. Player 1 has a hard preference and Player 2 has a soft preference which coincides with the preference with that of Player 1. Strategy P represents the common preference, O represents the opposite of the common preference.

Fig. 5.6 shows the evolution of frequency of strategies that occurred in both player populations in the Hard-Soft No Conflict game. Both player population's preference P are the same. As soon as the game started, the population of Player S playing P (dark blue) increased at a rate faster than the increase in the probability of Player

H playing P (red) resulting in roughly 60% of the times the joint strategy (P,C) was played by Player S and Player H and 40% of the time (C,P) was played, as opposed to 50% − 50% in the Soft-Soft No Conflict game. Otherwise, this process is also similar to the other two No Conflict games, where players generally coordinated smoothly and the final equilibria corresponded to the Nash equilibria.

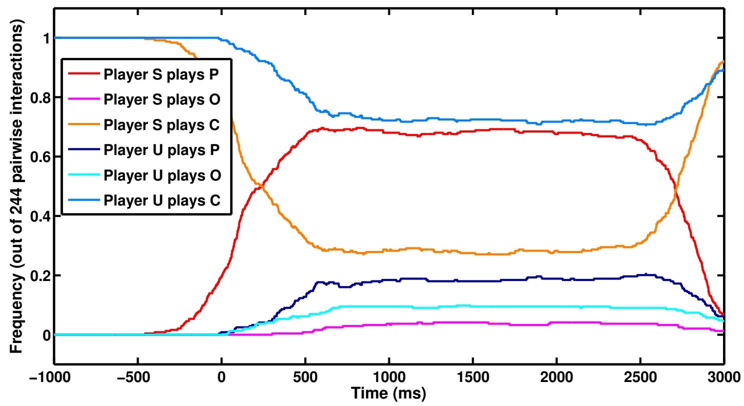

Figure 5.7: Evolution of strategies in the Soft-Unknown game. Strategy P represent the preference of Player S. Strategy O represents the opposite to P. Player U has no preference.

Fig. 5.7 shows the evolution of frequency of strategies that occurred in both player populations in the Soft-Unknown game. In this game Player S (red) started much earlier than Player U (blue) and the resulting process is similar to the Hard-Soft No Conflict game.

Fig. 5.8 shows the evolution of frequency of strategies that occurred in both player populations in the Soft-Soft Conflict games. At around −500 ms both player populations start to change strategies from C to L or R. In particular, about half of the players preferring L (red) change from initial state C to strategy P (means left for Player L), and 25% of the players preferring R (blue) change to strategy P (means right for Player R) and the another 25% of player R play O (means left for Player R). The remaining roughly half of Player L still play C, and the remaining half of Player R also still play C. This corresponds to an equilibrium distribution of joint strategies

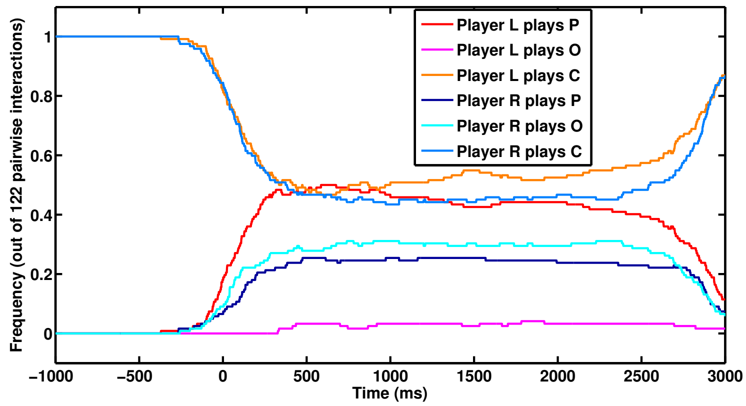

Figure 5.8: Evolution of strategies in the Soft-Soft Conflict game. Player L has a preference for left (L), hence the P strategy for Player L represents L. Player R has a preference for right (R), hence the P strategy for Player R represents R.

where roughly 50% of the whole population of Player L and Player R play (P,C) and 25% play (C,P) and 25% play (C,O). The fact that Player R are more likely to choose the opposite of their preference in the course of the game may be due to other factors not predictable from a game theoretic analysis. It also suggests possible interaction bias between players who have a preference for left versus those who have a preference for right which might be due to the way the experiment was conducted or the habits of the participants.

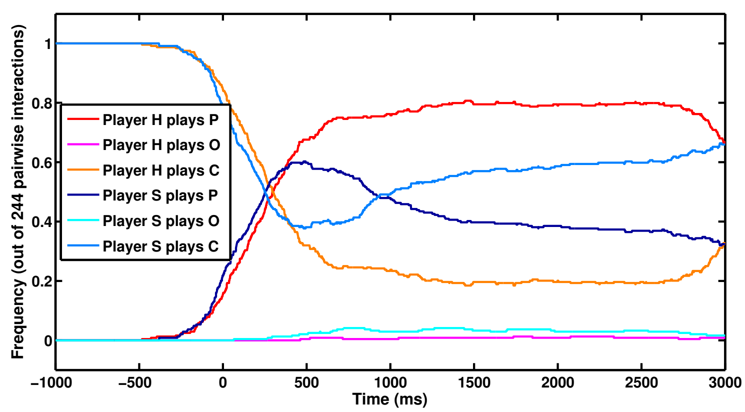

Figure 5.9: Evolution of strategies in the Hard-Soft Conflict game. Strategy P for Player H is opposite to the strategy P for Player S. In other words, the strategy P for Player H is equal to the strategy O for Player S and vice versa.

Fig. 5.9 shows the evolution of frequency of strategies that occurred in both player populations in the Hard-Soft Conflict game. At around -500 ms both players started to change strategies at almost identical rates. Within one second, the majority of Player H (red) changed their strategy from C to P. At around 800 ms (which is roughly one second after the first strategy change), 80% of Player H chose to play P and 20% still remained playing C. Player S reacted similarly fast and the number of Player S choosing to play their preference (which is the opposite of the hard preference) increases until around 400 ms reaching a peak. The time of the peak frequency of changing strategies from C to P for Player S also occurs around one second after the first player initiating the game.

Comparing the processes of how strategies in populations change across different game types as shown in Figs. 5.4-5.9 leads to the following observation. First, it is noticeable that the peak of the curve representing Player S playing P, which means the maximum number of trials when players having a soft preference insisted on the preference, is higher when Player S played against a player who had no soft preference. In other words, when Player S played against a player with a hard preference or no preference, more of Player S in the population will insist on their preference during the game play. In all these cases of Hard-Soft Conflict, Hard-Soft No Conflict and Soft-Unknown games, the peak of Player S playing P reached or even exceeded 0.6. Interestingly, when Player S played against a player who also had a soft preference, the peak was at most 0.5. This can be due to a bias in the experimental design due to the different starting times of the players caused by the difference in path widths at the split of the "T", as discussed in Chapter 4, or it can suggest that the incentive due to the hard preference was actually weaker than that due to the soft preference.

Evolutionary game theory was invented by Maynard Smith [60], when he applied game theory to study evolution of biological populations in competition. Replicator dynamics [65] is one of the descriptive methods that explains how an evolutionarily stable strategy is achieved from a given initial distribution of strategies in the population. Replicator dynamics is the product of merging both ideas of game theory and dynamical systems. In particular, it assumes that the strategies reproduce (or spread) proportionally to the success of the strategy measured by the rewards players receive from playing the strategy. The name "replicator" simply means that the individuals in this population playing a game replicate those strategies that are most successful. The fixed points of the replicator dynamics have two properties. First, every Nash equilibrium is a fixed point of the replicator dynamics but not every fixed point is a Nash equilibrium [31]. Second, for pairwise games (like the ones we consider), any asymptotically stable fixed point of the replicator dynamics is an evolutionarily stable strategy and replicator dynamics imply that an evolutionary process can produce rational behavior even though agents in the group may not consciously do so [31].

Using replicator dynamics to describe and predict human and other organisms collective decision-making behaviors in pairwise interactions has gained wide interest since the invention of the concept. It has advanced the understanding of interactive behaviors across many fields, from mathematical biology to economics and behavioral finance [34]. Recently there has been an increasing acknowledgement that the replicator dynamics are especially suitable for understanding multi-agent learning in both artificial and biological systems. They inspire simple and biologically plausible learning algorithms that require no assumption of rationality, or common information, or high cognitive capacity so that it is easy and efficient to implement on autonomous agents, or be used to describe various multi-agent learning behaviors [66].

We use a two-population three-strategy replicator dynamics model to capture the fact that the player may choose among three different strategies, left (L), right (R) and center (C), as well as having a different reward structure from her co-player (thus two sets of population states evolving simultaneously). General convergence results to the Nash equilibrium exists for replicator dynamics of homogenous populations, but convergence to the Nash equilibrium is not guaranteed for dynamics involving heterogenous populations [65]. Next we show through simulation what equilibrium states can be reached given an initial distribution of strategies for the Hard-Soft Conflict game and Soft-Soft Conflict game as an example.

Denote two populations (population 1 and 2) playing a game, where they have possibly different reward matrices such as reward matrix $\mathbf{A}$ for population 1 and reward matrix $\mathbf{B}$ for population 2. Both populations have three strategies to choose from that are the same for both populations. Denote the population states as $\mathbf{x} = \{\mathbf{x}_i\}$ for population 1 and $\mathbf{y} = \{\mathbf{y}_i\}$ for population 2, where $i \in \{1, 2, 3\}$ represents the index of strategies. $(\cdot)_i$ is used to denote the i-th entry of a vector. We also denote the three strategies 1, 2 and 3 as preference (P), opposite to the preference (O) and center (C) or left (L), right (R) and center (C) as before. Population states $\mathbf{x}_i$ and $\mathbf{y}_i$ represent the shares of the population playing strategy i in their respective population 1 and 2. By definition, $\sum_{i=1}^{3} \mathbf{x}_i = 1$ and $\sum_{i}^{3} \mathbf{y}_i = 1$. For better simulation of the model to capture the dynamic process in the data, we define two time parameters, one for each population, namely the "group" starting times t_1 and t_2 that represents the onset of evolution of strategies in the respective player populations 1 and 2. Like before with individual behaviors, we define time constants τ_1 and τ_2, assumed to be a constant for all strategies in the same population. With these two extra parameters, we write the replicator dynamics for $i = 1, 2, 3$ as

$$\tau_1 \dot{\mathbf{x}}_i = [(\mathbf{A}\mathbf{y})_i - \mathbf{x}'\mathbf{A}\mathbf{y}]\mathbf{x}_i H(t - t_1) \tag{5.1}$$

$$\tau_2 \dot{\mathbf{y}}_i = [(\mathbf{B}\mathbf{x})_i - \mathbf{y}'\mathbf{B}\mathbf{x}]\mathbf{y}_i H(t - t_2). \tag{5.2}$$

We use $(\cdot)'$ to denote the transpose of a matrix. As before, the function $H(t, t_i)$ is a Heaviside function and takes the value of 1 after $t > t_i$. In the following, we show the simulations of the replicator dynamics for a Hard-Soft Conflict game and a Soft-Soft Conflict game and compare to the empirical observations from the data.

First, we define the reward matrices for the Hard-Soft Conflict game for simulation. In the Hard-Soft Conflict game, the preference strategy is opposite for Player H and Player S, and the reward matrices are defined by $\mathbf{A_H}$ and $\mathbf{B_S}$ representing the rewards for Player H in population 1 and Player S in population 2. The P and O strategies in the reward matrices mean opposite sides for the two reward matrices $\mathbf{A_H}$ and $\mathbf{B_S}$. In other words, the P (O) strategy for Player H with reward matrix $\mathbf{A_H}$ is the O (P) strategy for Player S with reward matrix $\mathbf{B_S}$.

Fig. 5.10 shows a simulation of the replicator dynamics Eqs. 5.1-5.2 for a Hard-Soft Conflict game, with the parameter values $\tau_1 = 625$ ms, $\tau_2 = 425$ ms, $t_1 = -400$ ms and $t_2 = -420$ ms. The reward matrices are defined below. Initial conditions are $\mathbf{x}(0) = [0.02, 0.02, 0.96]'$ and $\mathbf{y}(0) = [0.01, 0.01, 0.98]'$. The parameters are chosen to match the simulation as closely as possible to observation in the data as shown in Fig. 5.9. However, no optimization fitting procedure was carried out and the parameters were chosen based on intuition and trial and error. In particular, the starting times t_1 and t_2 were chosen based on observation from the data. The values for the reward matrices were chosen such that Player H has more incentive in playing P than Player S playing their respective P. As a result, the time constants was chosen based on trial and error and satisfy the relation that $\tau_1 > \tau_2$, implying that the evolution of strategies in the Player H population is slightly slower than the Player S population. Intuitively it means that the Player S population changes in strategy faster than the Player H population in the finite number of rounds of repeated play.

$$\mathbf{A_H} = \begin{array}{c|ccc} & P & O & C \\ \hline P & 0 & 0 & 5 \\ O & 0 & 0 & 0 \\ C & 5 & 0 & 0 \end{array}$$

$$\mathbf{B_S} = \begin{array}{c|ccc} & P & O & C \\ \hline P & 0 & 0 & 4 \\ O & 0 & 0 & 1 \\ C & 4 & 1 & 0 \end{array}$$

The resulting simulation resembles the empirical results of Fig. 5.9. In particular, the simulation captures the time of the peak of strategy evolution of Player S at around 500 ms (blue line with blue circles), as the number of Player S increases to play C rather than P.

While the simulation of the replicator dynamics resembles the data, what's different is the equilibrium values. In particular, replicator dynamics suggest that the whole population of Player H and Player S will converge to the Nash equilibrium (P,C) whereas in data, more decision outcomes are possible. Even though the replicator dynamics may not predict the equilibrium accurately, it captures the features of the transient of the evolution of strategies.

Fig. 5.11 shows a simulation of the replicator dynamics Eqs. 5.1-5.2 for a Soft-Soft Conflict game and for the parameter values $\tau_1 = 225$ ms, $\tau_2 = 225$ ms, $t_1 = -300$ ms and $t_2 = -300$ ms. Initial conditions are $\mathbf{x}(0) = [0.01, 0.01, 0.98]'$ and $\mathbf{y}(0) = [0.01, 0.01, 0.98]'$. Reward matrices $\mathbf{A_L}$ for Player L and $\mathbf{B_R}$ for Player R defined below. In the Soft-Soft Conflict game, the highest individuals rewards for the two players correspond to opposite strategies. As before, the initial conditions are chosen based on the data and happen to be identical. However, the dynamics is very sensitive to the initial conditions and slight perturbation away from identical initial conditions can produce very different results, for example leading to a unique Nash equilibrium. The resulting simulation resembles the empirical results of Fig. 5.8. In particular, the evolution of strategies of Player L playing L (red line with red circle) and the evolution of Player R playing C (blue line blue triangle). The replicator dynamics simulations suggest that Player R playing R should also increase instead of playing L.

$$\mathbf{A_L} = \begin{array}{c|ccc} & L & R & C \\ \hline L & 0 & 0 & 4 \\ R & 0 & 0 & 3.5 \\ C & 4 & 3.5 & 0 \end{array}$$

$$\mathbf{B_R} = \begin{array}{c|ccc} & L & R & C \\ \hline L & 0 & 0 & 3.5 \\ R & 0 & 0 & 4 \\ C & 3.5 & 4 & 0 \end{array}$$

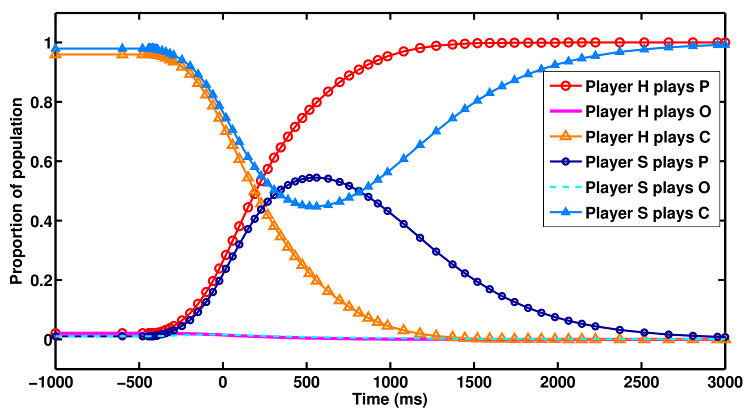

Figure 5.10: Simulation of Eqs. 5.1-5.2 with parameters $\tau_1 = 625$ ms, $\tau_2 = 425$ ms, $t_1 = -400$ ms and $t_2 = -420$ ms and initial conditions $\mathbf{x}(0) = [0.02, 0.02, 0.96]'$ and $\mathbf{y}(0) = [0.01, 0.01, 0.98]'$. The reward matrices are defined by $\mathbf{A_H}$ for Player H and $\mathbf{B_S}$ for Player S.

Replicator dynamics assume that individuals play myopically (meaning that decisions are driven by immediate individual rewards and not by future rewards). The fact that in this game, players' strategies evolve in a similar fashion as predicted by replicator dynamics suggests the possibility that human decision-making among alternatives, when there is incomplete information, is based on myopic decision rules. At the group level, this suggests that successful coordination (corresponding to a Nash

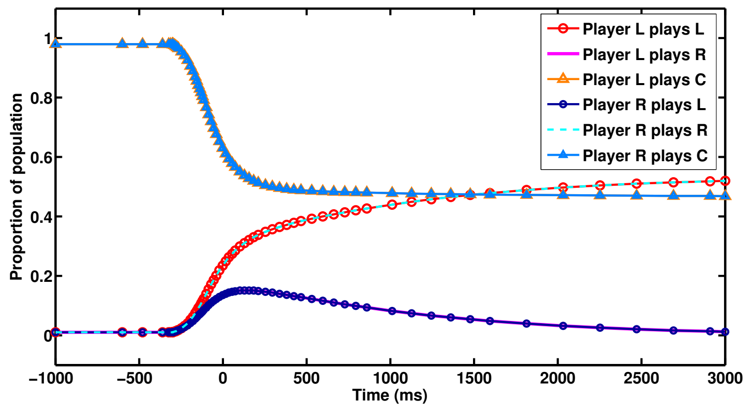

Figure 5.11: Simulation of Eqs. 5.1-5.2 with parameters $\tau_1 = 225$ ms, $\tau_2 = 225$ ms, $t_1 = -300$ ms and $t_2 = -300$ ms and initial conditions $\mathbf{x}(0) = [0.01, 0.01, 0.98]'$ and $\mathbf{y}(0) = [0.01, 0.01, 0.98]'$. The reward matrices are defined by $\mathbf{A_L}$ for Player L and $\mathbf{B_R}$ for Player R.

equilibrium or correlated equilibrium) is possible even without the communication between the players and that players are able to adapt "naturally" by playing the strategies that are best responses for themselves given the strategies of others.

Chapter 6

Conclusions and future work [1]

In this dissertation we studied collective decision-making among heterogeneously informed individuals with dynamic interactions using differential equation models and experimental data validation. In particular, we investigated the influences of parameters in collective decision-making problem on the emergent group level outcome. We also examined decision-making behaviors and how behaviors can be quantified and compared both at the individual level and the collective level.

In Chapter 2 we studied the role of uninformed individuals and individual sensing range in collective decision-making using a previously developed model on animal collective motion in the plane. The continuous-time, deterministic, dynamical system model was defined and analyzed in [50], [51] and [41] and shown to approximate well the decision-making of a group of informed and uninformed individuals on the move as studied with a computational model in [19]. The continuous-time model has the advantage of analytical tractability. By analyzing parametric conditions for the stability of solutions on the invariant manifolds of the reduced continuous-time model, we provided formal evidence that an increase in uninformed population size

[1] Discussions in the following on the analysis of Chapter 2 have been mainly taken from [41] verbatim with minor adjustments.

N_3 can improve decision-making for a group in motion by increasing the likelihood that the group will make a decision rather than compromise.

The evidence consists of three results. First, we showed that the presence of a sufficient number of uninformed individuals prevents the existence of the worse compromise solution (one that corresponds to motion in the direction opposite to the mean of the two preferred directions) on the manifold where there can be two stable compromise solutions. Further, we showed that a large enough N_3 limits the attractiveness of the remaining stable compromise solution, making the sufficient condition for stability of the manifold $\mathcal{M}_{111}$ corresponding to compromise also a necessary condition.

Second, we showed that the minimum difference in preference direction required for a group decision decreased with a decreasing individual sensing range (equivalently, an increasing threshold r on synchrony of directions sensed). This result suggests that the more local the sensing of an individual, the better the sensitivity to the conflict in preference as a collective; when individuals sense too much of the group, the result is a filtering of the local influences and a mean (compromised) collective response. By increasing the density of the group, even by adding uninformed individuals, an individual can reduce its sensing range and keep track of the same number of neighbors; in such a way an increase in population size of uninformed individuals lowers the critical difference in preference direction, making a group decision more likely.

Third, we showed that an increasing uninformed population size N_3 increases the region of parameter space for which a decision solution is exclusively stable among the eight solutions derived in [41].

The improvements that have been shown in collective decision-making with increased uninformed population size provide a testable hypodissertation about the advantages of groups of heterogeneously informed individuals. Experiments that tested and further explored the beneficial role of the uninformed individuals are described in [28].

In addition, these results provide ideas for more cost-efficient engineering designs of multi-agent systems performing tasks together. Adding individuals that do not invest directly in an external preference provides a low cost way in which groups can enhance better decision-making. Despite the fact that the model was deliberately designed as deterministic and results are formally proven for the case of symmetric populations, we showed through simulation that the results also remain robust to noise and modestly asymmetric informed sub-populations.

In Chapter 3, motivated by the animal collective motion model of [50, 41], we proposed and analyzed a continuous-time dynamical system model for human decision-making in a continuous-time interactive tracking task where individual decision makers have little information about the true preferences and incentives of other decision makers in the group. The abstract collective decision-making problem involves multiple decision makers coordinating their individual choices continuously in time for a group level (mean) decision outcome by only observing the mean of their individual decisions. Individuals in the group may have conflicting preferences for one of two alternatives. We define a model for multiple individuals deciding between two alternatives, but we focus our analysis on the case of two individual decision makers.

Our model has two features not present as far as we know in the current animal motion or human coordination literatures, namely a conditional tradeoff between two possibly different preferences and consensus-enhancing *heterophilious* interactions between agents. In particular, we proposed that without direct communication, individual decision-making depends on two critical distances in the real-valued decision space over time. We refer to an individual as a player and we represent an individual's decision state as a position on the real line. The critical distances are (1) the distance between the player's position and the group mean, and (2) the distance between the group mean position and the position of the player's preferred alternative. Each player i then makes decisions, represented as motion in decision space based on how these distances compare to their decision thresholds, which depend on two threshold parameters: the social threshold parameter θ_i and the preference threshold parameter δ_i. These parameters represent the tolerances that players hold for how far these distances have to be to affect their decisions. A higher value of the social threshold parameter represents a higher tendency to ignore the associated distance. For example, the higher the social threshold parameter θ_i of player i, the more likely it is that player i is going to neglect the social force and pursue her decision-making without caring about how far she is from the group mean. A high preference threshold parameter δ_i, on the other hand, represents a tendency for player i to stick to her preference, as opposed to an alternative choice, such as the current closer alternative. An individual with a higher preference threshold parameter is more likely to insist on pulling the group mean towards her preference, even when another alternative option is right nearby.

During the course of the decision-making, the players cannot know the preference or the strength of the preference of the other player. However, they may guess about the other player's intention by observing the mean of their decisions as it changes continuously in time. If the mean does not move according to one player's own decision-making, she would infer that it must be the result of the other player's decision-making in the opposite direction. Various studies have proposed explanations in terms of intention integration and having shared mental models when two or a small number of humans perform similar tasks [26, 38, 8, 47]. Such complex processes are hard to accurately quantify, and we do not claim to directly have such a component about integrating intentions or shared mental models in our model. Our proposed model allows sufficient autonomy for each decision maker to make adaptive decisions without having to rely on a direct measurement of the other player's decision-making.

The advantage of our model is that it can easily describe decision-making behaviors in a large group of individuals, where no one can guess the intention of the rest of the group.

We used bifurcation analysis, with threshold parameters as bifurcation parameters, to study the model for two players, in which one had a hard preference for one alternative and the other a soft preference for the other alternative. We showed bistability of decision outcomes for certain parameter ranges and a single stable solution for other ranges, suggesting the subtle role that the decision threshold parameters play in affecting the decision. In the region where there were two stable solutions, initial conditions would be the deciding factor between the two solutions.

While our model is relatively simple in contrast to previous research on modeling human decision-making in social settings, we were able to clearly identify factors that are critical in influencing the individual behaviors and explaining the emergence of group decision out of self-organized behaviors even in the presence of conflicting preferences and limited feedback.

In Chapter 4, we analyzed human behaviors in a shared tracking experiment by Groten and Feth et. al. [26] using the model developed in Chapter 3. We showed how statistical analysis of the start and end status of the decision behaviors alone was not sufficient to explain why the players reached certain decision as Player S started out more often than Player H, but did not win the decision more often. This motivates our model-based investigation of decision-making process. We fit the model to data and showed that it reproduced a wide range of human behaviors surprisingly well, suggesting that the model may have captured the mechanisms behind some of the behaviors observed in the experiment.

In particular, we found that successful coordination of decisions by the two players was achieved when either Player S had a low preference threshold, or Player H had a high social threshold. The more intransigent Player S was to her preference, the more impervious to the social force Player H had to be in order to "win" the coordinated decision. However, we also saw cases when Player H "compromised" soon and let Player S win. Even though initial conditions only affect decision outcomes for some cases (as predicted by the bifurcation plots in Chapter 3), there is evidence from the human behavior experimental results that in some cases better shared decision-making is reached with more favorable initial conditions. In this experiment, the initial positions are almost identical for the two players and therefore the starting times become the deciding initial conditions.

Our model has limitations in that it could not fit all cases of human behavior in the data. While there was a small portion of data for which we could not reproduce the transient trajectories, we could always at least reproduce the correct decision outcome.

Our approach of using a continuous-time dynamical systems model offers a distinctive advantage that allows us to gain insight into continuous-time decision-making. The experimental data that we have validated our theory on may be less complex as compared to behaviors in real-world decision scenarios: however, the experimental conditions did test the essential features of decision scenarios where communications between decision makers are restricted and individual preferences are conflicting. The data allowed us to apply our theory and gain understanding of human behaviors in shared decision-making in coordination tasks. As traditional data analysis alone does not suffice in identifying and quantifying the critical factors and mechanisms, using mathematical models such as ours to help understand experimental data may be further developed and used in future studies of human behaviors in interactive decision-making.

The model can be extrapolated to higher dimensions in two different ways. The first is to increase the number of players, making the game a real game of incomplete information since now no one can infer the decision state of the other players. One can investigate if there will be periodic solutions, where the group mean stays fixed but individual relative positions cycle indefinitely. If there will be some cycles in the model, it then remains to be tested experimentally and see if there is indeed periodic behavior. In a controlled experimental setting, we should be able to influence the thresholds through task and rewards design.

A second way to extrapolate the model is to increase the number of alternatives. When individuals have more than two alternatives to choose from, there may be complex group level dynamic by which individuals assess and eventually decide on a single alternatives.

Our model is applicable to a wide range of decision situations. It is of particular interest for future work to see how our proposed model can predict decision outcomes for different decision scenarios with different types of feedback limitations between the players. In an experimental setting, the starting times and starting positions can be controlled and new types of conflict scenarios can be introduced. To induce a higher or lower preference threshold of Player S, a higher or lower cost for losing the decision may also be imposed on the players. We hope that our model-based investigation of human behaviors can help towards the design of a human-robot interactive experiment to investigate human behaviors in interactions with autonomous co-players of various personalities that are played out by robots with personalities imposed by model parameters.

In Chapter 5, we took a game theoretic perspective to study human behaviors in the experiment of Chapter 4. We formulated the aforementioned coordination problem into a normal form game and showed that the majority of the population could converge onto the game-theoretic equilibrium strategy by the final rounds of the game. We then showed through simulations of the replicator dynamics for the Hard-Soft Conflict and Soft-Soft Conflict games that the simulated evolution of populations of strategies resembled empirical observations, suggesting that the underlying individual-based strategic responses may be myopic. Even when individuals did not know what game was being played, the population as a whole could learn to play the game-theoretic equilibrium strategies in time as a result of repeated pairwise game playing and updating strategies.

While numerous learning algorithms exist in the literature for game theoretic problems and especially for coordination games, comparison studies of game theoretic formulation with experimentally controlled human behaviors are rare. Most of the existing theoretical predictions that are compared to human behavioral data consider strategic interactions where players are able to perceive the entire game structure (both her own and the opponent's rewards), or are able to deduce complete game information iteratively using a given prior and Bayesian updates, or to keep a certain account (memory) of their opponent's strategy history in order to compute the best reply (as in regret-matching algorithms and fictitious play) [10, 9]. Other studies on human game play in experimental settings have questioned whether players use complex computations that involve, for instance, Bayesian updates. The most natural algorithms are those that don't require a lot of computations or memories or common rationality and information knowledge. Using regret-based learning and replicator dynamics to explain overall population level learning is an approach gaining increasing attention [34], as well as using coupled drift-diffusion models where the players have possibly different and stochastic perceptions of the rewards [61].

One can continue to investigate the role of learning in human subjects performing interactive tasks with incomplete information. Learning in an interactive setting is inherently more complex than learning in a single-agent setting, because during process of learning and updated decisions of other players change the environment to be learned. As we have already seen from the models in this dissertation, feedback is central to adapting to the environment, yet how individuals use feedback to update their decision-making can lead to different group level outcomes, some better than others. A possible future direction is to conduct new experiments with motor interaction tasks that are similar to the one we studied and formally design them in a game setting to study how individuals learn through repeated interaction and strictly enforced incentives.

In this dissertation we have used two very different approaches in understanding collective decision making in conflict situations. The two different approaches provide insights from two different perspectives on how decision outcomes on the collective level emerge out of individual-level decision rules and interactions. In the dynamical systems modeling approach (in Chapters 2, 3 and 4), we have seen that the collective decision outcome emerges based on how decision makers balance between the social and preference influences. It is one decision maker's tendencies relative to the other's decision-making tendencies that determines the mean decision outcome. We have also seen that initial conditions affect the final mean decision outcome, especially when two decision makers have comparable decision thresholds. We fitted the model predictions to human trajectories and gained understanding on the transients of the behavior. The fact that we could use a simple dynamical systems model to predict transient features in human decision-making makes the approach of using dynamical systems useful in designing robotic systems or human-robot systems for decision-making tasks in continuous-time while maintaining group cohesion.

However, with the dynamical system's approach, there is no notion of optimizing a collective decision, or responding in a best way to the decisions of other decision makers or to the environment. In examining the human behavioral data, we hypothesized that it was however possible, that the players played by not dynamically balancing between social and environmental influences, but to best respond to the other player's decisions. In many engineering applications, it may be desirable that not only the right collective decisions can be achieved but also be optimized while individual incentives need not be communicated. To develop systems that achieve optimal collective decisions, it is important as a first step, to examine if human players can achieve such a goal in the experimental data. While we can predict or describe optimal behaviors for one individual with optimal control theory, for decision behaviors of groups consisting more than one decision maker requires tools from game theory.

With the game theoretic modeling approach (in Chapter 5), we have seen that decision outcomes that correspond to the optimal individual rewards at equilibrium can be predicted using the reward structure (i. e. incentives in the game) and the rationality assumption that individuals maximize their own rewards. Being able to describe the incentives of the game with a parameterized reward matrix (i. e. the model of the game) is important in predicting the game outcome. Replicator dynamics then further explains how such equilibrium can be reached in continuous-time in a population, suggesting that the individual level decision rules may be very simple. The game-theoretic approach can be used in engineering applications when the incentives of the individual can be clearly defined and learning algorithms that guarantee the convergence to an equilibrium corresponding to an optimization goal are available and can be computed cost-efficiently. In Chapter 5 we've only provided some evidence from data that human players are able to play game-theoretic equilibria in games with incomplete information. We have not studied but have suggested that one could continue to study the learning algorithms that guarantee for each individual to reach a game-theoretic equilibrium.

With this dissertation we hope to provide additional methodology and mathematical models for understanding the process of continuous-time collective decision-making among heterogeneously informed individuals. Decision-making is a central part of control and by studying individual level decision rules and mechanisms for how group level decisions arise out of individual level decision-making, we hope to contribute to the design of collective control laws for solving a wide range of problems ranging from engineering to social applications.

Appendix A

Proofs for Chapter 2

A.1 Sufficient conditions for $\mathcal{M}_{111}$ to be unstable

Here we prove the sufficient conditions for $\mathcal{M}_{111}$ to be unstable.

Lemma A.1.1 *A sufficient condition for $\mathcal{M}_{111}$ to be unstable is $|\cos\frac{\bar{\theta}_2}{2}| < r$ and $N_3 > 2N_1$.*

Proof: The manifold $\mathcal{M}_{111}$ is one of compromise and can have up to two stable solutions. To show that the compromise manifold is unstable near its first stable solution, is to show conditions for which the Jacobian of the boundary layer dynamics gives at least one positive eigenvalue. This is equivalent to showing $|\cos\frac{\Psi_1-\Psi_2}{2}| < r$, where $\Psi_{1,2}$ is the stable equilibrium of interest (see [50]). The equilibrium satisfies the following equations defined for $0 < \Psi_1 < \frac{\bar{\theta}_2}{2} < \Psi_2 < \bar{\theta}_2$:

$$\begin{aligned} \Psi_1 + \Psi_2 &= \bar{\theta}_2 && \text{(A.1)} \\ \Psi_3 &= \frac{\bar{\theta}_2}{2} && \text{(A.2)} \\ \sin(\bar{\theta}_2 - \Psi_2) + \frac{K_1 N_1}{N}\sin(\bar{\theta}_2 - 2\Psi_2) &= \frac{K_1 N_3}{N}\sin(\frac{\bar{\theta}_2}{2} - \Psi_2). && \text{(A.3)} \end{aligned}$$

The solution Ψ_1, Ψ_2 and Ψ_3 defined by Eqs. A.1-A.3 is the first stable equilibrium on $\mathcal{M}_{111}$ and is denoted by $\Psi_{\mathcal{M}_{8,7}}$ in [50] (Eq. [6.32-34]). For the additional condition $N_3 > 2N_1$, this is the only equilibrium that exists on this manifold. We show that this solution is unstable when it is the only equilibrium, and therefore $\mathcal{M}_{111}$ is unstable as long as $|\cos\frac{\bar{\theta}_2}{2}| < r$ and $N_3 > 2N_1$.

To begin, we define $\frac{\Psi_1 - \Psi_2}{2} = \Delta_{12}$. From the domain of Ψ_1 and Ψ_2, $0 < \Psi_1 < \frac{\bar{\theta}_2}{2} < \Psi_2 < \bar{\theta}_2$, we can infer the following:

$$\Delta_{12} < 0, \qquad |\Delta_{12}| \in (0, \pi/2) \tag{A.4}$$

$$\cos\Delta_{12} > 0 \tag{A.5}$$

$$\sin\Delta_{12} < 0. \tag{A.6}$$

We can rewrite Eq. (C.1) as

$$\frac{\Psi_1}{2} + \frac{\Psi_2}{2} = \frac{\bar{\theta}_2}{2} \tag{A.7}$$

$\Longleftrightarrow$

$$\frac{\Psi_1}{2} + \frac{\Psi_2}{2} - \Psi_2 = \frac{\bar{\theta}_2}{2} - \Psi_2 \tag{A.8}$$

$\Longleftrightarrow$

$$\frac{\Psi_1 - \Psi_2}{2} = \Delta_{12} = \frac{\bar{\theta}_2 - 2\Psi_2}{2}. \tag{A.9}$$

Using Eq. (C.9), we can rewrite (C.3) as

$$\sin(\Delta_{12} + \frac{\bar{\theta}_2}{2}) + \frac{K_1 N_1}{N}\sin(2\Delta_{12}) = \frac{K_1 N_3}{N}\sin(\Delta_{12}) \tag{A.10}$$

$\Longleftrightarrow$

$$\sin\Delta_{12}\cos\frac{\bar{\theta}_2}{2} + \cos\Delta_{12}\sin\frac{\bar{\theta}_2}{2} + 2\frac{K_1 N_1}{N}\sin\Delta_{12}\cos\Delta_{12} = \frac{K_1 N_3}{N}\sin\Delta_{12}. \tag{A.11}$$

Divide both sides by $\sin\Delta_{12}(\neq 0) \iff$

$$\cos\frac{\bar{\theta}_2}{2} + \cos\Delta_{12}\frac{\sin\frac{\bar{\theta}_2}{2}}{\sin\Delta_{12}} + 2\frac{K_1N_1}{N}\cos\Delta_{12} = \frac{K_1N_3}{N} \tag{A.12}$$

$\iff$

$$\cos\frac{\bar{\theta}_2}{2} = \frac{K_1N_3}{N} - 2\frac{K_1N_1}{N}\cos\Delta_{12} + \cos\Delta_{12}\frac{\sin\frac{\bar{\theta}_2}{2}}{(-\sin\Delta_{12})}. \tag{A.13}$$

From here we prove by contradiction. The idea is as follows: Suppose $\cos\Delta_{12} \geq r$, which is contrary to what we want to prove. We will show that this implies a result that contradicts our assumption $r > \cos\frac{\bar{\theta}_2}{2}$ when $N_3 > 2N_1$. Thus $\cos\Delta_{12} < r$.

So, suppose $\cos\Delta_{12} \geq r$, and $\Delta_{12} < 0$, $|\Delta_{12}| \in (0, \frac{\pi}{2})$. Then

$$-1 < -(\cos\Delta_{12})^2 \leq -r^2 \tag{A.14}$$

and thus

$$\sin\Delta_{12} = -\sqrt{1-(\cos\Delta_{12})^2}. \tag{A.15}$$

From Eq. A.14 we get

$$-\sin\Delta_{12} \leq \sqrt{1-r^2} \tag{A.16}$$

$\iff$

$$\frac{1}{-\sin\Delta_{12}} \geq \frac{1}{\sqrt{1-r^2}}. \tag{A.17}$$

We assumed that $\cos\frac{\bar{\theta}_2}{2} < r$, and $\frac{\bar{\theta}_2}{2} \in (0, \frac{\pi}{2})$; therefore

$$\sin\frac{\bar{\theta}_2}{2} > \sqrt{1-r^2}. \tag{A.18}$$

Using Eqs. A.14- A.18, the last term on the RHS of Eq. A.13 becomes

$$\cos\Delta_{12}\frac{\sin\frac{\bar{\theta}_2}{2}}{(-\sin\Delta_{12})} > r\frac{\sqrt{1-r^2}}{\sqrt{1-r^2}} = r. \tag{A.19}$$

By definition, $\cos\Delta_{12} < 1 \iff$

$$-\cos\Delta_{12} > -1 \tag{A.20}$$

$\iff$

$$-2\frac{K_1N_1}{N}\cos\Delta_{12} > -2\frac{K_1N_1}{N}. \tag{A.21}$$

We can show that $\cos\frac{\bar{\theta}_2}{2}$ is bounded by the following:

$$\begin{aligned}
\cos\frac{\bar{\theta}_2}{2} = \frac{K_1N_3}{N} - 2\frac{K_1N_1}{N}\cos\Delta_{12} + \cos\Delta_{12}\frac{\sin\frac{\bar{\theta}_2}{2}}{(-\sin\Delta_{12})} && \text{(A.22)}\\
> \frac{K_1N_3}{N} - 2\frac{K_1N_1}{N} + r && \text{(A.23)}\\
(\text{ if } N_3 > 2N_1) && \text{(A.24)}\\
> r. && \text{(A.25)}
\end{aligned}$$

This is a contradiction since we assumed in the first place that $\cos\frac{\bar{\theta}_2}{2} < r$. Therefore, $\cos\Delta_{12} < r$ and therefore, $\mathcal{M}_{111}$ is unstable near $\Psi_{\mathcal{M}_{8,7}}$. Hence, a sufficient condition for $\mathcal{M}_{111}$ to be unstable is

$$|\cos\frac{\bar{\theta}_2}{2}| < r, \text{and } N_3 > 2N_1. \tag{A.26}$$

■

A.2 Sufficient conditions for $\mathcal{M}_{100}$ to be unstable.

Here we prove two conditions. First we show that when $K_1 < 2N/N_1$, the second stable solution of $\mathcal{M}_{100}$ does not exist. Then we show the condition for which when it does exist, it is unstable.

Lemma A.2.1 *The second stable solution of $\mathcal{M}_{100}$ does not exist when $K_1 < 2N/N_1$.*

Proof: According to [50] page 148, the second solution exists if and only if $K_1 \in \left[\frac{2N}{N_1}\left(\cos\left(\frac{\bar{\theta}_2}{2}\right)^{\frac{2}{3}} + \sin\left(\frac{\bar{\theta}_2}{2}\right)^{\frac{2}{3}}\right)^{\frac{3}{2}}, \frac{4N}{N_1 \sin\bar{\theta}_2}\right]$, and $\bar{\theta}_2 \in [\pi/2, \pi]$.

Let us define $G(\bar{\theta}_2) = \left(\cos\left(\frac{\bar{\theta}_2}{2}\right)^{\frac{2}{3}} + \sin\left(\frac{\bar{\theta}_2}{2}\right)^{\frac{2}{3}}\right)^{\frac{3}{2}}$. First notice that $G(\bar{\theta}_2)$ is a decreasing function of $\bar{\theta}_2$ in the given domain of $\bar{\theta}_2$ and takes minimum value when $\bar{\theta}_2 = \pi$. The resulting lower bound on K_1 becomes $\frac{2N}{N_1}\left(\cos\left(\frac{\pi}{2}\right)^{\frac{2}{3}} + \sin\left(\frac{\pi}{2}\right)^{\frac{2}{3}}\right)^{\frac{3}{2}} = \frac{2N}{N_1}$.

Therefore, if $K_1 < 2N/N_1$, according to the above necessary and sufficient condition, the second solution on $\mathcal{M}_{100}$ does not exist. ■

Lemma A.2.2 *When $K_1 < 2N/N_1$, the second solution on $\mathcal{M}_{100}$ is unstable when*

$$r > \sqrt{1-d^2}, \quad d = \frac{N\sin(\bar{\theta}_2/2)}{2N_1K_1}. \tag{A.27}$$

Proof: According to [50] page 99 Lemma 5.2.4, the stable equilibrium (denoted by ρ_{sync}), when it exists for $K_1 < \frac{2N}{N_1}$, satisfies

$$0 < \rho_{sync} < \sqrt{1-d^2}, \quad d = \frac{N\sin(\bar{\theta}_2/2)}{2N_1K_1}. \tag{A.28}$$

For the manifold to be not attracting near this equilibrium, the Jacobian of the boundary layer dynamics has to have at least one positive eigenvalue. Therefore, we look for condition such that $-(\rho_{sync} - r) > 0$ ([50] page 149). This is equivalent to requiring $r > \rho_{sync}$. As long as r is greater than the upper bound of ρ_{sync}, the condition will be satisfied. Therefore, the sufficient condition for $\mathcal{M}_{100}$ to be unstable near its second solution ρ_{sync} is

$$r > \sqrt{1-d^2}, \quad d = \frac{N\sin(\bar{\theta}_2/2)}{2N_1K_1}. \tag{A.29}$$

■

A.3 Proof for $\mathcal{M}_{011}$ to be stable within the parameter space for stable collective decision

Lemma A.3.1 *$\mathcal{M}_{011}$ can be stable within the parameter space for which $\mathcal{M}_{010}$ and $\mathcal{M}_{001}$ are stable.*

Proof: The necessary and sufficient condition for $\mathcal{M}_{011}$ to be stable is given by (from [50]).

$$\frac{1}{\sqrt{1+\nu^2}} < r < \sqrt{\frac{1}{2} + \frac{1}{2\sqrt{1+\nu^2}}} \tag{A.30}$$

where

$$\nu = \frac{N \sin(\bar{\theta}_2/2)}{N_3 K_1 + N \cos(\bar{\theta}_2/2)}.$$

The necessary and sufficient condition for $\mathcal{M}_{010}$ and $\mathcal{M}_{001}$ to be stable is given by

$$\left|\cos\left(\frac{\bar{\theta}_2}{2}\right)\right| - r < 0.$$

We can prove that $\mathcal{M}_{011}$ can be stable within the parameter space for which $\mathcal{M}_{010}$ and $\mathcal{M}_{001}$ are stable by showing that the following is always satisfied:

$$\frac{1}{\sqrt{1+\nu^2}} > |\cos\frac{\bar{\theta}_2}{2}|. \tag{A.31}$$

For simplicity, let $LHS = \frac{1}{\sqrt{1+\nu^2}}$, and $RHS = |\cos\frac{\bar{\theta}_2}{2}|$. We have

$$LHS^2 = \frac{1}{1+\nu^2}, \;\; RHS^2 = \cos^2\frac{\bar{\theta}_2}{2}. \tag{A.32}$$

Define $C = \frac{K_1 N_3}{N}$. We rewrite LHS in terms of C as

$$LHS^2 = \frac{1}{1+\nu^2} = \frac{1}{(\frac{\sin\frac{\bar{\theta}_2}{2}}{C+\cos\frac{\bar{\theta}_2}{2}})^2+1} = \frac{(C+\cos\frac{\bar{\theta}_2}{2})^2}{C^2+2C\cos\frac{\bar{\theta}_2}{2}+1} = 1 - \frac{\sin^2\frac{\bar{\theta}_2}{2}}{C^2+2C\cos\frac{\bar{\theta}_2}{2}+1}. \tag{A.33}$$

We rewrite RHS as

$$RHS^2 = 1 - \sin^2\frac{\bar{\theta}_2}{2}. \tag{A.34}$$

Subtracting the two, we have for $\bar{\theta}_2 > 0$,

$$LHS^2 - RHS^2 = \sin^2\frac{\bar{\theta}_2}{2} - \frac{\sin^2\frac{\bar{\theta}_2}{2}}{C^2+2C\cos\frac{\bar{\theta}_2}{2}+1} = \sin^2\frac{\bar{\theta}_2}{2}\frac{C^2+2C\cos\frac{\bar{\theta}_2}{2}}{C^2+2C\cos\frac{\bar{\theta}_2}{2}+1} > 0. \tag{A.35}$$

By definition, $LHS > 0$, $RHS \geq 0$, therefore $LHS > RHS$, i. e.,

$$\frac{1}{\sqrt{1+\nu^2}} > |\cos\frac{\bar{\theta}_2}{2}| \tag{A.36}$$

Therefore $\mathcal{M}_{011}$ can be stable within the parameter space for a collective decision. ■

Appendix B

Methods and additional figures for Chapter 3

Here we show the details of methods for computing the bifurcation plots, and an additional figure for Chapter 3.

B.1 Computing the bifurcations

To make the bifurcation plots, we redefine the closer path c to change smoothly from -1 to 1 in a sigmoid fashion. This way we avoid the discontinuity in the system caused by c:

$$c = \frac{2}{1 + e^{-100\bar{x}}} - 1 \tag{B.1}$$

The equilibrium of the system is the pair of solutions at which the derivative terms become zero. Since we are most interested in the equilibrium values of $\bar{x}$ instead of the individual positions, it is useful to make a change of coordinates into y_1 and y_2

coordinates, defined as the following:

$$
\begin{aligned}
y_1 &= \frac{x_H + x_S}{2} \\
y_2 &= \frac{x_H - x_S}{2}.
\end{aligned} \tag{B.2}
$$

For the bifurcation plots, we further ignore the step function H and use a general time constant of 1, instead of 100 ms as in the original equations. These differences do not affect the equilibrium solutions, nor the stability of the original system.

The resulting system equations in y_1 and y_2 coordinates are

$$
\begin{aligned}
\dot{y}_1 &= -y_1 + \frac{1}{2}\alpha_S(c+1) + \frac{1}{2}y_2(\beta_S - \beta_H) \\
\dot{y}_2 &= 1 - \frac{1}{2}\alpha_S(c+1) - \frac{1}{2}y_2(\beta_S + \beta_H).
\end{aligned} \tag{B.3}
$$

$$
\begin{aligned}
\alpha_S &= \frac{1}{1 + e^{-B_S(|1+y_1| - \delta_S)}} \\
\beta_H &= \frac{1}{1 + e^{-R_H(|y_2| - \theta_H)}} \\
\beta_S &= \frac{1}{1 + e^{-R_S(|y_2| - \theta_S)}}.
\end{aligned} \tag{B.4}
$$

At equilibrium, $\dot{y}_1 = 0$, and $\dot{y}_2 = 0$. Simplifying the equations leads to the following, which define, in general, all equilibrium points to the system Eqs. B.3:

$$
\begin{aligned}
1 - y_1 &= y_2\beta_H \\
1 + y_1 - \alpha_S(c+1) &= y_2\beta_S.
\end{aligned} \tag{B.5}
$$

Local stability of the equilibria can be found by evaluating the eigenvalues of the Jacobian matrix at the equilibria. If the Jacobian eigenvalues carry negative real parts, then the equilibrium is locally asymptotically stable. If, however, at least one eigenvalue has a positive real part, then the equilibrium is locally unstable. We denote the Jacobian matrix by $\mathbf{J}$. First we define the following terms:

$$\begin{aligned} D_1 &= 25\alpha_S(1+c)(1-c) + \frac{1}{2}B_S(c+1)\alpha_S(1-\alpha_S)\mathrm{sgn}(1+y_1) \\ D_2 &= \frac{1}{2}\beta_S + \frac{1}{2}y_2R_S\beta_S(1-\beta_S)\mathrm{sgn}(y_2) \\ D_3 &= \frac{1}{2}\beta_H + \frac{1}{2}y_2R_H\beta_H(1-\beta_H)\mathrm{sgn}(y_2). \end{aligned} \tag{B.6}$$

The sign function is defined as

$$\mathrm{sgn}(x) = \begin{cases} -1 & \text{if } x < 0 \\ 0 & \text{if } x = 0 \\ 1 & \text{if } x > 0. \end{cases}$$

The Jacobian matrix is then

$$\mathbf{J} = \begin{bmatrix} -1 + D_1 & D_2 - D_3 \\ -D_1 & -D_2 - D_3. \end{bmatrix}$$

The eigenvalues of the Jacobian are defined by the characteristic polynomial:

$$\lambda^2 + (1 - D_1 + D_2 + D_3)\lambda + D_2D_3 - 2D_1D_3 = 0. \tag{B.7}$$

The Routh-Hurwitz criterion for second-order polynomials to have roots with negative real-parts requires

$$\begin{aligned} 1 - D_1 + D_2 + D_3 &> 0 \\ D_2 + D_3 - 2D_1D_3 &> 0. \end{aligned} \tag{B.8}$$

Computations were carried out in MATLAB. Function fsolve was used to compute the solutions for the equilibria for a range of initial guesses and parameter values. Then the eigenvalues of the Jacobian were evaluated to determine stability of the equilibria for the bifurcation plots. The initial guesses of the solutions were found using the nullclines (see Fig. B.1). The two-parameter bifurcation plot is produced by mapping all bifurcation points onto the two-parameter plane.

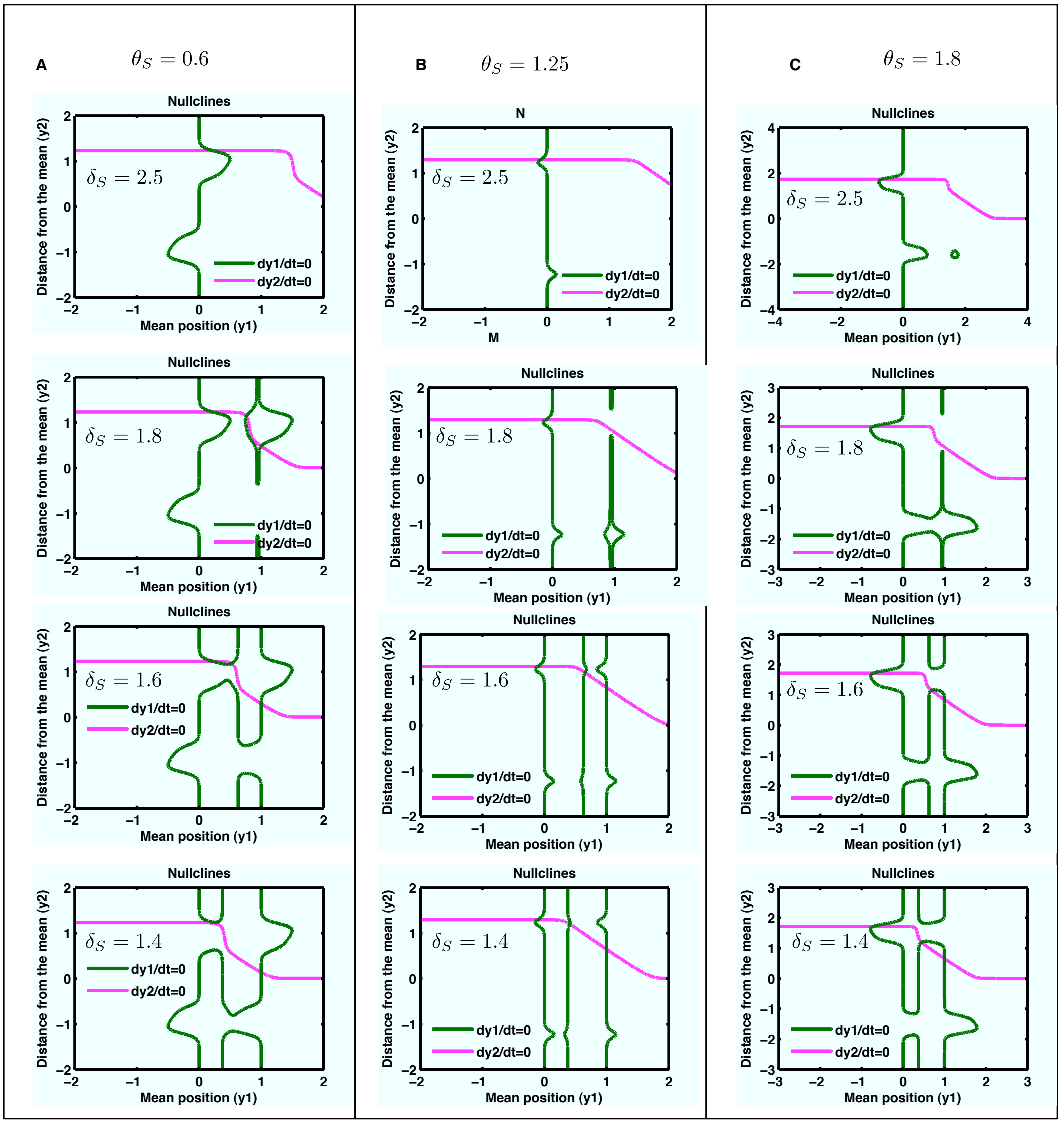

Figure B.1: Nullclines of the system equations as parameters θ_S and δ_S change. Nullclines of the system equations in (y_1, y_2) coordinates are plotted for parameters $\theta_H = 1.2$, $R_H = R_S = B_S = 20$. The horizontal axis is y_1, and the vertical axis is y_2. The green lines are the set of points where $\frac{dy_1}{dt} = 0$. The magenta lines are set of points where $\frac{dy_2}{dt} = 0$. The panels A-C show the nullclines for three different values of θ_S. Inside each panel, the values of θ_S are the same. The values of δ_S for each figure in the panels decrease from top to bottom.

Appendix C

Methods and additional figures for Chapter 4

Here we list our methods and additional figures for Chapter 4.

C.1 Data and statistics

We collected statistics for the decision outcome in the following way. For a given trial, if the mean trajectory entered a certain neighborhood of one of the two alternative reference paths and stayed there for a sufficiently long time, then the pair of players is said to have reached a decision, and we define the decision outcome to be for that particular path. When the trajectory was in the close neighborhood of zero (centerline), it is referred to as deadlock. When the trajectory was somewhere other than these classifications, it is called a "no decision", or "unclassified". We also allow a separate class corresponding to "multiple" decision outcomes.

The bounds of the neighborhood for the thick path, thin path and centerline, were defined by μ_{thick}, μ_{thin}, and μ_0 respectively. Each neighborhood is defined as a box surrounding the path, with length equal to the signal duration (3000 ms) and width equal to twice the bounds centered around the path or centerline. The bounds μ_{thick},

μ_{thin}, and μ_0 are percentages of the distance between the reference paths and the centerline.

Fig. C.1 below illustrates the boxes used to compute the statistics. We denote by $T_{preference}$ (ms) the minimum length of time necessary to stay within a neighborhood in order to qualify as the associated decision outcome. We vary the bounds μ_{thick}, μ_{thin}, and μ_0 from 0.1 to 0.35, by increments of 0.05, and we compare the corresponding statistical distribution of outcomes. We also vary the duration $T_{preference}$ from 50ms to 2000ms, by increments of 50ms, and again compare results. Trajectories that are sensitive to small changes in the bounds and thresholds are rare in the data set. For the ranges of μ_{thick}, μ_{thin}, μ_0, $T_{preference}$ and T_{center}, the outcome statistics is relatively robust with error bars less than 10% of the present values. As shown in Fig. C.1B, the decision can be classified as a soft preference, or as 'unclassified', depending on the width of the boxes and duration required to stay in the box.

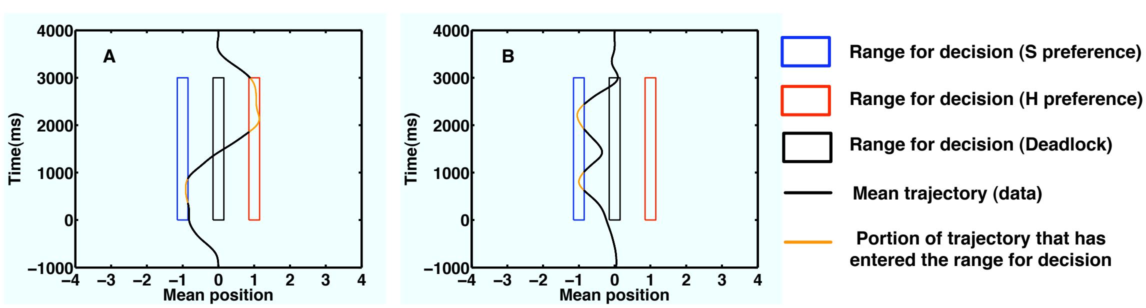

Figure C.1: Illustrative example for criteria on the statistics of decision outcomes. μ_{thick}=μ_{thin}=μ_0 = 0.15 A. Double decision: both the hard and soft preferences are reached. B. Classification of these types of outcomes A and B are sensitive to the choice of the bounds and threshold. If $T_{preference}$ increases or if μ_{thick} decreases, the decision in A would not be counted as a double decision but a single decision for the hard preference stead, and the decision in B) would not be counted as a soft preference but as an unclassified outcome.

Let player i's waiting position be her position at -1000 ms, i.e. one second before the time of the "T". We define the starting time t_i of player i to be the first time when player i has deviated from her waiting position by a distance exceeding a fixed threshold ϵ. The player who starts first will be referred to as the "initiator". This player has complete control over the mean for some time until the other player also starts moving. Depending on how big the difference is between the two players' starting times, the extent of dominance of the initiator can differ. The starting time is sensitive to the threshold ϵ. However, the starting order (i.e. who starts first) is generally not sensitive to changes in ϵ within the range of 0.01 and 0.3 for the majority of data sets, i.e., there is less than 10% variation in the statistics.

C.2 Pre-processing of the data for fitting to the model

Data for each decision-making process pertains to three continuously running parts: the decision-making period (0 ms to 3000 ms), the waiting period (-1000 ms to 0 ms), and the ending period (3000 ms to 4000 ms). Accordingly, we fitted to the data segment lasting from -1000 ms to 4000 ms for each decision scenario, where 0 ms is defined as the onset of the decision "T". The split in the reference paths lasts from 0 ms to 3000 ms. Furthermore, we normalized the data to the track position, so that the normalized target track locations are at 1 and -1 (on the horizontal axis), where 0 is the centerline.

We assume that players did not know their relative distance to the mean initially, and collapsed all players' trajectories to the starting position of the mean. Statistics of the absolute starting positions (i.e. position at -1000 ms) of the mean and Player S were collected. The histograms and statistics of the starting positions are shown in Fig. C.2. The mean of the starting positions for the mean trajectory was -0.0025, and the standard deviation was 0.0246, suggesting that the mean position started almost at centerline. The mean of the starting positions for Player S was -0.028, with a standard deviation of 1.0627, suggesting that the starting positions of Player S spread out from the centerline.

In order to see if starting on a particular side would lead to decision outcomes for that side, we compared the starting sides with the decision outcomes based on the measurements for Fig. 4.5 in Chapter 4. We found that the ratio between the number of times that Player S started on the decision side versus that for the opposite side is 1.22, which is very close to 1. We think that this is not a strong enough evidence to suggest that absolute starting positions correlate with decision outcomes. Therefore, by collapsing the players' trajectories to the starting position of the mean, we have not excluded important factors that influence the decision outcome.

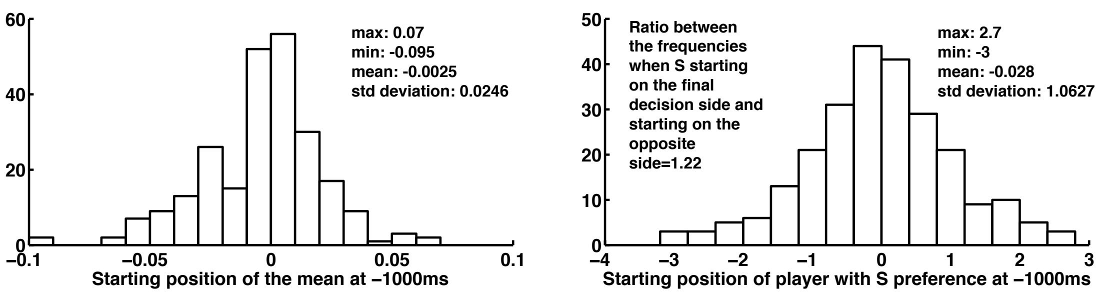

Figure C.2: Histograms of absolute starting positions of the mean and Player S. The starting positions of the mean and Player S are defined as the positions at −1000 ms. We compared the starting positions to the decision outcomes and found that there is no evident correlation between a starting side and final decision.

C.3 Fitting a dynamical system to continuous-time data

We fit the model equations to each set of trajectories by minimizing the sum of the error squared between the model simulation and the pre-processed data for each time step in the 5000 ms length for each data set in the hard soft conflict decision type.

Parameters were in confined ranges for optimization. In particular, $\theta_H, \theta_S, \delta_H, \delta_S$ were bounded between 0.1 and 6. R_H, R_S, B_H, B_S were bounded between 1 and 25, and t_H, t_S were bounded between -1000 ms and 1000 ms. The bounds were found through preliminary fitting which suggest that the ranges were appropriate for the majority data set.

All of 244 data sets for the Hard-Soft Conflict decision scenario were fitted and the corresponding parameters analyzed. The data we fit the model to are sequences of positions in time, denoted by $\mathbf{x}(\mathbf{t})$, where $\mathbf{t} = -1000, ..., 0, 1, 2, ...4000$ in milliseconds. Denote our model by $\dot{\mathbf{y}} = \mathbf{f}(\mathbf{y}, \Pi)$, where Π is the set of all parameters to be optimized. We set the initial conditions $\mathbf{y}(0)$ for our model equal to $\mathbf{x}(0)$. The optimization problem is then to seek Π that minimizes the mean squared error:

$$E(\Pi) = \frac{1}{5001} \sum_{t=-1000}^{4000} ||\mathbf{x}(\mathbf{t}) - \mathbf{y}(\mathbf{t}|\Pi)||^2 \tag{C.1}$$

subject to the constraint of $\dot{\mathbf{y}} = \mathbf{f}(\mathbf{y}, \Pi)$ and $\mathbf{y}(0) = \mathbf{x}(0)$.

C.4 Parameter ranges and conditions for optimization routine

The ranges for parameter search and fit optimization were found through repeated pre-fitting and adjustments to see if the optimization routine would hit the boundaries of the ranges. The optimization routine (lsqnonlin in MATLAB) searches for the best-fit parameters, until the changes in the errors between data and fit, are below a threshold of 10^{-5}, or until the number of iterations have reached a maximum of 10^5. The fit was then examined and the root mean squared error computed. The fit was then improved if the root mean squared error was too large, by varying the initial values of the parameters.

Bibliography

[1] D. Angeli, Jr. J. E. Ferrell, and E. D. Sontag. Detection of multistability, bifurcations, and hysteresis in a large class of biological positive-feedback systems. *Proceedings of the National Academy of Sciences of the United States of America*, 101(7):1822–1827, 2004.

[2] I. Aoki. A simulation study on the schooling mechanism in fish. *Bull. Jap. Soc. Sci. Fish*, 48:1081–1088, 1982.

[3] R. J. Aumann. Subjectivity and correlation in randomized strategies. *J. Math. Econ.*, 1:67–96, 1974.

[4] R.J. Aumann. Correlated equilibrium as an expression of bayesian rationality. *Econometrica*, 55(1):1–18, 1987.

[5] D. S. Bassett, D. L. Alderson, and J. M. Carlson. Collective decision dynamics in the presence of external drivers. *Physical Review E*, 86:036105(14), 2012.

[6] D. Biro, D.J.T. Sumpter, and J. Meade. From compromise to leadership in pigeon homing. *Current Biology*, 16:2123–2128, 2006.

[7] R. Bogacz, E. Brown, J. Moehlis, P. Holmes, and J. D. Cohen. The physics of optimal decision making: A formal analysis of models of performance in two-alternative forced choice tasks. *Psychological Review*, 113(4):700–765, 2006.

[8] T. Bosse, M. Hoogendoorn, C.A. Klein, J. Treur, C. N. van der Wal, and A. van Wissen. Modelling collective decision making in groups and crowds: Integrating social contagion and interacting emotions, beliefs and intentions. *Auton Agent Mult-Agent Syst*, 27:52–84, 2013.

[9] D. A. Braun, P. A. Ortega, and D. M. Wolpert. Motor coordination: when two have to act as one. *Exp. Brain Res.*, 211:631–641, 2011.

[10] D. A. Braun, P.A. Ortega, and D.M. Wolpert. Nash equilibria in multi-agent motor interactions. *PLoS Computational Biology*, 5(8), 2009.

[11] S. Camazine, J.L. Deneubourg, N.R. Franks, J. Sneyd, G. Theraulaz, and E. Bonabeau. *Self-Organization in Biological Systems.* Princeton University Press, Princeton, 2003.

[12] M. Cao, A. Stewart, and N.E. Leonard. Convergence in human decision-making dynamics. *Systems and Control Letters*, 59:87–97, 2010.

[13] G. Cardillo. Myfisher22: a very compact routine for fisher's exact test on 2x2 matrix, 2007.

[14] G. Cardillo. Myfisher33: a very compact routine for fisher's exact test on 3x3 matrix, 2007.

[15] J. M. Carlson, D. L. Alderson, S.P. Stromberg, D.S. Bassett, E.M. Craparo, F. Guiterrez-Villarreal, and T. Otani. Measuring and modeling behavioral decision dynamics in collective evacuation. *PLoS ONE*, 9(2):1–17, 2014.

[16] C.Eikenaar, T. Klinner, K.L. Szostek, and F. Bairlein. Migratory restlessness in captive individuals predicts actual departure in the wild. *Biol. Lett.*, 10, 2014.

[17] C.S. Chapman, J.P. Gallivan, D.K. Wood, J.L. Milne, J.C. Culham, and M.A. Goodale. Reaching for the unknown: Multiple target encoding and real-time decision-making in a rapid reach task. *Cognition*, 116(2):168–76, 2010.

[18] L. Conradt. Collective animal decisions: preference conflict and decision accuracy. *Interface Focus*, 3(6):1–12, 2013.

[19] I. D. Couzin, J. Krause, N.R. Franks, and S.A. Levin. Effective leadership and decision-making in animal groups on the move. *Nature*, 433(7025):513–6, 2005.

[20] I.D. Couzin. Collective cognition in animal groups. *Trends in cognitive sciences*, 13:36–43, 2009.

[21] I.D. Couzin, J. Krause, R. James, G.D. Ruxton, and N.R. Franks. Collective memory and spatial sorting in animal groups. *J. theor. Biol.*, 218:1–11, 2002.

[22] I.D. Couzin and Jens Krause. Self-organization and collective behavior in vertebrates. *Advances in the study of behavior*, 32, 2003.

[23] J. R.G. Dyer, C. C. Ioannou, L. J. Morrell, D. P. Croft, I. D. Couzin, D. A. Waters, and J. Krause. Consensus decision making in human crowds. *Animal Behavior*, 75:461–470, 2008.

[24] J.R.G. Dyer. Leadership, consensus decision making and collective behavior in human crowds. *Phil. Trans. R. Soc. B*, 364:781–89, 2009.

[25] J. I. Gold and M. N. Shadlen. The neural basis of decision-making. *Annu. Rev. Neurosci.*, 30:535–74, 2007.

[26] R. Groten, D. Feth, R. L. Klatzky, and A. Peer. The role of haptic feedback for the integration of intentions in shared task execution. *IEEE Transactions on Haptics*, 6(1):94–105, 2013.

[27] S. Gueron, S. A Levin, and D. I. Rubenstein. The dynamics of herds: From individuals to aggregations. *J. theor. Biol.*, 182:85–98, 1996.

[28] V. Guttal and I. D. Couzin. Leadership, collective motion and the evolution of migratory strategies. *Commun. Integr. Biol.*, 4(3):294–298, 2011.

[29] P. Haazebroek, S. van Dantzig, and B. Hommel. A computational model of perception and action for cognitive robotics. *Cogn Process*, 12:355–365, 2011.

[30] S. Hart and A. Mas-Colell. A simple adaptive procedure leading to correlated equilibrium. *Econometrica*, 68(5):1127–1150, 2000.

[31] Sergiu Hart. Commentary: Nash equilibrium and dynamics. *Games and Economic Behavior*, 71:6–8, 2011.

[32] A. Heathcote and J. Love. Linear deterministic accumulator models of simple choice. *Frontiers in Psychology*, 3(292):1–19, 2012.

[33] R. Hegselmann and U. Krause. Opinion dynamics and bounded confidence models, analysis, and simulation. *Journal of Artificial Societies and Social Simulation*, 5(3), 2002.

[34] C. Hilbe. Local replicator dynamics: A simple link between deterministic and stochastic models of evolutionary game theory. *Bull Math Biol*, 73:2068–2087, 2011.

[35] B. Hommel. Dancing in the dark: no role for consciousness in action control. *Front. Psychol.*, 4(380), 2013.

[36] J. A. S. Kelso. *Dynamic Patterns: the Self-Organization of Brain and Behavior*. The MIT Press, 1995.

[37] P.V. Kokotovic, H.K. Khalil, and J. O'Reilly. *Singular Perturbations Methods in Control: Analysis and Design*. Academic Press, New York, 1986.

[38] A. Kucukyilmaz, T.M. Sezgin, and C. Basdogan. Intention recognition for dynamic role exchange in haptic collaboration. *Haptics, IEEE Transactions on*, 6(1):58–68, 2013.

[39] L.Conradt. Models in animal collective decision-making: Information uncertainty and conflicting preferences. *Interface Focus*, 2(2):226–240, 2012.

[40] L.Conradt and C.List. Group decisions in humans and animals: A survey. *Phil. Trans. R. Soc. B*, 364:719–743, 2009.

[41] N. E. Leonard, T. Shen, B. Nabet, L. Scardovi, I. D Couzin, and S. A. Levin. Decision versus compromise for animal groups in motion. *Proceedings of the National Academy of Sciences of the United States of America*, 109(1):227–232, 2012.

[42] P.B.S. Lissaman and C.A. Shollenberger. Formation flight of birds. *Science*, 168:1003–1005, 1970.

[43] E.J. Masicampo and R.F. Baumeister. Conscious thought does not guide moment-to-moment actions-it serves social and cultural functions. *Front Psychol.*, 4(478), 2013.

[44] M. McPherson, L. Smith-Lovin, and J. M. Cook. Birds of a feather: homophily in social networks. *Annu. Rev. Sociol.*, 27:415–44, 2001.

[45] J. Memelink and B. Hommel. Intentional weighting: a basic principle in cognitive control. *Psychological Research*, 77:249–259, 2013.

[46] N. Miller, S. Garnier, A. T. Hartnett, and I. D. Couzin. Both information and social cohesion determine collective decisions in animal groups. *Proceedings of the National Academy of Sciences of the United States of America*, 110(13):5263–5268, 2013.

[47] J.B. Misyak, T. Melkonyan, H. Zeitoun, and N. Chater. Unwritten rules: virtual bargaining underpins social interaction, culture, and society. *Trends in cognitive sciences*, 18(10), 2014.

[48] S. Mohammed and E. Ringseis. Cognitive diversity and consensus in group decision making: The role of inputs, processes, and outcomes. *Organizational Behavior and Human Decision Processes*, 85(2):310–335, 2001.

[49] S. Motsch and E. Tadmor. Heterophilious dynamics enhances consensus. *SIAM Review*, 56(4):1–43, 2014.

[50] B. Nabet. *Dynamics and Control in Natural and Engineered Multi-Agent Systems*. PhD thesis, Princeton University, 2009.

[51] B. Nabet, N.E. Leonard, I.D. Couzin, and S.A. Levin. Dynamics of decision making in animal group motion. *Journal of Nonlinear Science*, 19:399–435, 2009.

[52] A. Nedic, D. Tomlin, P. Holmes, D.A. Prentice, and J.D. Cohen. A decision task in a social context: Human experiments, models, and analyses of behavioral data. *Proceedings of the IEEE*, 100(3):713–733, 2012.

[53] M. J. Osborne. *An Introduction to Game Theory*. Oxford University Press, 2002.

[54] D. Paley, F. Zhang, and N. E. Leonard. Cooperative control for ocean sampling: The glider coordinated control system. *IEEE Transactions on Control Systems Technology*, 16(4):735–744, 2008.

[55] J.K. Parrish and L. Edelstein-Keshet. Complexity, pattern, and evolutionary trade-offs in animal aggregation. *Science*, 284:99–101, 1999.

[56] K.M. Passino and T.D. Seeley. Modelling and analysis of nestsite selection by honeybee swarms: the speed and accuracy trade-off. *Behav. Ecol. Sociobiol.*, 59:427–442, 2006.

[57] P. Reverdy, V. Srivastava, and N. E. Leonard. Towards human-robot teams: Modeling human decision making in generalized gaussian multiarmed bandits. *Proceedings of the IEEE*, 102(4):544–571, 2014.

[58] A. Ross-Gillespie and R. Kuemmerli. Collective decision-making in microbes. *Frontiers in Microbiology*, 5:1–11, 2014.

[59] T. Shen, M. Schwemmer, R. Groten, D. Feth, E. Ludvig, and N. E. Leonard. On the dynamics of social coordination for shared decision-making with continuous-time feedback. *in preparation*, 2014.

[60] J.M. Smith. *Evolution and the Theory of Games*. Cambridge University Press, 1982.

[61] V. Srivastava and N.E. Leonard. Collective decision-making in ideal networks: The speed-accuracy tradeoff. *Transactions on Control of Network Systems*, 1(1):121–132, 2014.

[62] A. Stewart, M. Cao, A. Nedic, D. Tomlin, and N.E. Leonard. Model-based analysis of human decision making in two-alternative choice tasks with social feedback. *Proceedings of the IEEE*, 100(3):751–775, 2012.

[63] D. J. T. Sumpter. *Collective Animal Behavior*. Princeton University Press, Princeton, 2010.

[64] B.L. Taylor, I.B. Zhulin, and M.S. Johnson. Aerotaxis and other energy-sensing behavior in bacteria. *Annu. Rev. Microbiol.*, 53:103–128, 1999.

[65] P.D. Taylor and L.B. Jonker. Evolutionary stable strategies and game dynamics. *Mathematical Biosciences*, 40:145–156, 1978.

[66] K. Tuyls and S. Parsons. What evolutionary game theory tells us about multiagent learning. *Artificial Intelligence*, 171:406–416, 2007.

[67] P.K. Visscher, T. Seeley, and K. Passino. Group decision making in honey bee swarms. *American Scientist*, 94(3):220–229, 2006.

[68] K. Vittori. Path efficiency of ant foraging trails in an artificial network. *J. Theo. Biol.*, 239:507–515, 2006.